Agent-Based Modeling of Infected Cell Killing Mediated by Cytotoxic T-cells

Von der Fakultät für Lebenswissenschaften

der Technischen Universität Carolo-Wilhelmina zu Braunschweig

zur Erlangung des Grades einer

Doktorin der Naturwissenschaften

(Dr. rer. nat.)

genehmigte

D i s s e r t a t i o n

von: Ananya Rastogi

aus: Lucknow, India

1. Referent: Prof. Dr. Michael Meyer-Hermann

2. Referent: Prof. Dr. Dieter Jahn

eingereicht am: 09.03.2020

mündliche Prüfung (Disputation) am: 03.07.2020

Druckjahr 2021

Vorveröffentlichungen der Dissertation

Teilergebnisse aus dieser Arbeit wurden mit Genehmigung der Fakultät für Lebenswissenschaften, vertreten durch den Mentor der Arbeit, in folgenden Beiträgen vorab veröffentlicht:

Publikationen

- Robert PA, *Rastogi A*, Binder SC, Meyer-Hermann M. How to simulate a germinal center. InGerminal Centers 2017 (pp. 303-334). Humana Press, New York, NY.
- *Rastogi A*, Robert P, Halle S, Meyer-Hermann M. Evaluation of CD8 T cell killing models with computer simulations of 2-photon imaging experiments. bioRxiv. 2019 Jan 1:830505.

Tagungsbeiträge

- *Rastogi A*, Modelling of Cooperativity Mechanisms in T cell Killing. Workshop on Computational Models in Biology and Medicine, 8 - 9 March 2018, University of Regensburg, Germany.

Posterbeiträge

- *Rastogi A*, Computational Analysis of Microvesicle Dynamics in Germinal Centres. 14th B Lymphocyte Forum Zeist, 18 - 20 February 2016, Zeist, Netherlands.
- *Rastogi A*, Modelling of Cooperativity Mechanisms in T cell Killing. FEBS Advanced Course-19th International Summer School on Immunology, 23 - 30 September 2017, Hvar, Croatia.

This research project (2015-2019) was supported by the Human Frontier Science Program (RGP0033/2015).

Abstract (English)

Cytotoxic T lymphocyte (CTL) mediated killing of infected cells is an indispensable machinery of the immune system to remove infected cells from the host body. *In vivo* imaging of CTL killing activity revealed infected cells need multiple contacts with CTLs to die. The impact of increasing number of contacts with CTLs on infected cell death remained unexplored.

In this study, a novel method of analysis called probability of transition analysis (PTA) was proposed to study the effect of increasing number of interactions with CTLs on the probability of infected cell death. The versatility of the PTA makes it a viable analysis method for various systems. The application of PTA on CTL experimental data shows a higher probability of dying after multiple contacts with CTLs. The increase in observed probability of killing infected cells at each contact suggests a change in behaviour of CTLs or infected cells with increasing number of contacts. It is not known whether CTLs become more lethal with increasing contacts with infected cells or if infected cells become more susceptible to cell death with increasing number of contacts with CTLs.

To study and discriminate between possible killing mechanisms employed by CTLs, an agent-based model was developed. This model accurately mimics the behavior of a lymph node by incorporating experimentally observed properties into the system. The model was then used to discriminate between proposed hypotheses of CTL mediated killing that could give rise to an increase in probability of killing infected cells. The most credible scenario implied an increase in susceptibility of infected cells at each CTL contact. However, when allowing T cells to interact with already apoptotic target cells (zombie contacts), a contact history independent killing mechanism was also in agreement with the experimental datasets. The duration taken by an infected cell to die as well as the per capita killing rate (PCKR) were predictive read-outs that could be used to differentiate the CTL killing mechanism. The agent-based model and the comparison of observed datasets to model data helped us better understand the experimental data by shedding light on factors that cannot be measured experimentally.

We also explored the impact of temporal factors such as variable observation window and unknown history by using the agent-based model and PTA. The results indicated a difference that arose as a consequence of varying observation time duration and observations initiated at different time points. The obtained result shows the importance of uniformity of experimental setups to ensure accurate comparisons.

Zusammenfassung (Deutsch)

Die durch cytotoxische T-Lymphozyten (CTL) vermittelte Abtötung von infizierten Zellen ist ein unverzichtbarer Mechanismus des Immunsystems, um infizierte Zellen aus dem Wirtskörper zu entfernen. Durch in vivo-Bildgebung der CTL-Abtötungsaktivität konnte gezeigt werden, dass infizierte Zellen mehrere Kontakte mit CTLs benötigen, um abzusterben. Die Auswirkungen eines Anstiegs von Kontakten mit CTLs auf den Tod infizierter Zellen sind bisher unerforscht.

Um die Auswirkung eines solchen Anstiegs von Interaktionen mit CTLs auf die Wahrscheinlichkeit des Absterbens infizierter Zellen zu untersuchen, wurde in dieser Studie eine neue Analysemethode, die so genannte Übergangswahrscheinlichkeitsanalyse (probability of transition analysis, PTA), erprobt. Die Vielseitigkeit der PTA macht sie zu einer praktikablen Analysemethode für verschiedene Systeme. Die Anwendung der PTA auf experimentelle CTL-Daten zeigt, dass es nach mehrfachen Kontakten mit CTLs eine höhere Sterbenswahrscheinlichkeit gibt.

Die Zunahme der beobachteten Wahrscheinlichkeit, infizierte Zellen bei jedem einzelnen Kontakt zu töten, lässt auf eine Änderung des Verhaltens von CTLs oder infizierten Zellen mit zunehmender Anzahl von Kontakten schließen. Dabei ist nicht bekannt, ob CTLs bei mehr Kontakten mit infizierten Zellen tödlicher werden oder ob infizierte Zellen mit mehr Kontakten mit CTLs anfälliger für den Zelltod werden.

Um mögliche Tötungsmechanismen von CTLs zu untersuchen und zu unterscheiden, wurde ein agentenbasiertes Modell entwickelt. Dieses Modell ahmt das Verhalten eines Lymphknotens genau nach, indem es experimentell beobachtete Eigenschaften in das System einbezieht.

Dieses Modell wurde dann zur Unterscheidung zwischen vorgeschlagenen Hypothesen der CTL-vermittelten Abtötung verwendet, die zu einer erhöhten Tötungswahrscheinlichkeit infizierter Zellen führen könnten. Das zuverlässigste Szenario implizierte eine erhöhte Anfälligkeit der infizierten Zellen bei jedem CTL-Kontakt.

Wenn man jedoch T-Zellen mit bereits apoptotischen Zielzellen (Zombie-Kontakte) interagieren lässt, war ein Tötungsmechanimus, der unabhängig von vorherigen Kontakten ist, ebenfalls mit experimentellen Datensätzen zu vereinbaren.

Zwei Messwerte konnten als Prädiktoren zur Differenzierung des CTL-Abtötungsmechanismus verwendet werden: Die Dauer, die eine infizierte Zelle zum Absterben benötigte, sowie die Pro-Kopf-Abtötungsrate (per capita killing rate, PCKR).

Das agentenbasierte Modell und der Vergleich von tatsächlich beobachteten Datensätzen mit Modelldaten haben uns geholfen, die experimentellen Daten besser zu verstehen, indem sie solche Faktoren erklärten, die experimentell nicht gemessen werden können.

Wir untersuchten auch die Auswirkungen zeitlicher Faktoren wie variable Beobachtungsfenster und unbekannte Historien mit Hilfe des agentenbasierten Modells und der PTA. Die Ergebnisse wiesen auf einen Unterschied hin, der als Folge der unterschiedlichen Beobachtungszeitdauer und der zu verschiedenen Zeitpunkten initiierten Beobachtungen entstand. Das Ergebnis zeigt, wie wichtig die Einheitlichkeit der Versuchsaufbauten ist, um genaue Vergleiche zu gewährleisten.

Acknowledgements

I left this part of my thesis for last thinking that this would be a cakewalk. Yet, now as I think back to all the people who have helped me reach this point, I can't help but feel overwhelmed and it suddenly seems that it was easier to write the discussion than this. Well... That's not true.

I want to begin by thanking Michael Meyer-Hermann for his patience and enthusiasm, and for being the best supervisor I could have had. Thank you for motivating me to do better everyday. Plus, I don't think that there are many PhD students who can claim to have partied with their supervisor till 4 am in Lisbon and that is a story that never gets old!

My post-doc supervisor, Philippe Robert, is the reason I believe in angels because if devils like him can exist, there's no reason angels can't, right? The fact that he asked me to include something mean about him in my acknowledgments goes to show just how much fun he made these last 4 years. I truly couldn't have asked for a better supervisor and a friend. Of course, my PhD experience is incomplete without mentioning Anastasios Siokis. We have discussed what we would do if we were millionaires, we have annoyed each other with old Indian and Lebanese songs and we have planned just how we wanted to destroy our computers when the codes didn't run. Basically, all normal things that you discuss with your colleagues. I am grateful to all members of the lab for creating a wonderful and pleasant environment. A special thanks to Stephan Halle for his constant enthusiasm and feedback on my project.

I am thankful to all my wonderful friends who provided me with gentle and not-so-gentle reminders that there is life outside my PhD. A huge shout out to all my people: Rupali for listening to me rant and being the voice of reason in my life; Divya for understanding me so effortlessly; Sumer for being the unofficial encyclopedia and my go-to person for all questions about paper-work and adulting; Kalyani for being the counsellor for all us PhDs, we really needed you to keep us sane; Pragya for somehow making me feel like I was home whenever I visited her; Neha and Niharika for all the wonderful times we spent in Vapiano and watching terrible movies in Braunschweig.

None of what I have done would have been possible without my incredible family. My mother, Ruby Rastogi and my father, Atul K. Rastogi, who have been my constant cheerleaders and have never failed to remind me that they will support me in anything I choose to do, thank you for everything. My husband, Vivek B. Raina, who is truly the yin to my yang and is largely responsible for helping me stay (somewhat) calm during all the ups and downs of my work. Also, thank you for always reminding me that "experimental science is the only real science". You say that but you and I, both know what I am doing is way cooler. I also want to thank my *masi*, Monica Rastogi, and sister, Aditi Rastogi, for always listening to me ramble about my work with so much interest. I couldn't have asked for a better audience!

Lastly, I would like to thank two people who aren't here with us anymore but have inspired me in ways that they probably didn't even realize. All I have to say to them is: *naniji* and *babaji*, look, I am gonna be a doctor!

Abbreviations

CTL	Cytotoxic T lymphocyte
TCR	T cell receptor
PTA	Probability of transition analysis
PCKR	Per capita killing rate
MCMV	Murine cytomegalovirus

Contents

Chapter 1

Introduction

1.1 Functions of Immune System

Hundreds of years ago, before Edward Jenner rationalized the immunization process, it was assumed that diseases were punishments from God or curses from witches. But documentation from as early as 430 B.C shows theories that survivors of the Athenian epidemic of typhus and small-pox had acquired a partial immunity to the disease [1]. Our knowledge of the immune system is today much wider, and we have the chance to have a much clearer picture how the body is protected.

The immune system, a collection of a multitude of structures, processes and cells, mounts a response against harmful foreign substances and diseases within the body to ensure that we do not fall sick frequently. The ultimate function of the immune system is to prevent or limit infection, and keep the body under homeostasis by removing dead or malignant cells. New immune tasks have also been uncovered, for instance the regulation of the metabolic state [2], and also the social behavior during sickness [3, 4]. Various psychiatric conditions have been correlated with abnormal immune responses such as anorexia [5], depression [6], and in the case of obsessive-compulsive disorder, a bone marrow transplant has been shown to cure the abnormal behavior in mice [7].

To combat infections effectively, the immune system detects a wide variety of harmful foreign bodies known as pathogens. These pathogens include bacteria and viruses. The immune system must distinguish them from the organism's own healthy cells, and the commensal microbiota from the mucosal surfaces like the skin and the gut. Therefore, the decision to attack or tolerate is a constant dilemma of immune cells.

The layers of defense mounted by the immune system can be divided into three distinct groups (Figure 1.1).

1. **Physical and chemical barriers**: As first line of defense, the surface barriers of the body (mucosa) can restrict the entry of pathogens into the body [9], for instance by the secretion of antibacterial enzymes by the skin [10], or by tears from the eyes that rinse away

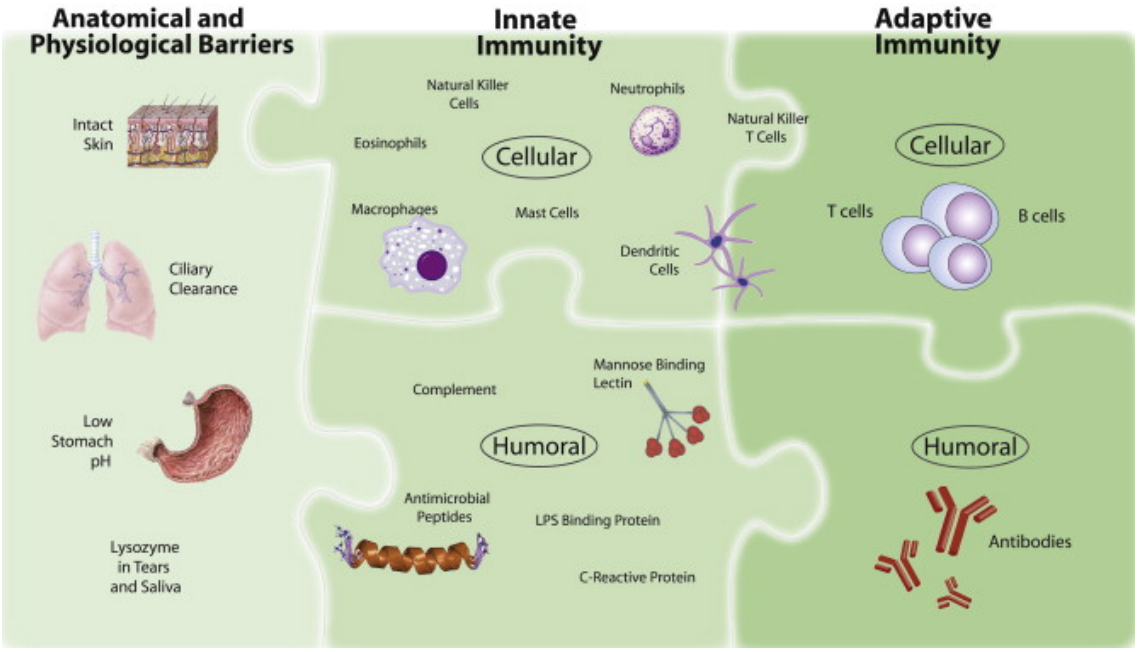

Figure 1.1: The three layers of the immune system are the physical barriers, innate immune system and the acquired immune system. Figure reproduced from [8].

pathogens [11]. Additional types of barriers include mucus and cilia that line the nasal passages [8] and in the gut mucosal.

But even in the presence of these barriers, sometimes pathogens can enter the host body. In that situation the body requires additional lines of defense.

2. **Innate immunity**: The next line of defense of the body is named the innate immune system. It is called innate as it recognizes predefined patterns and is less specific to one pathogen exclusively i.e. it recognizes broad types of pathogens. It is quick and effective against a wide range of pathogens.

   The innate immune system recognizes a type of conserved molecular motifs found in pathogens known as pathogen-associated molecular patterns (PAMP) that are essential for pathogen survival and hence difficult to modify [12, 13]. The immune receptors to those motifs are named pattern recognition receptors (PRRs) [14]. An interaction between PAMPs and PRRs initiates a cascade that leads to release of a variety of proinflammatory molecules which together coordinate the response to infection [15].

   Apart from these cells, innate immunity has a humoral component which is mediated by macromolecules. These include naturally occurring antibodies (NAb), pentraxins and the complement and contact cascades [16–18]. These macromolecules are soluble in the plasma and are well equipped to mount a strong response against pathogens. These ubiquitous innate immune proteins play important roles sensing microbes and initiating pathways to ensure removal of the infection.

Several molecules playing an important role in the innate immune system are highly conserved across plant and animal species implying that it arises from an ancient system that existed prior to the divergence between the plant and animal kingdom [19,20]. The different cells forming part of the innate immune system are macrophages, mast cell, neutrophils, eosinophils, natural killer (NK) cells, dendritic cells, and natural killer T cells [21–27]. These cells are involved in processes such as phagocytosis (ingestion of pathogenic fragments, viruses or bacteria) and eliciting an inflammatory response. Interestingly, the animal kingdom up till invertebrate fish, possess an innate immune system only, showing that innate mechanisms are already powerful enough to sustain the survival of such species against infections [28,29].

3. **Adaptive immunity**: Despite the efficient functioning of the innate immune system, it is complemented by an additional layer of cells and mechanisms known as "adaptive immune system". Especially, in mammals, the innate system is tightly controlled by the adaptive system and vice versa, and a lack of adaptive cells like T cells and B cells leads to strong immunodeficiencies for people carrying specific mutations [30,31].

While the innate immune systems mounts a general response against the pathogens, the adaptive immune system is highly specific. The adaptive immune response is mediated by receptors that arise through a highly regulated process of recombination of a diverse group of gene segments followed by selection. This leads to a clonally diverse repertoire of antigen receptors on lymphocytes that can recognize a wide array of pathogens [32,33]. Historically, the adaptive immune system was classified into two parts- the humoral immune response and the cell mediated immune response. The key players for the humoral immune response were B cells and antibodies while for cell-mediated immune response they are T cells [34–37].

There is now increasing evidence of cells that show properties of innate and adaptive immune system. One such example is NK cells which show properties of innate immune system such as inducing death of tumor cells and virus infected cells in absence of specific immunization. They also show properties of adaptive immune system such as antigen-specific immunologic memory [38,39].

B cells: B cells produce antibodies in response to a breach in the host system. Antibodies are immunoglobulin molecules with an antigen-binding site that facilitates its binding to an antigen in a highly specific manner [41]. B cells arise from the hematopoietic cells that are produced in the fetal liver during pregnancy, and at a later stage in the Bone Marrow (Figure 1.2) [42, 43]. Within these microenvironments, precursor cells undergo proliferation and diversification through a series of differentiation events involving the ordered rearrangement of variable (V), diversity (D), and joining (J) gene segments thus giving rise to a wide range of B cell receptors (BCRs) that can recognize many different types of molecules [44–46]. Immature, naive B cells constantly migrate between secondary lymphoid organs through the

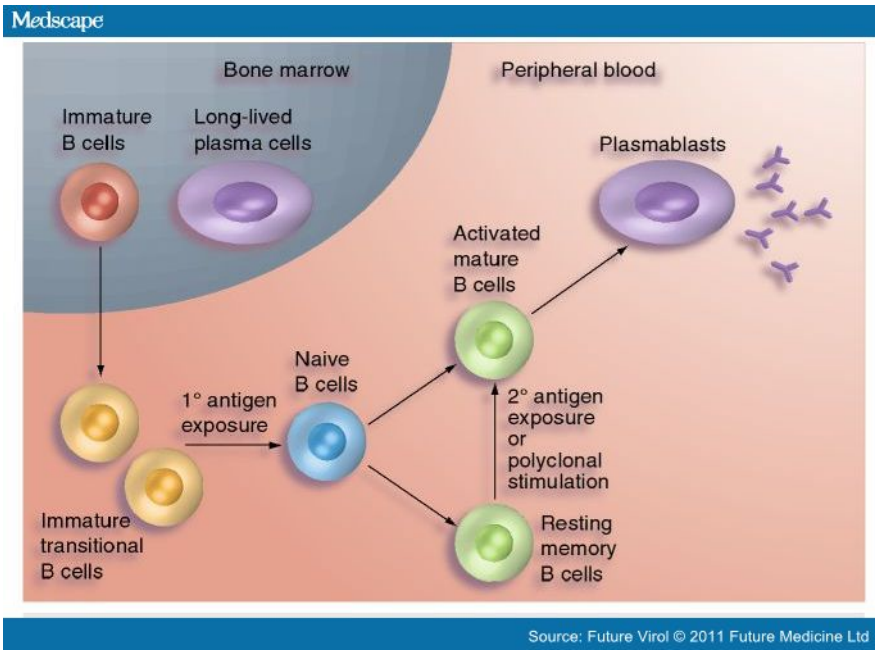

Figure 1.2: Immature B cells are made in the bone marrow after which they are exposed to antigens to give rise to either memory B cells or plasmablasts. Figure reproduced from [40].

blood where they search to meet their cognate antigen supplied by the circulating lymph and get activated [47]. Antigen loaded B cells then interact with antigen-specific helper T cells which give them signals to proliferate [48]. From this pool of B cells, some go on to become extrafollicular antibody-secreting plasma cells while some form germinal centres. Germinal centres serve as a site for B cell affinity maturation which involves repeated exposure of same antigen so that the antibodies produced have a higher affinity for the antigen and somatic mutation which involves diversification of B cell receptors to allow to combat new threats [49].

Throughout their development, B cells are tested for reactivity against autoantigens. These take part in two phases known as the central tolerance, which takes place at the immature B-cell stage [50] and peripheral tolerance which takes place once the B cell has left the primary lymphoid organs [51, 52]. B cells that encounter self-antigen are removed from B-cell repertoire by negative selection [53, 54]. Negative selection has been proposed to take place by three distinct mechanisms: deletion by apoptosis [55, 56], induction of anergy [57, 58], or alteration of the antigen receptor specificity by receptor editing [59, 60]. This is the first checkpoint that the B cells undergo and the site of a B cell's first antigen encounter is a determining factor in the mechanism of negative selection that is used [61].

By producing antibodies in response to the relevant antigens, B cells play an indispensable part in the immune system (Figure 1.2). Antibodies can (i) access all the body parts by diffusion (ii) opsonize small pathogens like viruses, by coating them and forbidding them to interact [62] and (iii) induces a strong recruitment of adaptive immune cells to an antigen so that those cells can eliminate the antigen [63]. In addition to the production of antibodies,

B cells have also been implicated in other functions such as cytokine production [64] and suppression of inflammatory responses [65].

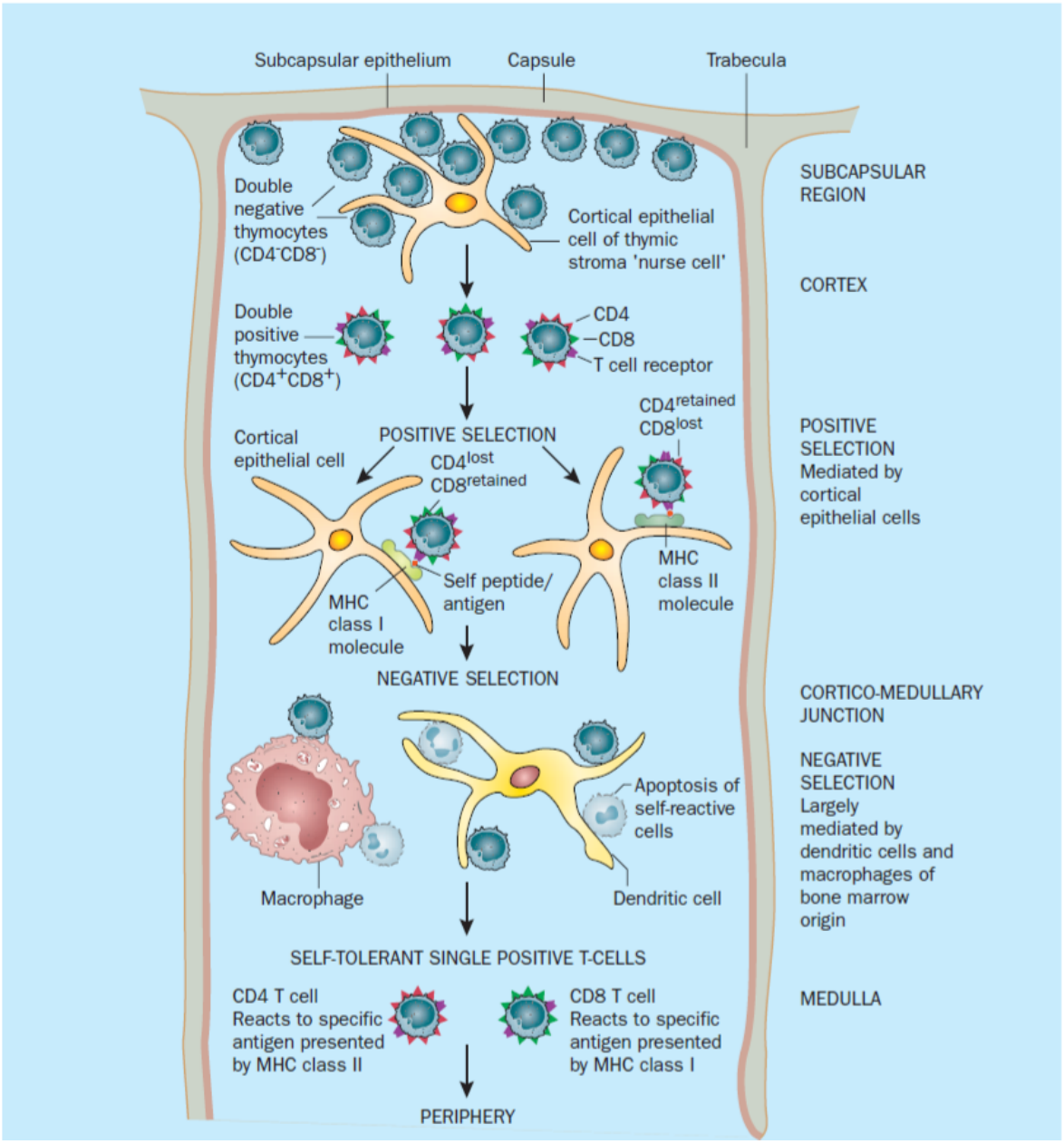

Figure 1.3: T cell development in the thymus: T cell progenitors enter the thymus in the subcapsular region. T cells with T-cell receptor that recognises self MHC are positively selected whereas T cells that react with self-antigens are removed through negative selection. The cells that egress are naive T cells. Figure reproduced from [66].

T cells: T cells play a range of functions in the immune system and originate from hematopoietic stem cells in the bone marrow and eventually migrate to the thymus [67,68]. Here, the T cell progenitors localize to the outer regions of the thymic cortex and through recombination of genomic DNA segments, unique T cell receptors (TCRs) are generated. In the thymus, the T cells undergo selection ensuring both functionality and self-tolerance. The thymus is divided into two parts- the cortex where T cell progenitors inhabit to undergo positive selec-

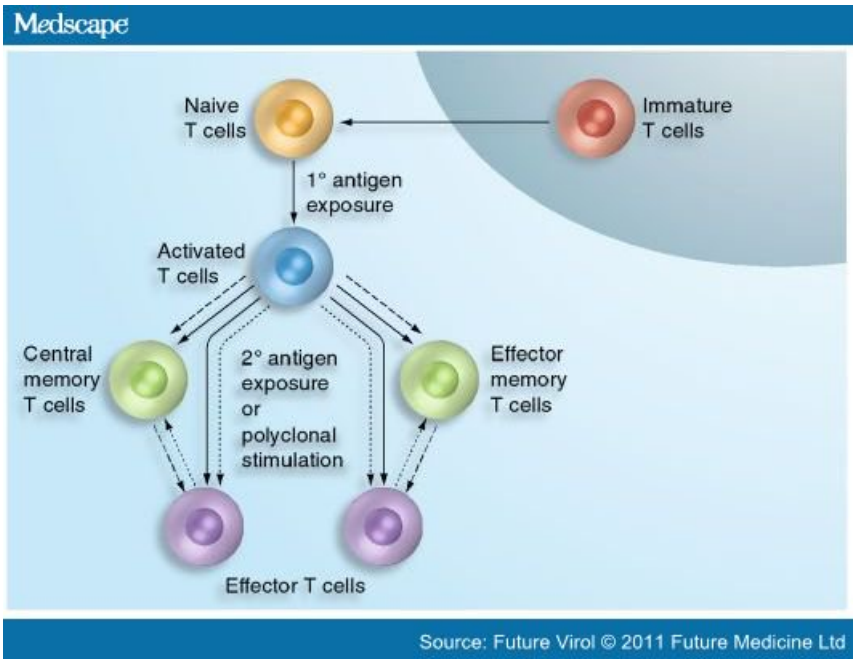

Figure 1.4: T cell differentiation pathway. Figure reproduced from [40].

tion and the medulla, where the T cells undergo negative selection and functional maturation after which they egress the thymus (Figure 1.3) [69]. Positive selection involves interaction of CD4+CD8+double positive (DP) T cells with antigen presenting cells (APCs). Successful recognition of the ligand gives rise to single positive (SP) T cells which are T cells committed to either the CD4+ or CD8+ T cell lineage. Other than lineage commitment, recognition of the ligand provides the signal for cell survival whereas a lack of interaction leads to death by neglect [70]. DP and SP T cells also undergo negative selection where T cells reactive to self-antigens are eliminated from the repertoire [71,72]. After positive and negative selection, T cells egress from the thymus. These T cells are in a naive, resting phase and are activated to protect the body in case of an infection (Figure 1.4) [73].

These T cells need activation to give immune response. T cells can only be activated in the presence of two independent signals to avoid against premature or excessive activation (Figure 1.5) [74,75]. The first signal is antigen specific and is received through the interaction of the TCR with an antigen peptide and MHC complex on the surface of APC. The second signal is antigen independent and involves the interaction of a co-stimulatory molecules on the APC and the T cell surface. One of the most researched co-stimulatory molecules is the CD28 receptor expressed on the T cell which recognizes and interacts with CD80 and CD86 expressed on the APC surface [76–78]. T cell activation is a tightly regulated process and in the absence of either of the signals described above, T cells fail to activate and it leads to T cell anergy [79–81], deletion or the development of immune tolerance. This regulation is part of peripheral tolerance [82, 83]. After infection, the time taken for activation of T

cells is nearly $\sim$ 48hours and this delay allows the innate response to combat the infection before the T cell mediated immune response is initiated [84]. The three main properties of T cell antigen recognition are sensitivity, specificity, and context discrimination [85]. T cell ligands are displayed at a low number which has led to T cells being highly sensitive. This allows them to recognize very few molecules of antigens on a synapse which is an interface between an APC and a T cell [86]. The recognition must be specific to allow for discrimination and identification of the relevant antigenic peptide–MHC complexes among the pool of homologous complexes of the same MHC molecules. Lastly, T cells are able to interpret the context of antigen presentation so as to initiate an effector response to harmful antigens while ignoring harmless or self-antigens.

Once the infection is removed, $\sim$ 95% effector T cells undergo a phase of contraction, where most cells die by apoptosis while a small pool remains as memory T cells and mount a faster response in face of renewed exposure to the relevant antigen [87–89].

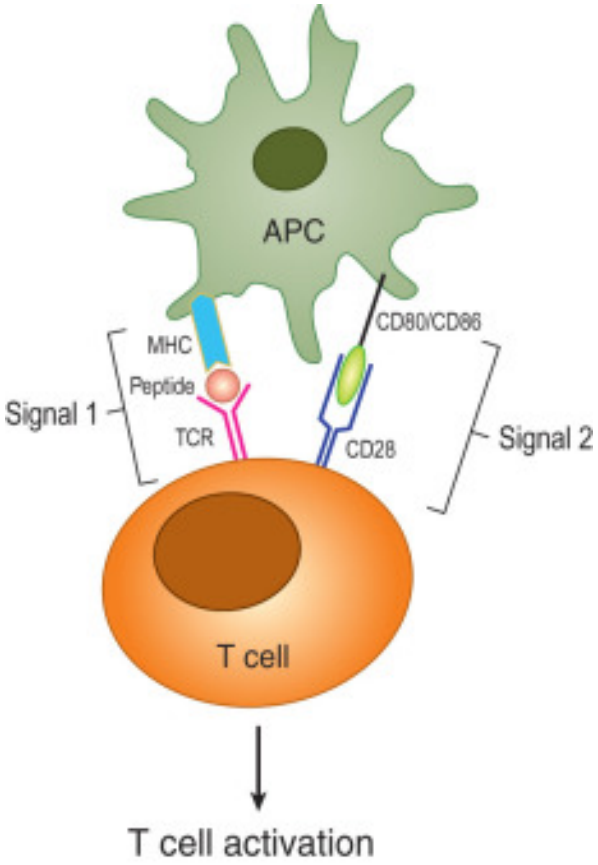

Figure 1.5: T cell activation requires the presence of two signals simultaneously. Figure reproduced from [90].

In response to activation signals, CD4+ T cells differentiate into T helper cells, Th1 Th2, Th9, Th17 and regulatory T cells [91, 92]. These cells differ on the basis of their respective cytokine profiles. On the other hand, CD8+ T cells differentiate into cytotoxic T lymphocytes (CTLs), Tc2, Tc9, Tc17 or CD8+ T regulatory fate [93–95].

My doctoral research topic pertained to T cells. In particular, I worked on two research projects about the activation of T cells and the killing mechanisms employed by CTLs *in vivo*.

1.2 T Cell Activation

Naive T+ cells constantly scan secondary lymphoid organs for the presence of non-self antigen. In response to infections, fragments of the pathogen are presented on APCs and naive T cells can get activated by interacting with APCs (Figure 1.6). T cell activation requires hours of interaction with APCs and the duration of antigen stimulation plays an important role in determining the fate of T cells [96]. Recent studies have also shown that T cells have transient interactions with APCs before forming stable T cell-APC complexes that eventually lead to T cell activation [97]. Thus, during the process of activation, T cells interact with cognate APCs for hours while alternating between forming stable synapses and motile kinapses [98, 99]. The activation of T cells through synapse formation is well studied and the TCR signaling that arises as a consequence of synapse formation has been shown to persist for several hours [100, 101]. Studies have also exhibited that an elevated signal strength as a consequence of a high peptide density or a high TCR ligand affinity leads to synapses rather than kinapses [102, 103].

T cell activation in the lymph node has been shown to take place in three different phases: (i) transient successive contacts during the first activation phase, (ii) stable contacts leading to cytokine production during the second phase, (iii) an enhanced motility and rapid proliferation during the third phase [104].

While interaction between APC and T cells is required for the activation of CD4 and CD8 T cells, the major difference lies in the MHC molecules employed by each type of T cell. The two types of MHCs that play an important role in antigen presentation are MHC class I and class II [105]. CD4 T cells bind with MHC class II molecules whereas CD8 T cells bind with MHC class I molecules.

A stable interaction between a T cell and APC involves the formation of an immunological synapse (IS) [106, 107] (Figure 1.7). The IS facilitates T cell activation also known as "priming" which brings about changes in the migration, cell growth and proliferation, expression of different gene programs that can be effector or memory phenotype, and an increase in the killing capacity of the cells [108]. The IS consists of an assembly of pMHC-TCR, co-stimulatory/inhibitory and adhesion interactions at the contact interface between the T cell and APC [109, 110].

The activation of T cells leads to the clonal expansion of specific effector T cells that will in turn leave the lymphoid organs and enter the bloodstream to move towards the sites of infection. One such example of an effector cell is the CTL which induces cell apoptosis by different mechanisms, including release of cytotoxic granules at the synapse interstitial area (described below).

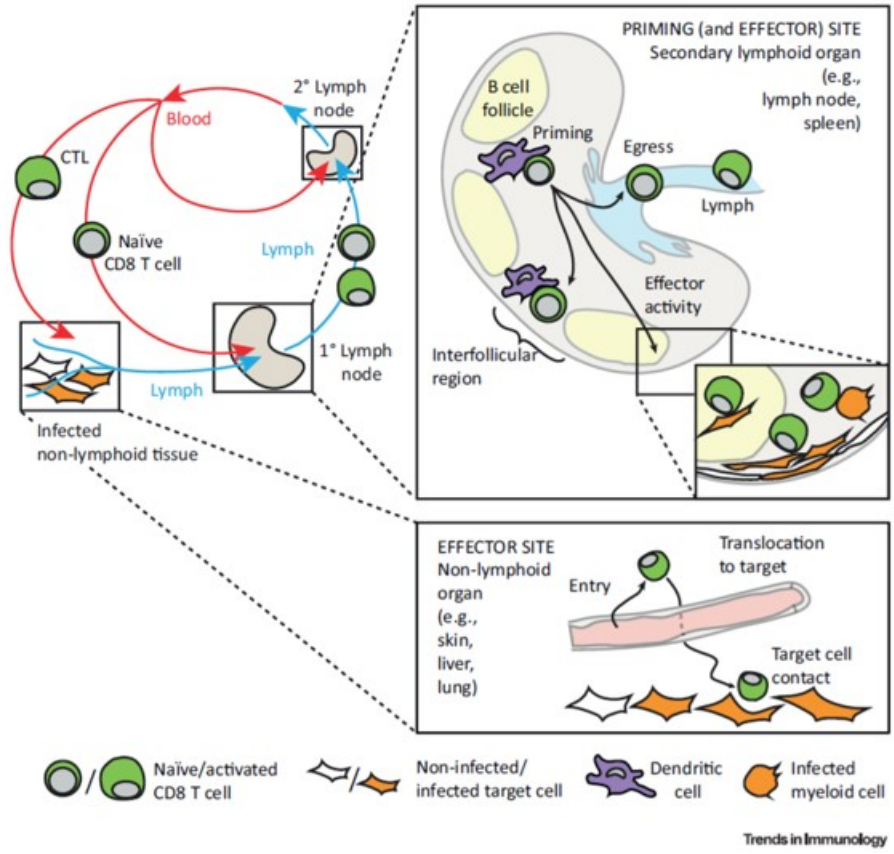

Figure 1.6: Naive CD8 T cells that are circulating through the secondary lymphoid organs can be activated by APCs such as dendritic cell. Once activated, CTLs can either undergo further maturation and act as effector T cells or they can exit into the lymph and migrate to the site of infection and interact with the target cells. Figure reproduced from [111].

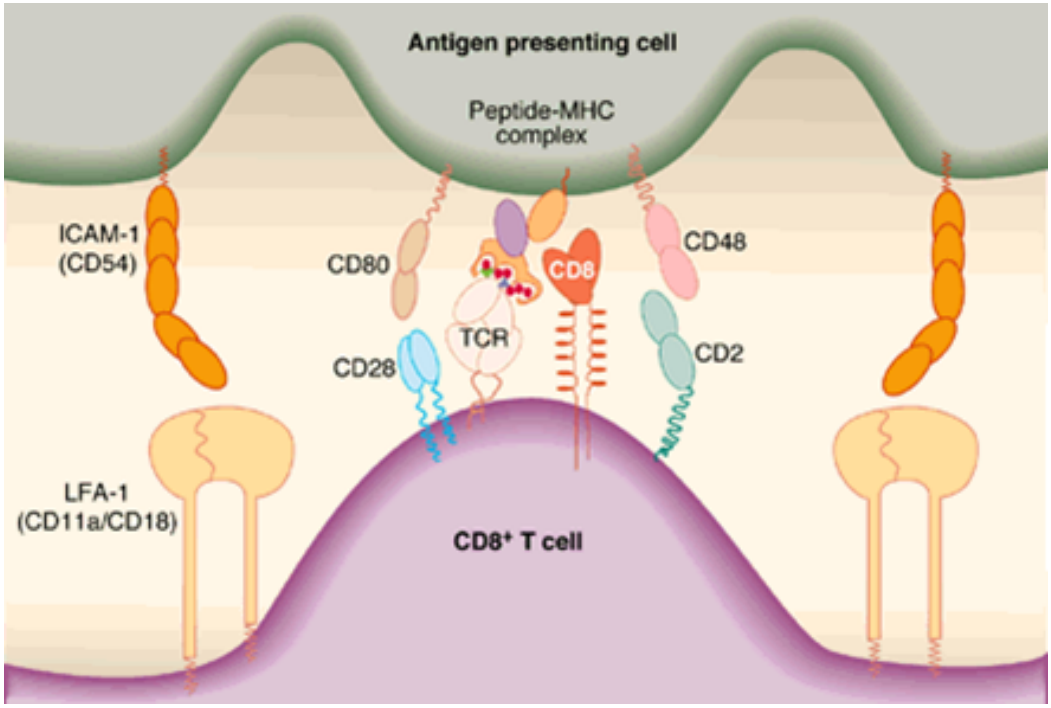

Figure 1.7: An immunological synapse and various molecules associated with it: CD8+ T cells interact with APCs in order to get activated. Figure reproduced from [112].

1.3 Signal Integration During Activation

Earlier studies, implicated synapses in the effector function [113] whereas kinapses were thought to be important for a better exploration of the area in the lymph node [114]. But recently, T cell activation has also been shown to be achieved through kinapses. T cells can engage multiple DCs consecutively and sum the signals obtained from the interactions [115, 116]. This implies that T cells retain some biochemical memory of previous encounters which accumulates until the T cell is activated. Certain *in vitro* studies have also shown that T cells can gather signal from recurring interactions with APCs despite a lapse in time between two consecutive interactions [117, 118].

Additionally, it has been shown that T cells "counted" the number of TCRs which were triggered in the course of interaction with APCs and a response was seen when $\sim$ 8000 TCRs were triggered. In the presence of costimulatory signals, T cells were more sensitive to antigen stimulation and a response was seen at $\sim$ 1500 TCRs [119]. As discussed in Section 1.2, T cells activation takes place in three different phases. It has been shown that T cells do not get activated or proceed to the phase two when the antigen is below a certain threshold [102]. Together, these results suggest that T cells get activated over a series of interaction with APCs and integrate the signals received at each interaction.

1.4 Killing by CTLs

On coming in contact with a target cell, CTLs initiate membrane-membrane contact between the TCR on the T cell and the peptide-MHC complex on the target cell. After a few minutes of initiating contact, the CTL cytoskeleton reorganizes such that the microtubule-organizing center (MTOC) moves toward the synaptic interface (Figure 1.8) [120, 121]. This rearrangment facilitates the transport of lysosomes which contain cytolytic proteins from the CTL to the target cell [122]. This mechanism is indispensable in ensuring the secretion of cytotoxic components such as perforin and granzymes [123]. In addition, an increase in perforin pore formation and target cell killing is seen as a consequence of mechanical force exerted by the killing synapse on the target cell membrane [124, 125].

CTLs kill infected cells by different pathways.

1. **Granzyme mediated pathway**: Granzymes are proteases implicated in the induction of target cell death by CTLs [127]. On being secreted by CTLs, granzymes cleave extracellular and intracellular proteins in the target cell [128]. The main types of granzymes are granzymes A, B, H, K and M [129]. Out of all the granzymes in humans, granzyme B is the most well researched granzyme and is the main force behind the efficient induction of caspase-dependent apoptosis [130, 131].

The original view regarding granzyme mediated cell death involved the function of perforin

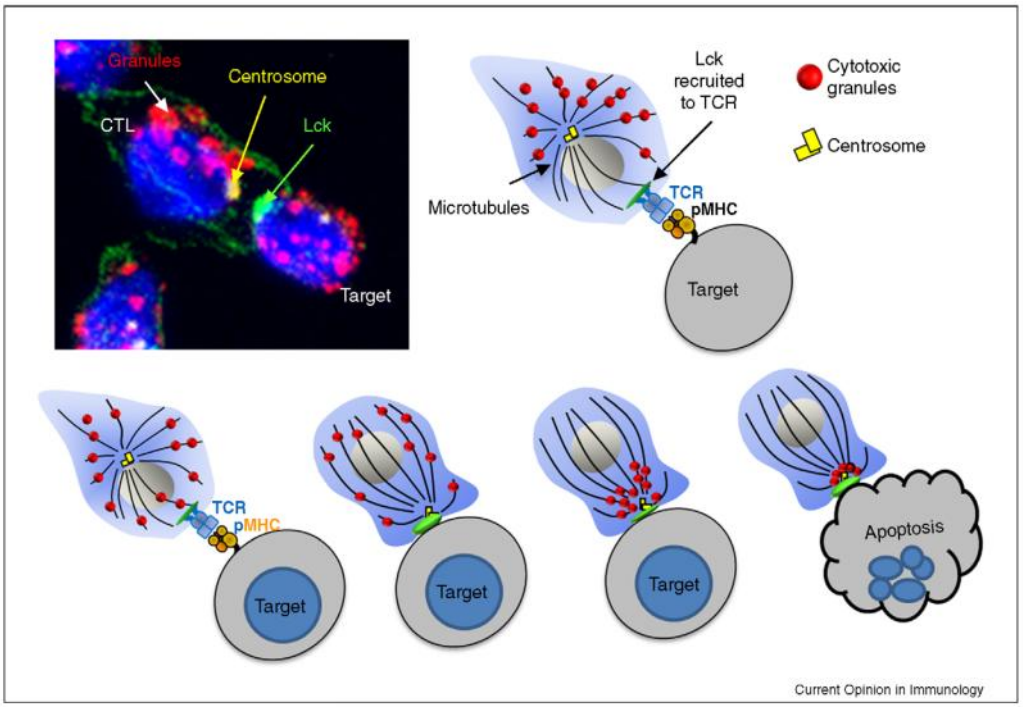

Figure 1.8: On recognizing MHC class I molecule and initiation of contact between TCR and peptide antigen, the centrosome polarizes towards the synapse and attaches to the plasma membrane. The granules then move towards the centrosome and they are ejected into the synaptic cleft leading to apoptosis. Figure reproduced from [126].

polymerization to induce a pore (Figure 1.9a) [132]. Perforin is a protein with multiple domains that is stored in the cytoplasmic granules of the CTL along with a family of serine proteases known as granzymes [133]. After establishing a contact with a target cell, these granules are secreted by the CTLs. Perforin monomers then assemble and insert into the plasma membrane of target cells to give rise to plasma membrane pores by polymerization [134,135]. These perforin channels then facilitate the entry of other granzymes into the target cell which cleave substrates at key aspartic acid residues leading to target cell apoptosis. This is at present the accepted view for functioning of perforin in CTL mediated cytotoxicity however there have also been studies showing that perforins can deliver granzymes to target cells without forming pore in the membrane [136].

The role of perforin is highly debated but in perforin deficient mice, it has been shown that the cytotoxicity of CTLs and NK cells is highly affected [137,138] implying that perforin plays an important role in CTL and NK cell mediated cytotoxicity. The exact role of perforin in killing of target cells came under scrutiny when a receptor for granzyme B was discovered. By means of the receptor, granzymes could be taken up by receptor-mediated endocytosis where perforin releases granzymes stored in endosomes into the target cell (Figure 1.9b). Additionally, granzymes have been shown to bind to target cell surface and enter the target cell through membranes damaged by perforin (Figure 1.9c).

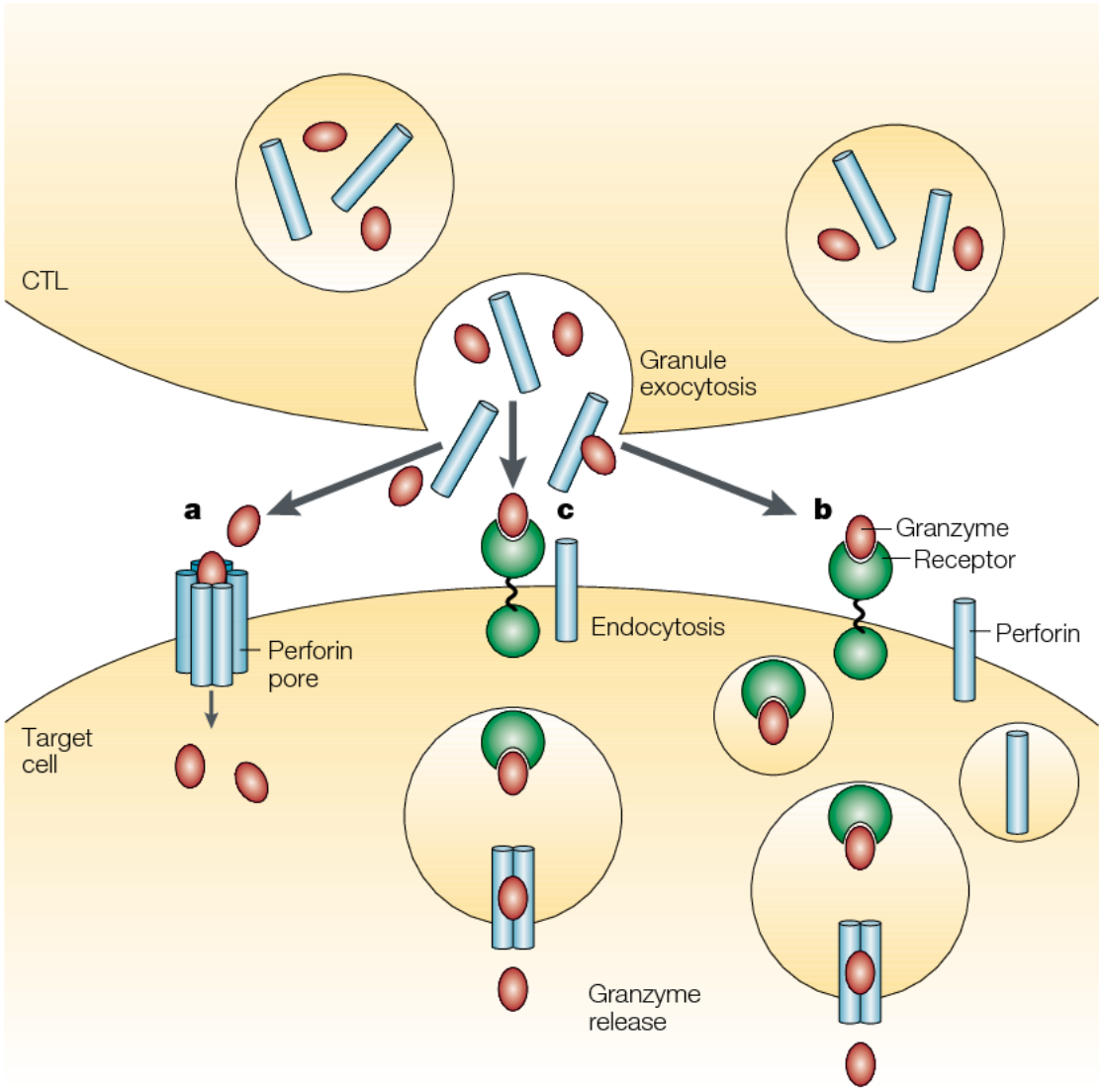

Figure 1.9: Pathways for entry of granymes: (a) Perforin pore dependent granzyme entry into target cell; (b) Uptake of granzymes by perforin mediated cell damage; (c) Receptor mediate endocytosis where perforin acts to release granzymes from the endosomes. Figure reproduced from [139].

2. **FAS mediated killing**: Fas (CD95) is a membrane protein expressed on many different tumor cells and belongs to the tumor necrosis factor (TNF) receptor superfamily. The interaction of Fas ligand (FasL) expressed on CTL membrane with Fas protein on the infected cell induces apoptosis of the target cell by triggering a cascade of caspases [140–142]. The association of Fas and FasL leads to the formation of a death-inducing signaling complex (DISC) which is a multi-protein complex which in turn activates caspase-8, belonging to the family of cysteine proteases [143,144]. This activated caspase-8 sets in motion the downstream apoptotic events [145]. The cascade of caspase activation culminates into the activation of caspase-3 [146]. Activated caspase-3 is partially or completely responsible for the proteolysis of a number of substrates, eventually leading to cell death [147].

   Other than Fas, studies have also shown that FasL can bind to other proteins such as DcR3 which belong to a group of proteins known as decoy receptors that can inhibit apoptosis and serve as regulators of immunity and inflammation [148, 149]. Due to the ubiquity of Fas on tumor and cancer cells, the modulation of FAS pathway has been an area of research that could lead to efficient anticancer therapy [150, 151].

The above two mechanisms are the most significant pathways of CTL mediated killing but it has also been shown to function through other pathways such as tumor necrosis factor (TNF) production [152].

A non-apoptotic pathway of cell death is necroptosis which is a much more rapid form of cell death [153–155]. While apoptotic death is an immunologically silent process, death by necroptosis releases molecules that lead to inflammation which is known as necroinflammation [156, 157].

The effector function of CTLs has been studied most in context to the response to HIV infection [158]. Studies have also shown that HIV in the blood shows a sharp increase followed by a peak and an eventual decline to a set point, where it persists for many years in absence of treatment HIV [159]. Recent studies have shown also that CTL mediated killing might not be a very efficient process and target cells may need multiple contacts with CTLs before they are killed [111, 160].

1.5 CTL Exhaustion

T cell exhaustion, also known as T cell dysfunction is seen in various chronic infections and cancer [161, 162]. It arises as a result of continued stimulation of the TCR in the presence of a large amount of antigen or in case of exposure to antigen for an extended period of time [163].

T cell exhaustion has been shown to take place in phases such that certain properties are lost before others [164–167]. A loss in proliferative capacity, *ex vivo* killing and the production of IL-2 is the first step of T cell exhaustion. Next, T cells lose the ability to produce tumor necrosis factor. Eventually, the T cell is unable to degranulate or produce beta-chemokines. In extreme cases, the

final stage of T cell exhaustion is the removal of virus-specific T cells [161]. In humans, HIV-specific CD8+ T cells have been shown to have a partially or no effector function [168]. Characterization of T cells at different levels of exhaustion shows that the level of expression of the inhibitory receptors such as PD-1, CTLA-4, and Tim-3, correspond to the extremity of exhaustion [169].

Understanding how T cell exhaustion can be reversed or prevented is a dynamic field as it opens up the possibility of identifying ways to combat diseases that are till now incurable [170–172].

1.6 Assays to Study CTL Mediated Killing Dynamics

The importance of T cells in viral infections such as HIV, pneumonia and other diseases such as cancer [173–176] along with their use in immunotherapies [177–181] makes the study of T cell mediated killing an incredibly fascinating field.

The main mechanisms of CTL killing rely on cell to cell contact, and the presentation of antigen by the infected cell. However, the efficiency and dynamics of CTL killing are poorly described. Different methods to monitor and extract quantitative information about CTL killings will be presented in this part.

1.6.1 *In Vitro* Assays

The first assay that gave an insight into the measurement of CTL mediated killing was ^{51}Cr release assay which involved the incubation of CTLs with target cells labeled with radioactive chromium [182]. When they are killed, target cells release the radioactive chromium which is measured and used as a quantification of the number of killed target cells and the duration in which these killings took place. But a study involving mathematical modeling of data obtained from the ^{51}Cr release toxicity assay showed that the release of chromium was not instantaneous and cannot be used as an accurate measure of killed target cells [183,184]. Additionally, a consequence of the experiment being carried out in a liquid suspension leads to a readout that does not reflect the 3D dynamics of CTL looking for target cells among other complexities that arise *in vivo* [185].

The chromium assay showed that target cell lysis proceeds linearly over the observed period of time but due to the cost and hazard of handling radioactive material, it is an expensive procedure. Alternative assays have been developed that do not make use of radioactive material such as a killing assay that makes use of a fluorescent dye called calcein [186]. Calcein enters the target cell cytosol through the plasma membrane and once the target cells are killed, calcein is released into the supernatant leading to a loss in fluorescence. It was shown that the intensity of fluorescence corresponds to the number of target cells with calcein in a linear manner. This information opens up the possibility of calculating the fraction of killed target cells at a particular time. An alternative assay involved loading target cells with calcein and observing the live fluorescent target cells with a cell-imaging multimode reader [187].

Despite providing insights into the fraction of killed target cells, the above assays did not answer questions about killing at an individual cell level. To this end, a single cell method was developed where complexes of CTL and target cells that were bound to each other were isolated and studied through microscopy [188, 189]. While this method gave a peek into the killing at an individual cell level, it lacked information about the complex 3D dynamics that take place in biological systems. To study the 3D dynamics, a collagen-gel assay was used. It consisted of a 3D fibrillar collagen matrix containing CTLs. The interface of the collagen gel and culture dish contained target cells and with this assay, we could monitor data that represented efficiency of CTL migration, conjugation and killing of target cells [190]. The number of surviving target cells in this assay are studied by flow cytometry and the gel can be observed by time-lapse microscopy to study killing dynamics.

1.6.2 *In Vivo* Assays

To study the dynamics of CTL mediated killing in a system that has all the complexities of a real system, *in vivo* assays were developed. Here, two different *in vivo* assays used to study the dynamics of CTL mediated killing are described.

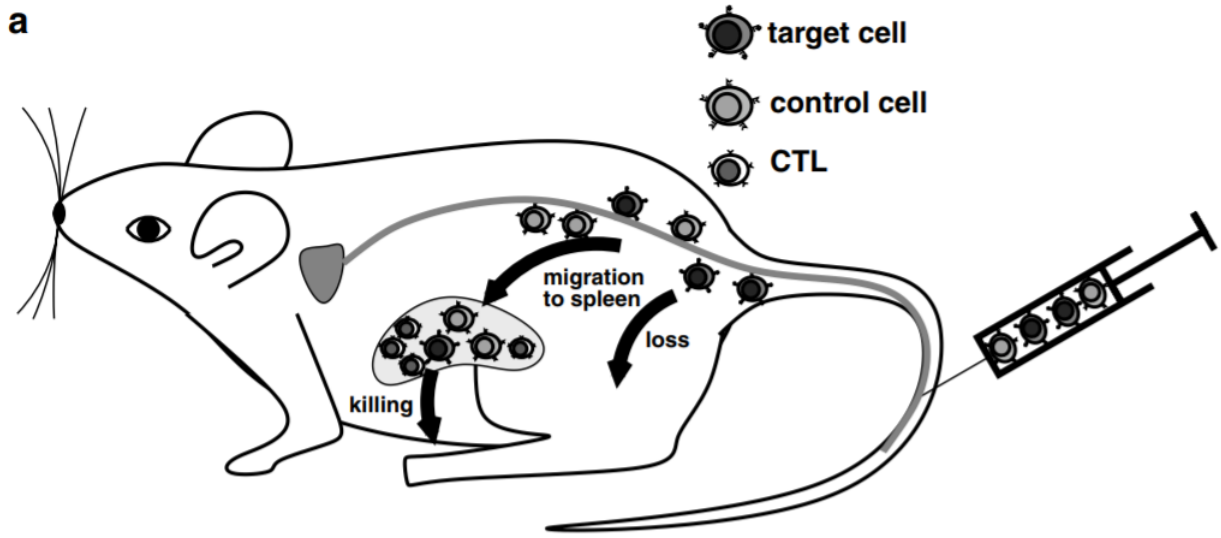

Figure 1.10: In vivo assays involves the injection of peptide-pulsed and unpulsed target cells into model organism. Some target cells are lost while others migrate to the spleen where they are killed by CTLs. Figure reproduced from [184].

1. Adoptive transfer of infected cells. Through the process of adoptive transfer, infected cells are transferred into the model organism (Figure 1.10). A widely used approach involves the transfer of equal peptide-pulsed target cells and unpulsed cells into the organism. Peptide-pulsed target cells are killed by CTLs whereas unpulsed target cells remain unaffected. By observing the ratio of surviving pulsed and unpulsed target cells at various time intervals,

the killing rates can be elucidated [191, 192].

2. Another approach involves labelling infected/target cells with a fluorescent protein, following which the dynamics can be observed using two-photon microscopy [111]. Two-photon miscroscopy is used to obtain three-dimensional imaging *in vivo* and employs two lasers to excite a fluorescent tag of a protein and recording the emitted light to study the behavior of the protein [193, 194]. The second method is an indirect way to observe CTL killing rate and is mostly used for viruses such as HIV and SIV. Some infected cells have been shown to have mutated CTL epitopes which cannot be recognized by CTLs and can thus, escape apoptosis [195]. The rate of increase in the frequency of the mutated epitope bearing cell is used to quantify the killing rate of CTLs and a higher increase in frequency of the cell implies a higher CTL mediated killing rate [196].

1.7 Mathematical Models of Cytotoxic T Lymphocytes

An important step in gaining new insights into a system is creating and studying mathematical models. A model can be used to interpret the observed experimental data, propose and test new hypotheses, and suggest new experimental approaches to further our knowledge of the system. The model recreates the behavior of the system being studied based on the known and observed properties. The benefit of such a model is that it can be used to explore aspects of a system that cannot be explored using only experimental approaches. Additionally, the ease and speed of testing hypotheses, makes an established model a powerful tool.

CTL mediated killing modeling and assays used to observe CTL mediated killing have always been entangled due to the complexity of linking observed killing to cellular decisions. The observed dynamic interplay between CTLs and infected cells raises many questions about the mechanisms and quantification of killing that can be answered by modeling of their behavior.

Modeling of CTL mediated killing follows three major paths: (i) equating CTL mediated killing to an enzyme substrate system, (ii) a differential equation approach and, (iii) creating *in silico* models that recreate the experimental environment and running simulations.

One of the simplest enzyme substrate model of CD8+ T cell mediated target cell killing has been shown to follow the law of mass action where the death rate of individual target cells is proportional to the total number of specific CD8 T cells in the spleen. This has been observed even in cases where the effector to target ratios vary [197]. On the other hand certain studies have shown saturation of death rate with CTL densities [198] or target cell densities [199]. Mathematical models also allow for comparisons between effector and memory CTL function which show that effector CTLs have approximately a double killing rate compared to memory CTLs [200]. In contrast, a model which takes into account the gradual migration of target cells into the spleen showed that effector CTLs do not kill significantly better than memory CTL [201].

In a series of studies consisting of a simulated environment made to resemble a portion of the lymph node by making use of a 2D cellular Potts model, Gadhamsetty et al explored killing regimes. These included monogamous, where one CTL can kill just one infected cell at a time; simultaneous killing, where one CTL can kill multiple infected cells at the same time; joint killing, where multiple CTLs kill a single infected cell; and mixed killing, where multiple CTLs can kill infected cells simultaneously. From this study, it can be seen that the killing rate saturates comparably when increasing the CTL or target cell density [202, 203].

To understand the dynamics of how CTLs interact and kill infected cells in a three-dimensional (3D) tissue *in vivo* Graw et al [198] developed a 3D model to look at CTL mediated killing through the lens of CTL motility where they showed that the killing is linear with respect to the frequency of target cells but saturates with respect to the frequency of CTL. Interestingly, Gadhamsetty et al also showed that the dimensionality of Potts models affects the efficiency of CTL mediated killing of target cells [204]. These models use an empirical probabilistic mechanism but the killing mechanisms at an individual cellular level remained unresolved.

1.8 Quantification of Killing Dynamics

A conceptual understanding of the mechanisms is imperative to understand the working of CTL mediated cytotoxicity. But a crucial step in enhancing our knowledge of the field is not possible without a clear understanding of the numbers associated with the process. Thus, an important aspect of understanding the behavior of a system that includes killing of infected cells is quantitative analysis.

Quantification of CTL mediated killing dynamics is studied by two major ways:

1. **Per capita killing rate (PCKR)**: This method gives the number of killed infected cells per CTL in 24 hours [111].

2. **Half life of target cell**: By using the chemical kinetics approach, this is the time taken for half the target cells to be killed and is computed as $\ln 2/r_{\mathrm{k}}$ where r_{k} is the rate of target cell killing [184].

Recently, Halle et al showed that infected cells need to be contacted by CTLs multiple times to initiate apoptosis [111]. While these quantitative methods provide a way to estimate the efficiency of CTLs, there is no established method to quantify the effect of increasing number of CTL contacts on infected cell death.

1.9 Scope of Doctoral Research

In 2016, Halle et al reported CTL-mediated killing kinetics analysed by 2-photon microscopy *in vivo*. They tracked CTLs interacting with virus-infected cells *in vivo* [111] inside lymph nodes with fluorescent reporter viruses that allow the direct observation of the infected target cell over time. These studies relied on morphological disruption of the target cell as evidence for irreversible target cell death. This study showed that infected cells need multiple contacts with CTLs to get killed.

In my doctoral research, I tackled the following questions:

1. Is there a way to quantify the effect of increasing number of contacts with CTLs on infected cell death probability? What are the properties of this quantification method and can it be used to study the dynamics of other systems? (Chapter 2)

2. Could the need for multiple contacts with CTLs for an infected cell to get killed indicate a mechanism whereby CTLs or infected cells change their properties? Can a modulation in system properties give an agreement with observed datasets? (Chapter 4)

3. Do experimental biologists need to care about the duration of experiments? Does this factor affect the observed results? (Chapter 5)

4. What is the impact of a higher antigen concentration on T cell activation? Do the motion properties of T cells change as a consequence of signal integration during T cell activation? (Chapter 6)

In the upcoming chapters, I have elaborated further on these problems and I have proposed solutions to all of the questions posed above.

Chapter 2

Experimental Setup and Data Analysis

2.1 Experimental Setup

In 2016, Halle et al studied *in vivo* CTL mediated killing of infected cells inside a lymph node by employing a modified MCMV reporter virus [111]. The experimental setup consisted of infecting mice with a modified murine cytomegalovirus (MCMV-Δ3D) which did not affect MHC presentation. The MCMV expressed a fluorescent protein (mCherry) that facilitates observing the system through two-photon microscopy. In addition, the MCMV expressed a specific ovalbumin (OVA) protein. Before infection, T cells specific for OVA, carry another fluorescent protein are adoptively transferred to the mice. The CTLs expressed a green fluorescent protein whereas the infected cells expressed a red fluorescent protein. The CTLs specifically recognized infected cells and killed them. The micro-anatomical regions containing virus infected cells inside lymph nodes were observed. In these experiments, just a small top portion of the tissue is observed where CTLs are recruited to kill infected cells. By making use of two-photon microscopy, the killing of infected cells mediated by CTL is recorded and studied. The observations include movement of T cells, the number of contacts between the infected cells and CTLs, the duration of these contacts, the number of contacts after which an infected cell dies and disappears.

In vivo imaging of CTL mediated killing activity revealed that infected cells need multiple contacts with CTLs in order to get killed. It is not known whether CTLs become more lethal with increasing contacts with infected cells or if infected cells become more susceptible to cell death with increasing number of contacts with CTLs. The need for multiple contacts with CTLs for infected cell death raised a question about how increasing number of contacts with CTLs affect cell death. To this end, a mathematical analysis was used in Halle et al. [111] to calculate the ratio of killed target cells at each contact to total cells at each contact. Here, I analyzed the used

mathematical analysis and show its dependence on time of measurement. In its place, I proposed a new probability of transition analysis (PTA) that gives the observed probability of killing infected cells at each contact.

2.2 Infected Cell Fates

In the experimental system described in [111], a single alive infected cell with 0 or more contacts with CTLs can either get a next contact with a CTL or it may not. At the end of this particular contact, the infected cell can then either die or stay alive. In order to understand a general system with these characteristics, I studied the behaviour of k_{i}, p_{i}, A_{i} and D_{i} (Table 2.1).

Symbol	Meaning
k_{i}	Fraction of infected cells with exactly $(i-1)$ contacts that get the i^{th} contact
p_{i}	Probability of cell death after getting the i^{th} contact with a CTL
A_{i}	Number of infected cells that are alive at exactly i contacts
D_{i}	Number of infected cells that are dead at exactly i contacts

Table 2.1: Format of data output of infected cells killed by CTLs

A decision tree of the system under study can be represented as shown in (Figure 2.1). The infected cells shows a cyclical behavior involving contact with CTL followed by cell death decision and for each infected cell, this cycle is observed until the infected cell dies or the experiment is over (Figure 2.2a). Thus, the number of contacts with CTLs that an infected cell gets is a function of time. An experiment with a longer duration would imply that more infected cells get higher number of contacts with CTLs. At time t_0, all infected cells have had no contacts and infected cells in the system continue getting contacts with CTLs until they die and are removed from the system. From the flowchart, we can also infer that each infected cell behaves independently and the number of contacts that it gets does not depend on the behavior of other infected cells. Thus, at the end of the observation window, the pool of infected cells remaining in the system have had different number of contacts with CTLs and the infected cells that died also did so after getting different number of contacts (Figure 2.2b).

2.3 Analysing *in vivo* CTL Killing Activity

To study the CTL killing activity, the number of CTL contacts received by a target cell to get killed were monitored. The data is organized in a table as shown in Table 2.2. The number of interactions are with respect to the infected cells and represent the times a CTL came in contact with a particular infected cell during the time-window of observation. The cells are tabulated based on whether they died during the observation window or if they remained alive at the end of

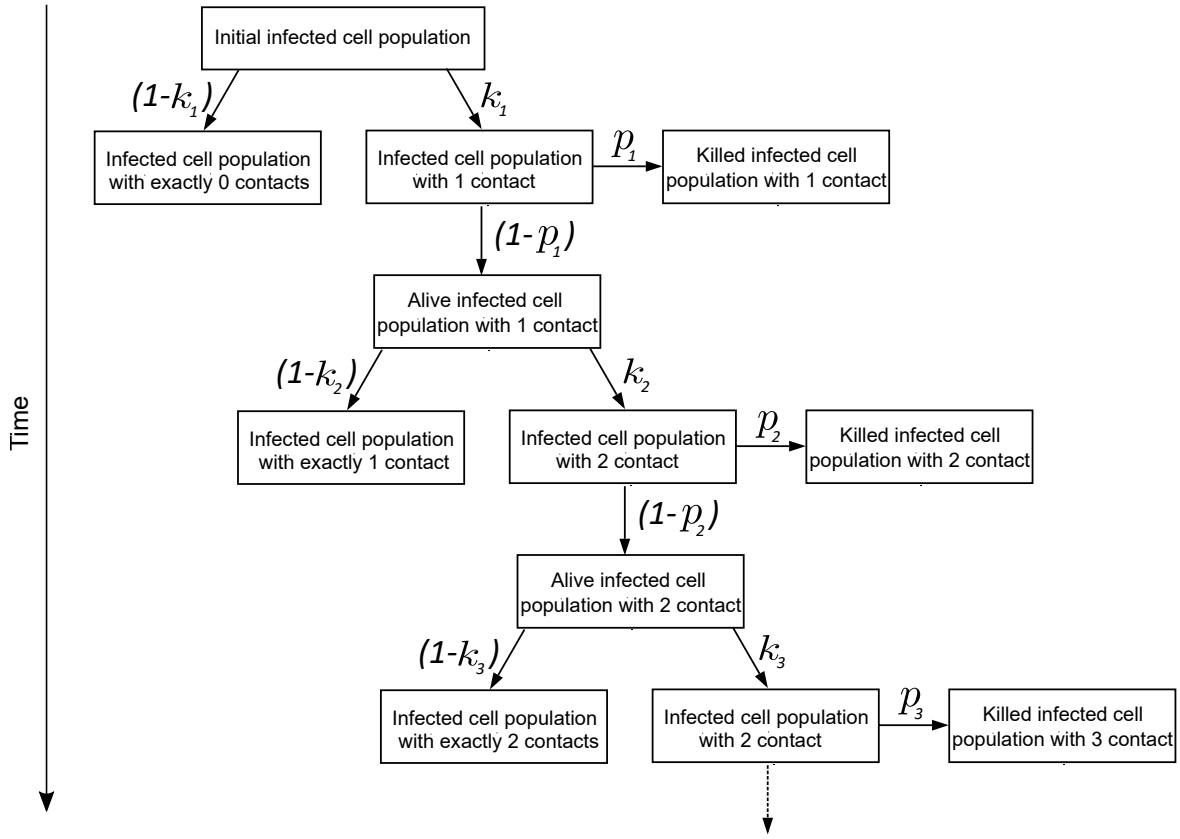

Figure 2.1: Decision tree for infected cell behavior.

the observation.

No. of interactions (i)	Dead infected cells at exactly i contacts	Alive infected cells at exactly i contacts
1	D_1	A_1
2	D_2	A_2
3	D_3	A_3
:	:	:
m	D_m	A_m

Table 2.2: Format of data output of infected cells killed by CTLs

To study the effect of increasing number of interactions with CTLs on target cell death, the ratio of killed target cells at each contact to total cells at each contact was calculated in [111]. For each value of i, the number of dead infected cells is normalized against the total number of infected cells, dead and alive, with i interactions with CTLs.

$$R_{\mathrm{dead,\,i}} = \frac{D_\mathrm{i}}{A_\mathrm{i} + D_\mathrm{i}} \tag{2.1}$$

In the study [111], it was shown that the value of $R_{\mathrm{dead,\,i}}$ increased with increasing values of i. But the significance of this ratio remains unexplored. In order to understand the physical

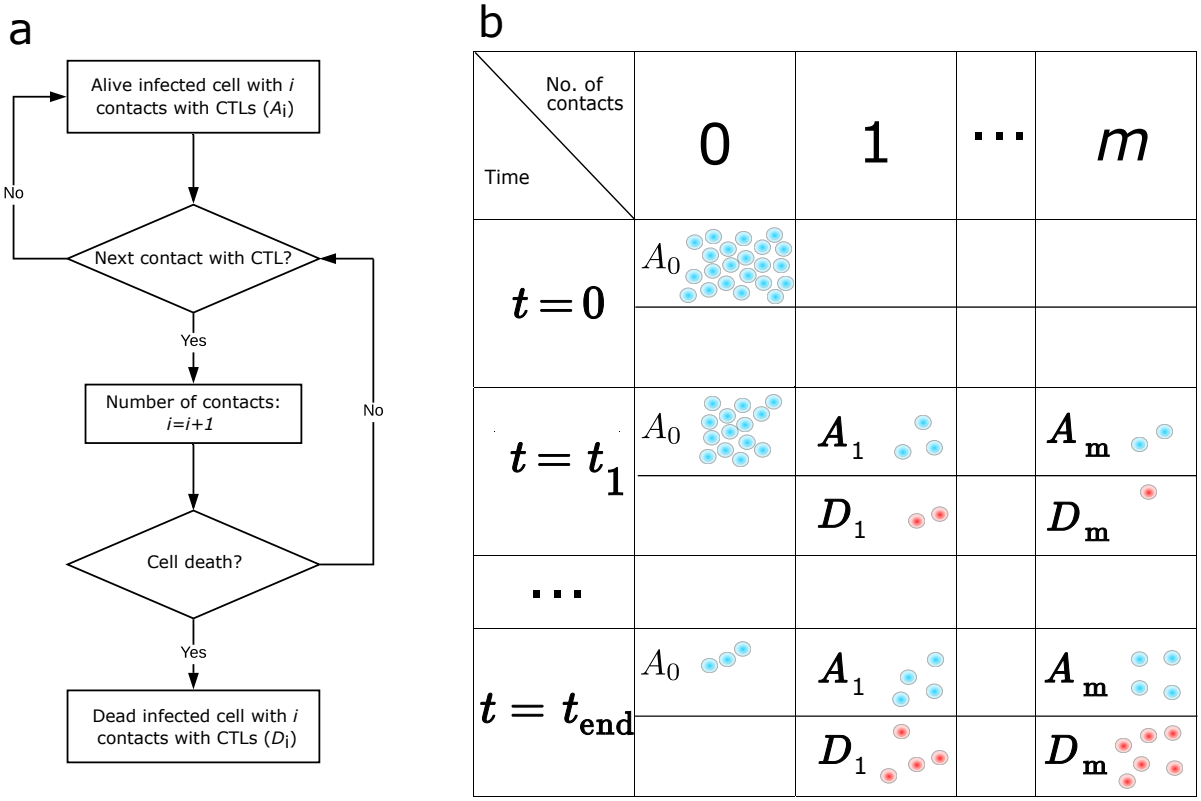

Figure 2.2: (a) Flowchart for infected cell fate, (b) The number of dead and alive infected cells have a variable number of CTL contacts throughout the observation time.

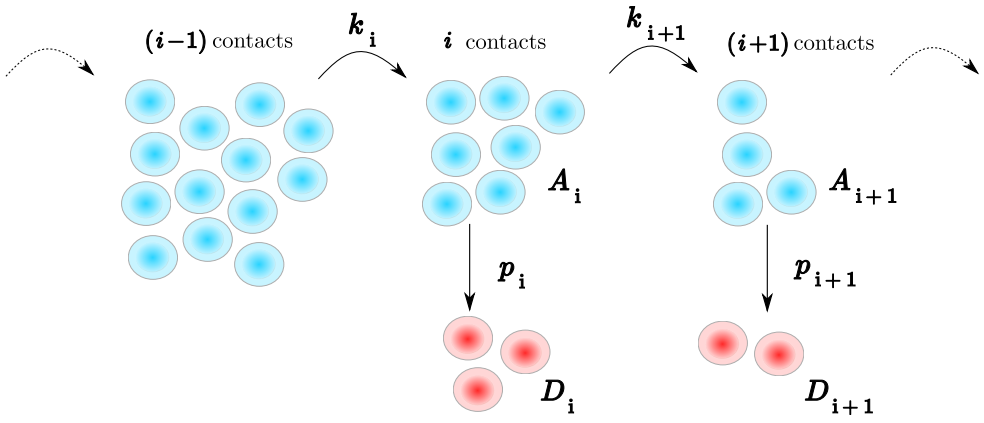

Figure 2.3: Basic properties of the experimental system: The fraction of cells with $(i-1)$ contacts that get the i^{th} contact is k_i and the probability of infected cell death at the i^{th} contact is p_i.

significance of this ratio, I derived a general expression for the values of A_{i} and D_{i} in a system of N infected cells (Figure 2.4a). Each target cell can get contacts with CTLs and each interaction has an associated probability of killing the target cell. The fraction of infected cells with exactly $(i-1)$ contacts that get the i^{th} contact is given by k_{i} (Figure 2.3). The value of k_{i} is a function of time, the density of infected cells, the density of CTLs and velocity of CTLs. At each interaction, an infected cell can either die or survive. In this system, the fraction of cells that die after getting the i^{th} contact is given by p_{i}. The behavior of p_{i} is unknown and could be constant or could be a function of time and/or previous contacts. The values of p_{i} for all values of i collectively also describe how the fraction of killed infected cells changes at increasing number of contacts with CTLs. The surviving cells at each interaction can either get more interactions with CTLs or remain alive at the same number of interactions. Using these constraints, I calculated the values for D_{i} (infected cells that are dead at exactly i contacts) and A_{i} (infected cells that are alive at exactly i contacts). It is important to note that any infected cell that has had $\geq i$ interactions has at least had i interactions with CTLs. Thus, I also calculated another set of cells given by $C_{\mathrm{min,i}}$ which are infected cells that have had at least i interactions. The value of $C_{\mathrm{min,\,i}}$ is given as:

$$C_{\mathrm{min,i}} = \sum_{x=i}^{m} (A_{\mathrm{x}} + D_{\mathrm{x}}) \tag{2.2}$$

where m is the maximum number of contacts that any infected cell has had.

Using these constraints, we calculated the values for D_{i}, A_{i} and $C_{\mathrm{min,\,i}}$ (Figure 2.4). Out of N infected cells, Nk_1 cells get the first contact with a CTL as calculated from the definitions discussed above (Figure 2.4b). Nk_1 are all infected cells that have at least 1 contact with a CTL and is the expression for $C_{\mathrm{min,\,1}}$. Out of these Nk_1 cells, Nk_1p_1 are killed and $Nk_1(1-p_1)$ survive (Figure 2.4c). Continuing this cycle further gives us the values of $C_{\mathrm{min,\,2}}$, A_2 and D_2 (Figure 2.4d-f). From this, we can see how a general population of N infected cells is partitioned into A_{i}, D_{i} and $C_{\mathrm{min,\,i}}$ (Figure 2.5).

The values derived in (Fig. 2.4) are tabulated in Table 2.3. By making use of these general expressions, we aim to derive a method of analysis that gives the probability of infected cell death with increasing number of contacts with CTLs.

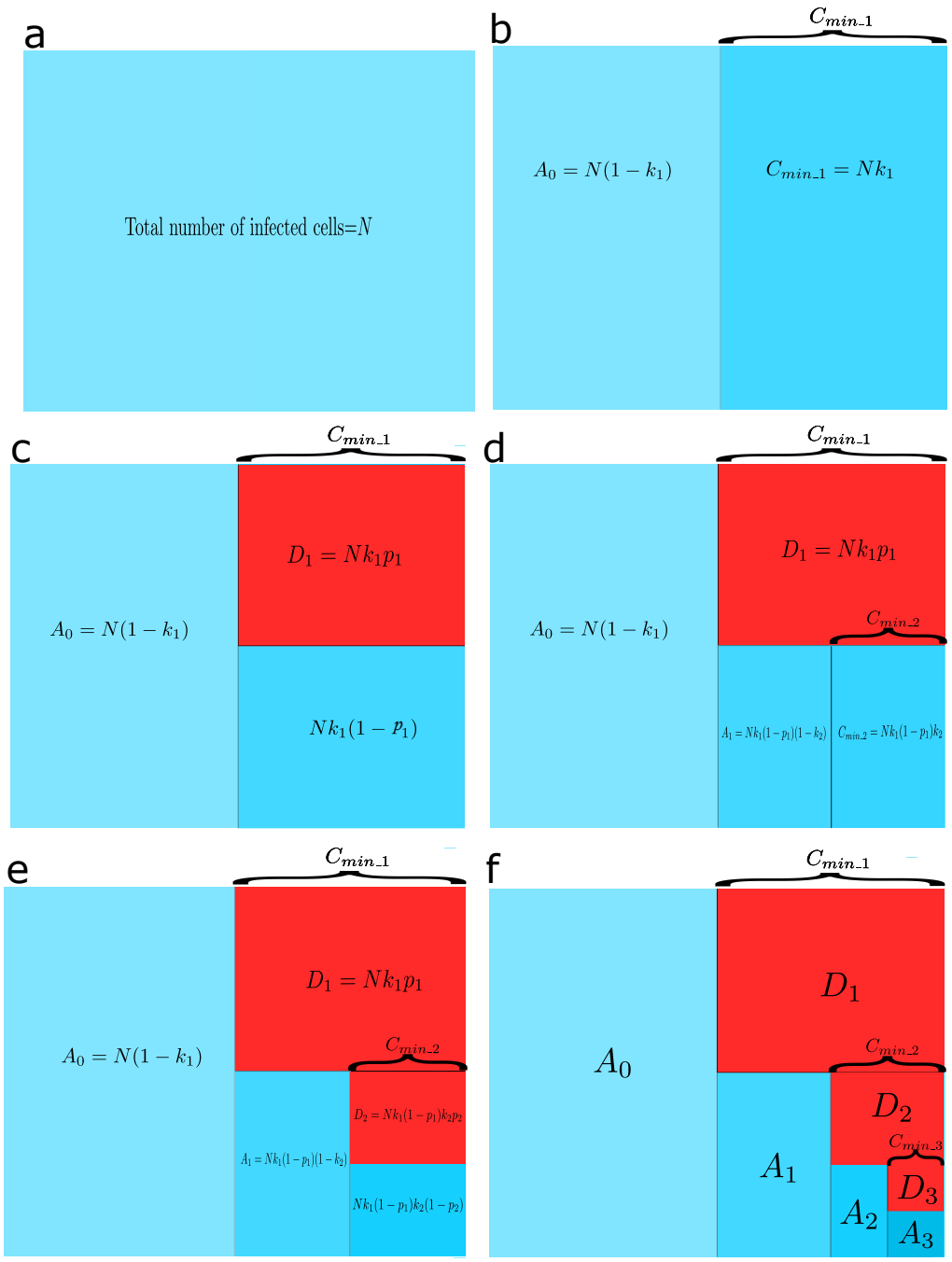

Figure 2.4: A visual representation of the distribution of infected cell states at the end of the experiment. For a population of N infected cells, I computed the value of A_{i}, D_{i} and $C_{\mathrm{min,\,i}}$ (Table 2.1): (a) The system consists of N cells, (b) Out of the N cells, a fraction of k_1 gets the first contact, (c) Of all cells that get the first contact, a fraction of p_1 cells die, (d) Out of the infected cells alive at the first contact, a fraction of k_1 get the first contact, (e) A fraction p_2 cells are killed out of all infected cells that get the second contact, (f) A general distribution of a system with the no infected cell with more than 3 contacts.

Contacts	$C_{\mathrm{min,\,i}}$	A_{i}	D_{i}
0	N	$N(1-k_1)$	0
1	Nk_1	$Nk_1(1-p_1)(1-k_2)$	Nk_1p_1
2	$Nk_1k_2(1-p_1)$	$Nk_1k_2(1-p_1)(1-p_2)(1-k_3)$	$Nk_1k_2(1-p_1)p_2$
:	:	:	:
m	$N(\prod_{j=1}^{m} k_{\mathrm{j}})[\prod_{j=1}^{m-1}(1-p_{\mathrm{j}})]$	$N(1-k_{\mathrm{m+1}})\prod_{j=1}^{m}[k_{\mathrm{j}}(1-p_{\mathrm{j}})]$	$Np_{\mathrm{m}}(\prod_{j=1}^{m} k_{\mathrm{j}})[\prod_{j=1}^{m-1}(1-p_{\mathrm{j}})]$

Table 2.3: Expression for A_{i} and D_{i} derived using the general rules of system

Contacts	A_{i}	D_{i}	$C_{\mathrm{min,\,i}}$	$\frac{D_{\mathrm{i}}}{C_{\mathrm{min,\,i}}}$
0	$N(1-k_1)$	0	N	0
1	$Nk_1(1-p_1)(1-k_2)$	Nk_1p_1	Nk_1	p_1
2	$Nk_1k_2(1-p_1)(1-p_2)(1-k_3)$	$Nk_1k_2(1-p_1)p_2$	$Nk_1k_2(1-p_1)$	p_2
:	:	:	:	:
m	$N(1-k_{\mathrm{m+1}})\prod_{j=1}^{m}[k_{\mathrm{j}}(1-p_{\mathrm{j}})]$	$Np_{\mathrm{m}}(\prod_{j=1}^{m}k_{\mathrm{j}})[\prod_{j=1}^{m-1}(1-p_{\mathrm{j}})]$	$N(\prod_{j=1}^{m}k_{\mathrm{j}})[\prod_{j=1}^{m-1}(1-p_{\mathrm{j}})]$	p_{m}

2.4 Ratio of Killed Target Cells at Each Contact to Total Cells at Each Contact

The values of A_{i}, D_{i} and $C_{\mathrm{min,\,i}}$ are dependent on p_{i} and k_{i}. As discussed above, the value of k_i is further dependent on a host of other system properties. This makes it difficult to conclude anything about the system dynamics by just observing these values.

The observations about the impact of time on the number of contacts that a target cell gets with CTLs raise the question if the quantitative analysis described in [111] is independent of time and if it accurately represents the change in infected cell death properties with increasing number of contacts with CTLs. In order to check this, I computed a general expression for $R_{\mathrm{dead,i}}$ as described in equation (2.1) for the system, using the values obtained in Table 2.3.

$$R_{\mathrm{dead,i}} = \frac{p_{\mathrm{i}}}{1 + k_{\mathrm{i+1}}(p_{\mathrm{i}} - 1)} \tag{2.3}$$

While the value computed for $R_{\mathrm{dead,i}}$ is dependent on the value of p_{i}, it is also dependent on the value $k_{\mathrm{i+1}}$. As discussed in Section 2.3, the value of k_{i} is a function of time, density of infected cells and CTLs and velocity of CTLs. Thus, the value of k_{i} is dependent on time as the fraction of cells that get more number of contacts will increase with time.

The simplified expression also shows that the ratio of killed target cells at each contact to total cells at each contact calculated in this way does not accurately represent the effect of increasing contacts on infected cell death. The fraction of dead infected cells at the i^{th} contact is given by p_{i} at different interactions. As seen in equation (2.3), the value of $R_{\mathrm{dead,i}}$ at each contact is a function of p_{i} and $k_{\mathrm{i+1}}$. An observed change in the value of $R_{\mathrm{dead,i}}$ could be an effect of change in p_{i} or $k_{\mathrm{i+1}}$ whereas the effect of increasing contacts on infected cell death is only represented by p_{i}. Thus, this value does not provide a quantification of only the intrinsic killing properties. This suggests that a new method to analyse the data is needed where the calculated values at an interaction i

Contacts	$p_{\mathrm{obs,\,i}} = D_{\mathrm{i}}/C_{\mathrm{min,\,i}}$
0	0
1	p_1
2	p_2
:	:
m	p_{m}

Table 2.4: Proposing a new analysis method ($p_{\mathrm{obs,\,i}}$) to study the killing probability of CTLs.

are functions of only p_{i}.

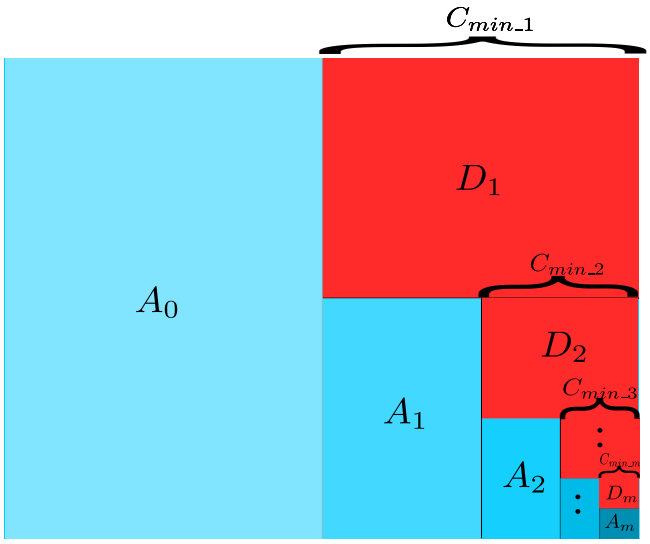

Figure 2.5: A general distribution of a system with the m being the maximum number of contacts that any infected cell has.

2.5 Requirements from New Analysis

For the system described above with N cells, the values that can be observed are A_{i} and D_{i} for different values of i. The value of $C_{\mathrm{min,\,i}}$ can be computed from values of A_{i} and D_{i} (equation (2.2)) but the values of k_{i} and p_{i} cannot be observed. As discussed, the probability of an infected cell getting killed at each contact is given by p_{i}. To understand the dynamics of the system, I would need to compute a way to calculate the observed probability of killing at each contact ($p_{\mathrm{obs,\,i}}$) that is only dependent on the value of p_{i}. By doing this, I can be sure that any change in the value of $p_{\mathrm{obs,\,i}}$ is a consequence of the change in killing properties of the system. The dependence of $R_{\mathrm{dead,\,i}}$ on $k_{\mathrm{i+1}}$ rules it out as a potential analysis method.

2.6 Probability of Transition Analysis

The analysis of the ratio of killed target cells at each contact to total cells at each contact is dependent on time and does not give a value for the rate of killing with number of interactions as shown above. Hence, I proposed a new probability of transition analysis (PTA) to analyse the experimental data that would accurately represent the killing properties of the system by making use of the general expressions shown in Table 2.3. The analysis calculates the probability at each contact for an infected cell to transition from alive to dead.

The analysis I proposed to understand the system is calculating the probability of infected cell death with increasing CTL contacts. The probability of dead cells at exactly the i^{th} interaction is given by normalizing the number of dead infected cells with exactly i interactions by the number of infected cells that have survived the i^{th} interaction. The number of infected cells that have survived the i^{th} interaction consist of all infected cells that have had i or more interaction ($C_{\text{min, i}}$). From Table 2.3, it can also be seen that the ratio of D_{i} to $C_{\text{min, i}}$ for each contact is p_{i} (Table 2.4). Thus, I propose that a more reliable measure to represent the killing dynamics is by calculating $p_{\text{obs,i}}$ which is the calculated probability of death at each contact and is given by:

$$p_{\text{obs,i}} = \frac{D_{\text{i}}}{C_{\text{min,i}}} \tag{2.4}$$

For experimental data that is obtained in the form of Table 2.2, this formula is given by:

$$p_{\text{obs,i}} = \frac{D_{\text{i}}}{\sum_{k=i}^{m}(A_{\text{k}} + D_{\text{k}})} \tag{2.5}$$

2.7 Understanding PTA

In the previous section, I have proposed PTA as an alternative to the analysis done in equation (2.1) [111]. It is extremely crucial to note that the value of $p_{\text{obs,i}}$ equals p_{i}. Thus, if the value of p_{i} is a function of other properties of the system, the PTA will reflect that.

As an example, in a given system the value of p_{i} for a given value of i increases with time and the system evolves such that CTLs become more lethal with time. For such a system, the property of CTLs changes accordingly. To carry out the PTA, if the values of A_{i} and D_{i} for the same duration of observation window are measured but at different time points, the $p_{\text{obs,i}}$ obtained will vary accordingly. Only for a system where the values of p_{i} for all values of i are constant, the PTA will give same values at all time points.

In concise terms, if the value of dp_{i}/dt is non-zero, the values of $p_{\text{obs, i}}$ calculated by applying PTA will vary at different time points.

2.8 CTL Data Analysis

Having established that the proposed method of analysis reflects the value of p_{i}, I applied the method to experimental data obtained by Halle et. al in [111]. The data given in Table 2.5 is used to make the plots.

No. of Contacts (i)	D_{i}	A_{i}	$C_{\mathrm{min,\,i}}$	$p_{\mathrm{obs,i}}$
0	0	96	191	0
1	9	26	95	0.095
2	4	12	60	0.067
3	10	1	44	0.227
4	8	0	33	0.242
5	9	1	25	0.36
6	8	0	15	0.533
7	4	0	7	0.571
>7	3	0	3	1

Table 2.5: Format of data output of infected cells killed by CTLs

As observed from Figure 2.6, using the method of analysis in equation 2.1 gave rise to an increase in the ratio of killed target cells at each contact to total cells at each contact. The increase in this ratio did not follow an identifiable pattern. But since the analysis was not solely dependent on the p_{i} values, I cannot comment further on the reason behind the increase. On the other hand, using the method of analysis described in equation (2.5), I can conclude that the value of observed probability of killing infected cells increases linearly.

The observed linear increase in probability of killing infected cells makes it easier to propose mechanisms that might be employed in the system to kill infected cells. A potential mechanism that gives rise to this linear increase could be a increase in infected cell susceptibility directly proportional to the prior number of contacts with CTLs.

2.9 Applications of PTA

With the plot in Figure 2.6, I have shown that the PTA gives results that represent the killing dynamics of the system. The efficiency of the analysis made me question if it can be used to study the transition in other systems. To this end, I investigated the versatility of the PTA and if it can be used to understand the dynamics of other systems.

The general description of the experimental system in [111] can be justified as a species (S) undergoing irreversible transition or change to give rise to C as a consequence of a recurring event (E) that the species experiences (Figure 2.7). In this case, the species undergoing the irreversible transition are the infected cells, the irreversible transition is cell death and the recurring event is

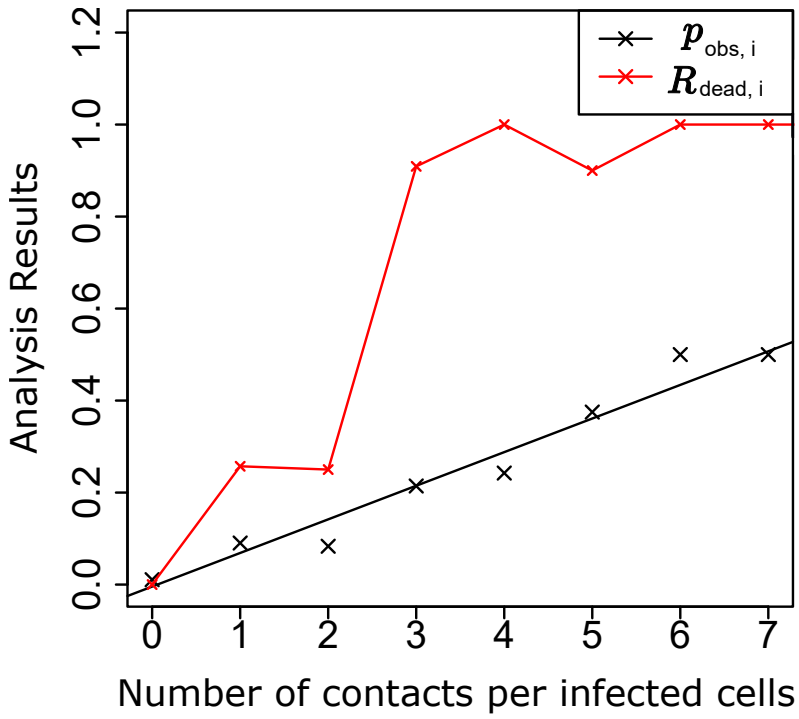

Figure 2.6: Comparing the ratio of killed target cells at each contact to total cells at each contact ($R_{\mathrm{dead,i}}$) to the plot obtained using PTA ($p_{\mathrm{obs,i}}$)

.

contact with CTLs.

Here, I propose that for any system that fulfills the criteria defined in Figure 2.7, the PTA can be used to study the dynamics of the system. This could include systems where cells are killed as a consequence of contacts with killer cells such as the one described above. An example of another system whose dynamics could be studied using the PTA is the activation of T cells as a consequence of contacts with antigen presenting cells (APCs).

A general equation of PTA is given by:

$$p_{\mathrm{calc,\,i}} = \frac{C_{\mathrm{i}}}{\sum_{k=i}^{m}(S_{\mathrm{k}} + C_{\mathrm{k}})} \tag{2.6}$$

where C_{i} is the number of elements that transitioned at exactly i recurring events and S_{i} is the number of number of elements that did not transition at exactly i recurring events.

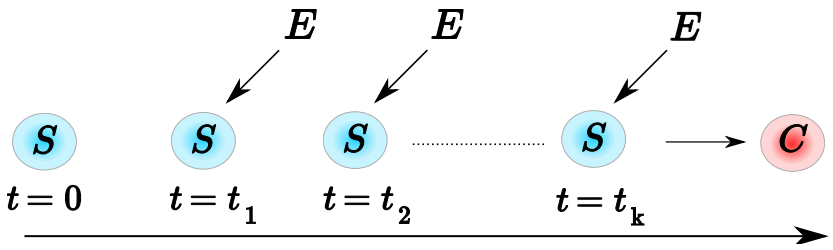

Figure 2.7: A general framework of a system on which PTA can be applied consists of a species (S) undergoing an irreversible transition to C due to a recurring event E.

2.10 Summary

In this chapter, I studied the properties of the experimental system described in [111]. This led me to the conclusion that the number of contacts that an infected cell has with CTLs is a function of time. Next, I studied the existing analysis, $R_{\mathrm{dead,\,i}}$ in [111] to understand what insight this analysis gives into the CTL mediated killing dynamics. I found that this analysis is dependent on other properties of the system and killing properties of CTLs. Thus, a change in value of cannot be attributed to just the killing properties. To counter this analysis, I proposed the PTA to analyse the experimental data. It is also interesting to note that the PTA is a versatile tool and can be used to analyse other systems.

Chapter 3

Agent Based Model of CTL Mediated Killing *In Vivo*

The observations and the analysis using PTA show that the observed probability of killing infected cells at the n^{th} contact increases with n. Additionally, with the experimental setup, we can observe the cell movement and interactions. Using the observations obtained from the experiments [111], I developed an agent based model (ABM) of 3D CTL killing that mirrors *in vivo* imaging experiments and fairly reproduces the same experimental setting. In this model, I have proposed multiple hypotheses for the mechanisms behind CTL mediated killing of infected cells and using the observed datasets, I have ranked the best hypotheses to get an insight into the system properties.

3.1 Agent Based Modeling

Agent-based modeling is a powerful tool that has been used in recent years to study diverse systems. It involves introducing a set of autonomous agents which can behave and interact with other agents based on a set of rules used to define them [205]. A major benefit of ABM as a technique is that by making use of individual properties of agents, it captures the emergent phenomena and it can be used to study the impact of changing one particular property on the emergent phenomena. Since different types of agents have different rules, it allows for heterogeneity in the system. Agent-based modeling is akin to a computational microscope and can be used to zoom into the system to look at properties in exhaustive detail. I chose to carry out my research using an ABM as it gives a peek into the mechanisms of killing that are previously unexplored.

In the system outlined above, the experimental setup by Halle et al. already made us privy to the emergent phenomena. Thus, by changing the rules of agents for different hypotheses of killing, I could make predictions about system behavior on a cellular level.

3.2 Three Dimensional Setting and Movement of Cells

The tissue of the lymph node under observation in experiments is visualized in the ABM as a three dimensional cube of dimensions 700*700*700 μm (Figure 3.1a). The agents of this ABM which are CTLs and infected cells, are positioned in this continuous three-dimensional space. The size of the cube is taken from the experimental settings. It is assumed that the distance along the x and y axes is periodic, such that as one cell exits from one side, it re-enters at the other end with the other properties remaining the same and maintaining the same velocity vector. In the experimental setup, cells can leave from the lower boundary but not from the upper boundary along the z-axis. The exit and entry of CTLs in the experimental system leads to a situation where CTLs with known history are replaced by CTLs with unknown history. We have assumed the system to be impermeable along the z-axis such that cells cannot leave from the upper or lower boundaries. CTLs are randomly located throughout the space, whereas the infected cells are placed only in the upper 40% (Z_{lim}) of the space with respect to the z-axis, similar to the observed layer of infected cells *in vivo*. The cells are represented as spheres. We assume a nucleus hard-core repulsion where C_{CF} known as the collision confinement factor defines the radial size taken by the nucleus. In view of this, the cells are positioned in the three-dimensional space to ensure that no two cells do physically overlap. The CTLs have a radius of 4.8 μm (R_{T}), and the infected cells have a radius of 5.1 μm (R_{I}) (mean calculated from experimental observations).

The CTLs in the ABM are motile while infected cells are stationary as seen in the experimental system. I modelled CTL migration to mimic T cell behaviour as observed by 2-photon microscopy. The motion of CTLs is described using a current direction of movement and a speed. The initial speed is taken from the distribution obtained from experimental observations (Figure 3.1d) and the initial directions are assigned at random. The CTLs have a constant persistence time of 2 minutes which is the time that a particular cell moves in one direction before changing directions [206]. When the persistence time of a CTL is reached, it is assigned a new direction of movement and a new speed taken from the distributions obtained from experimental data. Initially, the time that each cell has been moving in the same direction is assigned as a random value between 0 and the persistence time. This measure avoids synchronization between the movement of CTLs as they are all updated to have a new velocity at different time relative to each other.

3.3 Collision Detection and Interaction Between Cells

Once the cells have been placed in the three-dimensional space, the respective functions associated with each cell type are carried out every time step (0.1 minutes):

(a) **Collision**: CTLs that are not interacting with an infected cell at the given time are checked for motion. If the CTL has moved in the same direction for a duration equal to or longer than

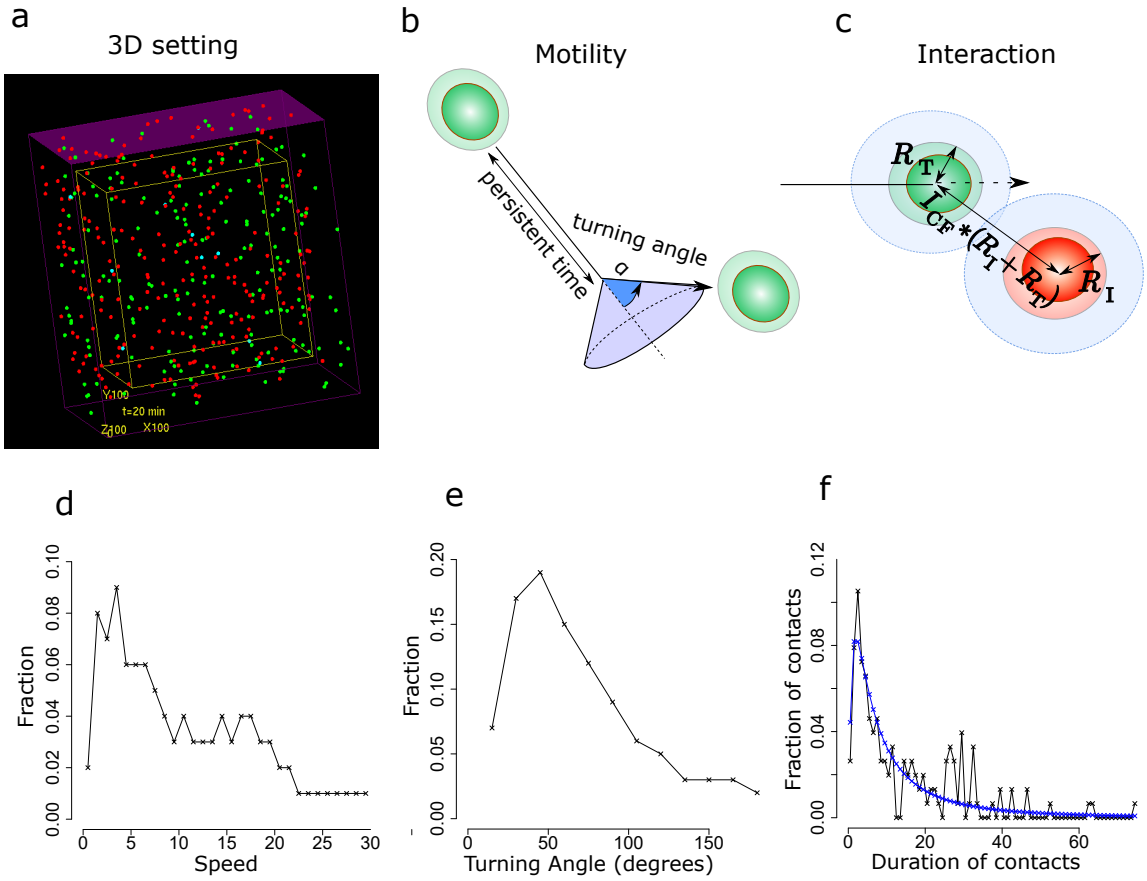

Figure 3.1: Design of the agent-based model for spatial CTL killing activity. (a) 3 dimensional view of the agent-based model where the infected cells are red and CTLs are green, (b) CTLs in the model move in a straight direction until a persistence time is reached, then a new direction is randomly set (α) according to an experimentally measured turning angle distribution, (c) CTLs interact with infected cells when they are in close proximity to each other (R_{T}- CTL radius, R_{I}- infected cell radius, I_{CF}- interaction confinement factor, refer to Section 3.3), (d) Speed distribution of CTLs obtained from experiments [111] and used in the model, (e) Turning angle distribution of CTL movement obtained from experiments [111] and used in the model, (f) Distribution of contact duration between infected cells and CTLs (Black- experimental data, blue- log normal plot fitted to experimental data [111] and used in the model).

the persistent time, the CTL is assigned a new speed and direction taken from the experimentally observed distribution (Figure 3.1d and e). The order of CTLs in which the movement is allowed is random to avoid any bias in results.

Before moving in the assigned direction, the CTLs are checked for collisions. Two cells in the system are said to collide if they are at a distance corresponding to the nucleus hard-core repulsion or less. More precisely, a CTL collides with a cell when the distance between the centre of the CTL under motion and the other cell (infected cell or CTL) is C_{CF}(CTL radius + Cell radius). We have set the value of C_{CF} as 0.5 to account for the behavior of a cytoplasm whereby it can change shapes to squeeze through smaller openings. Thus, the CTLs are moved in their direction of movement as much as possible within the maximum distance that can be covered in a single time step until they reach another cell. I have chosen the value of the time step such that it is small enough to ensure that a CTL can never pass through another cell in just one time step. Once CTLs reach at the threshold distance for collision, the CTL stops moving during that time step.

(b) **Interaction initiation**: At each time step, CTLs are checked for interaction. Each CTL can interact with only one infected cell at a time, but an infected cell can have interactions with multiple CTLs simultaneously. For an interaction to be initiated, the distance between a free infected cell and a CTL has to be less than I_{CF}(CTL radius + infected cell radius), where I_{CF} is the interaction confinement factor. For the entire interaction period, the CTL is stationary. The value for I_{CF} is set to 1.5 to account for the phenomenon that cells can expand pseudopodia to interact with another cell. As a consequence of the values taken for I_{CF}, the interaction can be initiated before the cells collide with each other.

(c) **Interaction termination**: For every interaction, the duration is determined based on a predefined distribution. The experimental data for duration of interaction has very few points and to achieve a better sampling, the distribution of interaction duration is chosen from a fitted log normal distribution, leading to a mean of 2.1 and a standard deviation of 1.2 (Figure 3.1f).

Once the duration of the ongoing interaction between a CTL and an infected cell equals or exceeds the initially assigned interaction time, the interaction is terminated and the CTL is reassigned a new speed and angle. After an interaction ends, CTLs are not allowed to interact during the first persistent time. This is done to ensure that the CTL has enough time to move away from the cell with which it was interacting previously and to avoid recurring contacts between the same two cells due to their proximity to each other.

3.4 Hypotheses for Cell Death

Infected cells that are interacting at a given time step are checked for death based on the following hypotheses (Figure 3.2):

1. Null hypothesis: The killing of infected cells is considered to be contact history independent.

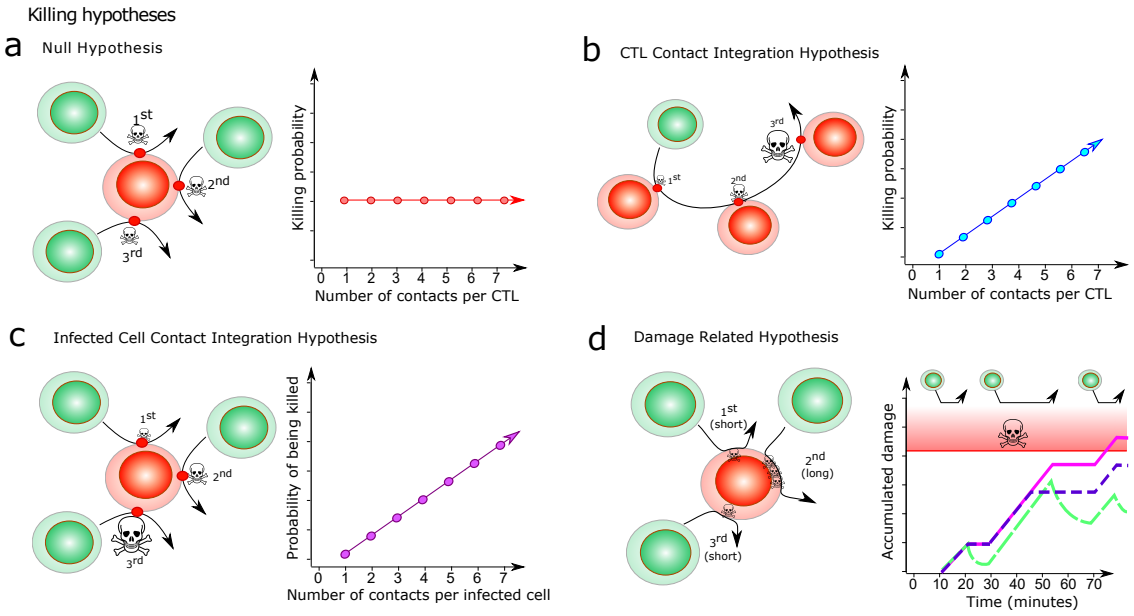

Figure 3.2: Killing hypotheses: (a) Null hypothesis: Infected cells and CTLs do not retain memory of prior contacts. Each contact is associated with a constant probability of death. The associated plot shows the behaviour of CTL killing properties with increasing number of interactions with infected cells; (b) CTL contact integration: The CTLs retain memory of contacts and at each contact. The associated plot shows the behaviour of CTL killing properties with increasing number of interactions with infected cells; (c) Infected cell contact integration: The infected cells retain memory of CTL contacts. The associated plot shows the behaviour of infected cell susceptibility to death with increasing number of interactions with CTLs; (d) Damage hypotheses: The CTLs induce damage to the infected cells. The associated plot shows the change in damage of infected cell for varying interaction times with CTLs for different hypotheses- constant damage (pink), damage and repair (green) and saturated damage (purple). The red area represents the damage greater than the threshold damage after which an infected cell dies.

The probability of CTL mediated infected cell killing (p_0) remains constant as the number of CTL contacts increases, and there is no modulation of cell characteristics as the number of contacts increases. Thus, neither the infected cells nor the CTLs retain memory of prior interactions. The CTL kills the infected cell at the end of an interaction.

2. Infected cell contact integration: The probability of CTL mediated infected cell killing increases linearly with the number of CTL contacts. For each contact, the probability of infected cell killing is given by $k_{\mathrm{I}}C_{\mathrm{I}}$, where k_{I} is constant and C_{I} is the number of contacts the infected cell has had, including the current one. In this hypothesis, infected cells become more susceptible to cell death with more contacts with CTLs. The increase in susceptibility could arise due to potential mechanisms involving storing the number of previous contacts by infected cells or signals left by the CTLs around the infected cells. Similar to the Null hypothesis, the CTL kills the infected cell at the end of an interaction.

3. CTL contact integration: Instead of infected cells, the T cells retain the memory of the contacts. T cell killing capacity is modulated such that they become more lethal as the number of contacts increases. For each contact, the probability of cell death is given by $k_{\mathrm{T}}C_{\mathrm{T}}$, where k_{T} is constant and C_{T} is the number of contacts the CTL has had. A value of a $k_T > 1$ implies that CTL becomes more lethal with increasing number contacts (positive maturation), while $k_{\mathrm{T}} < 1$ implies a long-term depletion of T cell killing capacity with increasing contacts (negative maturation). Similar to the previous hypotheses, the CTL kills the infected cell at the end of an interaction.

4. Constant damage: A potential mechanism through which infected cells retain memory of contacts with CTLs and become more susceptible to cell death, I proposed that CTLs damage the infected cells. The damage imparted by CTLs to infected cells is assumed to be proportional to the duration of contact between the CTL and infected cell and is calculated at every time step of the interaction for an infected cell according to the equation below.

$$\frac{dI_{\mathrm{d}}}{dt} = n_{\mathrm{CTL}}(t)d \tag{3.1}$$

Here I_{d} is the damage of an infected cell, d is the damage rate, and $n_{\mathrm{CTL}}(t)$ is the number of CTLs that are interacting with the infected cell at time t. From the above equation, it can be seen that for an infected cell to reach a damage of 1, a total contact period of $1/d$ minutes is required with CTLs. For an infected cell this is the shortest time from the first contact with a CTL after which apoptosis can be initiated. Once an infected cell reaches a threshold damage of 1, the death process is initiated. The interaction ends when the infected cell dies, or when the interaction time is complete, whichever comes first.

5. Saturated damage: Damage of infected cells during a single interaction with CTLs is limited to a certain duration $T_{\max}$. Once an interaction exceeds $T_{\max}$, the CTLs no longer damage the infected cells. This measure accounts for the short-term fatigue of CTL in contact. For each CTL, the damage inflicted on a particular infected cell during interaction is given by:

$$\frac{dI_{\mathrm{d}}}{dt} = \sum_{i=1}^{n_{\mathrm{CTL}}} \begin{cases} d, & \text{if } T_{\mathrm{c,i}} < T_{\max} \\ 0, & \text{if } T_{\mathrm{c,i}} \geq T_{\max} \end{cases}$$

where I_{d} is the damage of the infected cell, d is the damage rate, $T_{\mathrm{c,i}}$ is the time duration of the i^{th} interaction and n_{CTL} is the total number of CTL contacts that the infected cell is currently having.

6. Damage and repair: As a compensatory mechanism for infected cells, I have assumed that while infected cells can get damaged by CTLs, they can also repair themselves. Similar to the damage hypothesis, the damage is proportional to the duration of contact and the repair is proportional to the damage of the infected cell. At each time step, the damage for an infected cell is updated according to:

$$\frac{dI_{\mathrm{d}}}{dt} = n_{\mathrm{CTL}} d - r I_{\mathrm{d}} \tag{3.2}$$

where I_{d} is the current damage of the infected cell, d is the damage rate, n_{CTL} is the number of CTLs currently interacting with the infected cell and r is the repair rate.

To get an idea about the damage of an infected cell, I solved the above differential equation to get the following equation for damage.

$$I_{\mathrm{d}} = \frac{d}{r}(1 - e^{-\mathrm{rt}}) \tag{3.3}$$

Using the equation (3.3), the duration of the first contact needed to reach a damage of 1 (t_{complete}) is given by:

$$t_{\mathrm{complete}} = \frac{-1}{r} \ln\Big(1 - \frac{r}{d}\Big) \tag{3.4}$$

Once the decision for an infected cell to die is taken, the infected cells do not immediately disappear from the system. Instead, they persist for a period of time taken for cell to die called T_{death}. During this period, the infected cells are in state of activated apoptosis. The value of T_{death} is treated as an unknown parameter and is considered a constant value. A non-zero value of T_{death} raises the question of contacts between an infected cell in activated apoptosis and CTLs (zombie contacts). In the simulations, zombie contacts may or may not be allowed (in this case, CTLs ignore the dying cells). If zombie contacts are allowed, they do not contribute to the decision of cell death,

but are still observed as contacts in the analysis of the data. After expiration of T_{death}, the dying cell disappears from the simulation.

The ABM is embedded in a user-friendly interface (Figure 3.3) through which the parameter values can be entered without making changes within the code.

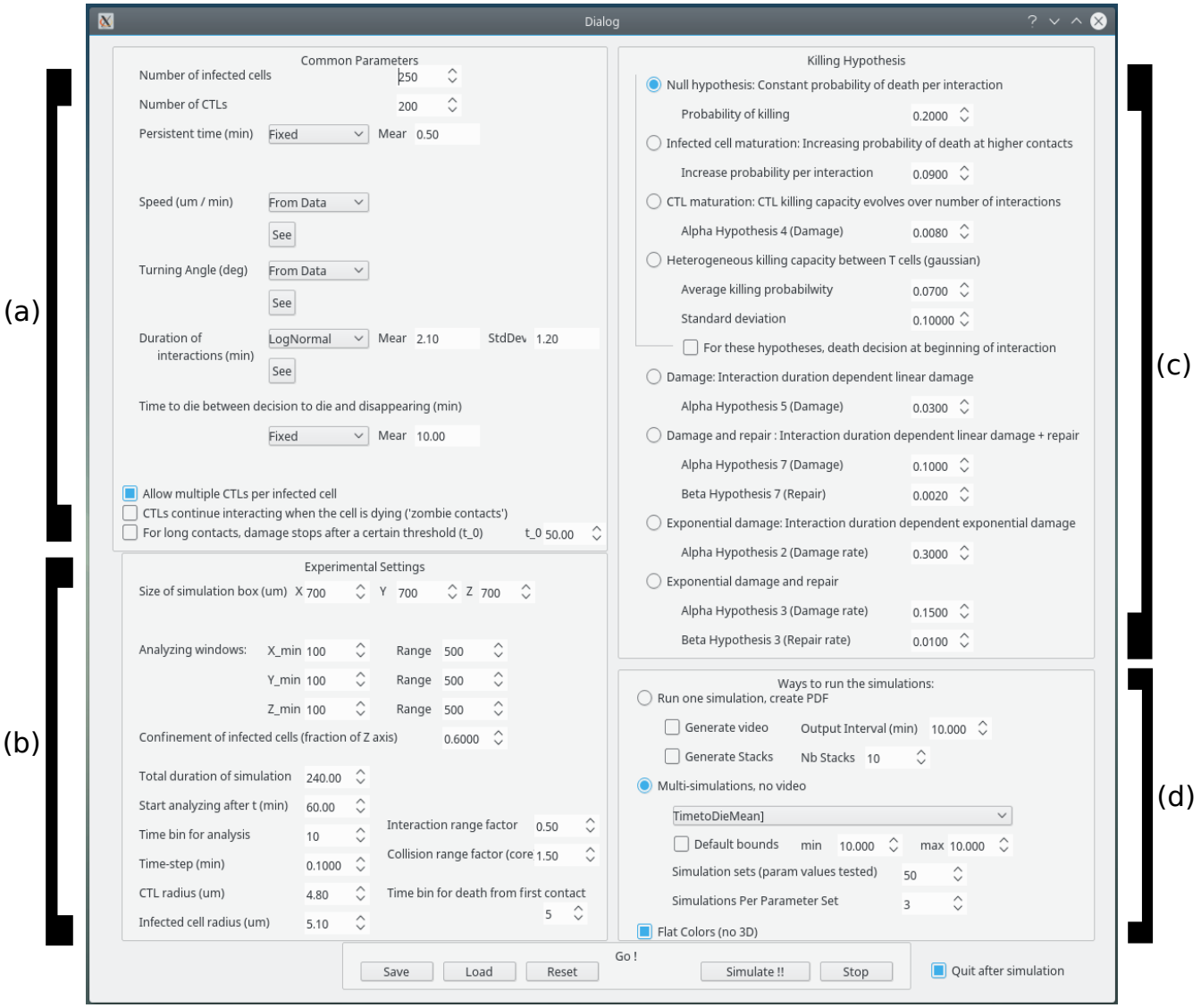

Figure 3.3: Agent-based model interface: (a) Datasets and experimental values taken from experimental data, (b) Parameters about general system settings, (c) Hypothesis dependent parameters, (d) Parameters based on the type of output the user wants.

3.5 Finding Best Parameter Sets

Although most parameters are taken directly from data, each hypothesis contains a set of associated unknown parameters, such as a killing rate or damage rate. Also, T_{death} is unknown. The unknown parameters associated with each hypothesis are:

1. Null hypothesis: Probability of death at each contact (p_0).

2. Infected cell contact integration: Probability of infected cells getting killed at first contact with CTLs (k_{I}).

3. CTL contact integration: Probability of CTLs killing infected cells at first contact with CTLs (k_{T}).

4. Constant damage: Damage rate (d).

5. Saturated damage: (i) Damage rate (d); (ii) Maximum time until which CTLs can damage infected cells ($T_{\max}$).

6. Damage and repair: (i) Damage rate (d); (ii) Repair rate (r).

The total cost is derived from the simulation of 8 experimental readouts at the same time (see Figure 3.4):

1. Observed probability of killing infected cells with a particular number of interactions with CTLs (Figure 3.4a). In the model, the number of infected cells that died at exactly the i^{th} interaction is normalized by the total number of infected cells with at least i interactions.

2. Distribution of the observed time between first CTL contact and the observed time of cell disruption (Figure 3.4b). In the model, this distribution is obtained by monitoring all cells from their first contact to a CTL, counting the number of killed cells in time bins, and normalising these with the total number of killed infected cells.

3. Distribution of the number of contacts with CTLs for infected cells that died during the observation period (Figure 3.4c). In the model, the number of CTL contacts is saved with each cell and a histogram is generated at the end of the simulation and normalized with the total number of dead cells at the end of the simulation

4. Distribution of the number of contacts with CTLs for infected cells that survived the observation period (Figure 3.4c). In the model, same procedure as in point 3 is used but for cells alive at the end of the simulation.

5. Total duration of contact with CTLs for infected cells that died during the observation period (Figure 3.4d). In the model, each cell in contact to CTL increases a clock and a histogram on time bins is generated at the end of the simulation and normalized by the total number of dead cells at the end of the simulation.

6. Total duration of contact with CTLs for infected cells that survived the observation period (Figure 3.4d). In the model, same procedure is used as in point 5 but for cells alive at the end of the simulation.

7. Distribution of single CTL contacts duration for infected cells that died during the observation period (Figure 3.4e). In the model, at each contact with CTLs a clock is running and the time when the cells detach is saved. For all dead cells, these times are recollected in a histogram on time bins at the end of the simulation and normalized with the total number of contacts of all dead cells.

8. Distribution of single CTL contacts duration for infected cells that survived the observation period (Figure 3.4e). In the model, same procedure as in point 7 but for cells alive at the end of the simulation.

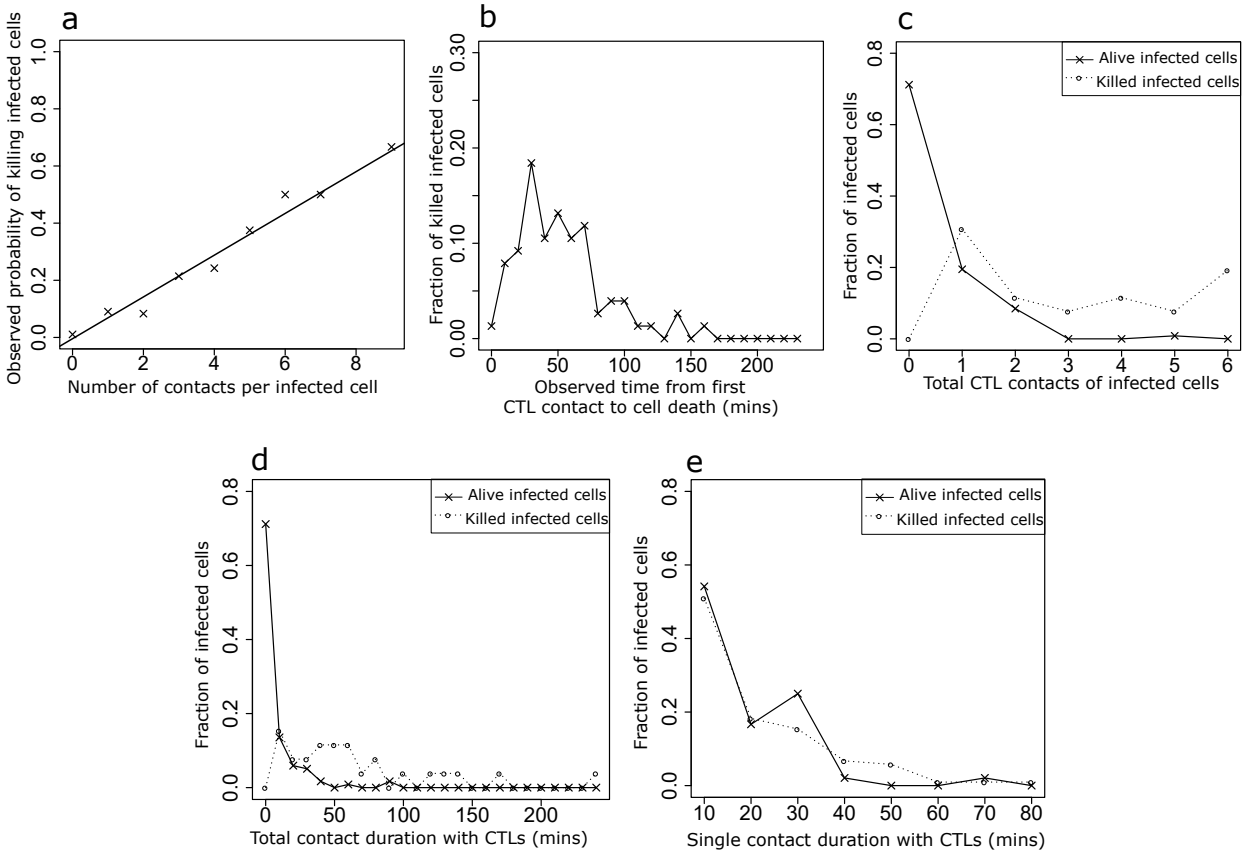

Figure 3.4: Experimental readouts used to compare experimental data [111] with model data: (a) Probability of killing infected cells with increasing number of interactions with CTLs, (b) Observed time between first CTL contact and cell death for killed infected cells, (c) Number of contacts with CTLs for infected cells, (d) Total duration of contact with CTLs for infected cells, (e) Single CTL contacts duration for infected cells.

When comparing different parameter sets, the formula in equation (3.5) is used to compute the cost for each of the 8 datasets described above:

$$C_{\mathrm{x}} = \frac{1}{n}\sum_{1}^{n}\Big[\sum_{i=1}^{N_{\mathrm{x}}}(E_{\mathrm{x,i}} - M_{\mathrm{x,i}})^2\Big] \tag{3.5}$$

where C_{x} is the average cost of the x^{th} dataset, n is the total number of simulations run for each

parameter set, N_{x} is the total number of data points of the x^{th} experimental dataset, $E_{\mathrm{x,i}}$ is the i^{th} data point of the x^{th} experimental dataset and $M_{\mathrm{x,i}}$ is the i^{th} data point of the x^{th} model dataset with this parameter set. The subscript x represents the 8 datasets described above.

The 8 separate costs were averaged to compute the mean cost (C) for a particular parameter set using equation (3.6):

$$C = \frac{1}{e}\sum_{x=1}^{e} C_{\mathrm{x}} \tag{3.6}$$

where e is the total number of datasets ($e = 8$ in the current study) and C_{x} is the average cost of the x^{th} dataset using equation (3.5).

For each hypothesis, the average costs are plotted in a heatmap comparing different combination of parameter values. Then, the parameter set with the lowest cost for each hypothesis was used to run the simulation to get the results. For the first dataset (Figure 3.4a), since the experimental data points beyond the 6th contact only represent a small number of cells, only the 6 first interactions are included in the cost calculation.

As all of the hypotheses do not have the same number of unknown parameters, I also computed the Akaike information criterion (AIC) for all the hypotheses using the following formulae:

$$\mathrm{AIC} = 2k + s\ln(C) \tag{3.7}$$

where k is the number of unknown parameters, s is the number of experimental readouts that are compared with the model readouts and C is the cost. A lower AIC value indicates a better fit of model with experimental data.

3.6 Table of Parameters Fixed from Data

The parameters that are common for all hypotheses such as the number of CTLs and infected cells are taken from experimental data. These parameter values are tabulated in Table 3.1.

3.7 Summary

To find out which killing mechanisms can explain the *in vivo* observed quantitative killing properties observed in [111], I used the ABM described in this chapter. The ABM simulates the movement and interactions of CTLs with non-motile infected cells in 3D as *in vivo* imaging experiments in [111] (Figure 3.1a). In short, CTLs move in a straight line at a certain speed until a persistence time is reached, and then, a new direction is selected based on the experimentally measured turning angle distribution (Figure 3.1e) and a new speed is selected from the distribution in Figure 3.1d. CTLs and infected cells initiate an interaction with each other, when they reach a threshold distance

Parameter	Value
Number of CTLs (N_{T})	200
Number of infected cells (N_{I})	250
Percent of z-axis occupied by infected cells (Z_{lim})	40%
Radius of CTLs (R_{T})	4.8 μm
Radius of infected cells (R_{I})	5.1 μm
Interaction Confinement Factor (I_{CF})	1.5
Collision Confinement Factor (C_{CF})	0.5
Persistent time (T_{pers})	2 minutes
X-axis dimension of space (X_{dim})	700 μm
Y-axis dimension of space (Y_{dim})	700 μm
Z-axis dimension of space (Z_{dim})	700 μm
Simulation (T_{Sim})	240 minutes
Speed	Taken from distribution (Figure 3.1d)
Turning angle	Taken from distribution (Figure 3.1e)
Interaction duration	Taken from distribution (Figure 3.1f)

Table 3.1: Parameter values taken from experimental data [111]

(Figure 3.1c). The duration of an interaction is directly taken from experimental data shown in Figure 3.1f.

The various killing hypotheses outlined in this chapter were tested (Figure 3.2). These include a constant killing rate (Null hypothesis) as seen in Figure 3.2a, a modulated killing capacity of CTLs with interactions as seen in Figure 3.2b, an increased susceptibility of death of infected cells at higher CTL contacts (infected cell contact integration) as seen in Figure 3.2c, and finally a damage rate of infected cells at each contact with CTLs (damage), possibly with repair of the cell (damage and repair) and with a maximal damage per contact (saturated damage) as seen in Figure 3.2d. The datasets used to discriminate between killing hypotheses are taken from [111] and are shown in Figure 3.4.

Chapter 4

Results From The Agent Based Model

Using the ABM described in the previous chapter, I ran simulations for the killing hypotheses and compared them with the observed experimental data.

4.1 Best Parameter Set

In the ABM, most of the parameters have been taken directly from experimental data (Section 3.6). But the parameters associated with each hypothesis and the time between activation of apoptosis and visual cell dissolution remained to be estimated (T_{death}). I ran simulations and then computed the cost for all observed 8 datasets from the experiments (equation (3.5)). Using these 8 costs from all datasets, I computed the average costs (equation (3.6)) for all hypotheses in absence of zombie contacts (Figure 4.1) and in presence of zombie contacts (Figure 4.2). The parameter set with the lowest cost has been marked with an 'X'. The heatmaps show that only a restricted range of parameters is consistent with the observed experimental data.

For the identified parameter sets, I ran simulations and plotted the data to compare model results with experimental data. Additionally since the number of unknown parameters is not the same for all hypotheses, I computed the Akaike information criterion (AIC) (equation (3.7)).

4.2 Null Hypothesis

First, I investigated whether the observed properties of CTL-mediated killing seen in quantitative 2-photon imaging (Figure 3.4) could be explained by a contact history independent killing mechanism (Null hypothesis).

For the Null hypothesis, the parameter associated with the hypothesis is the probability of

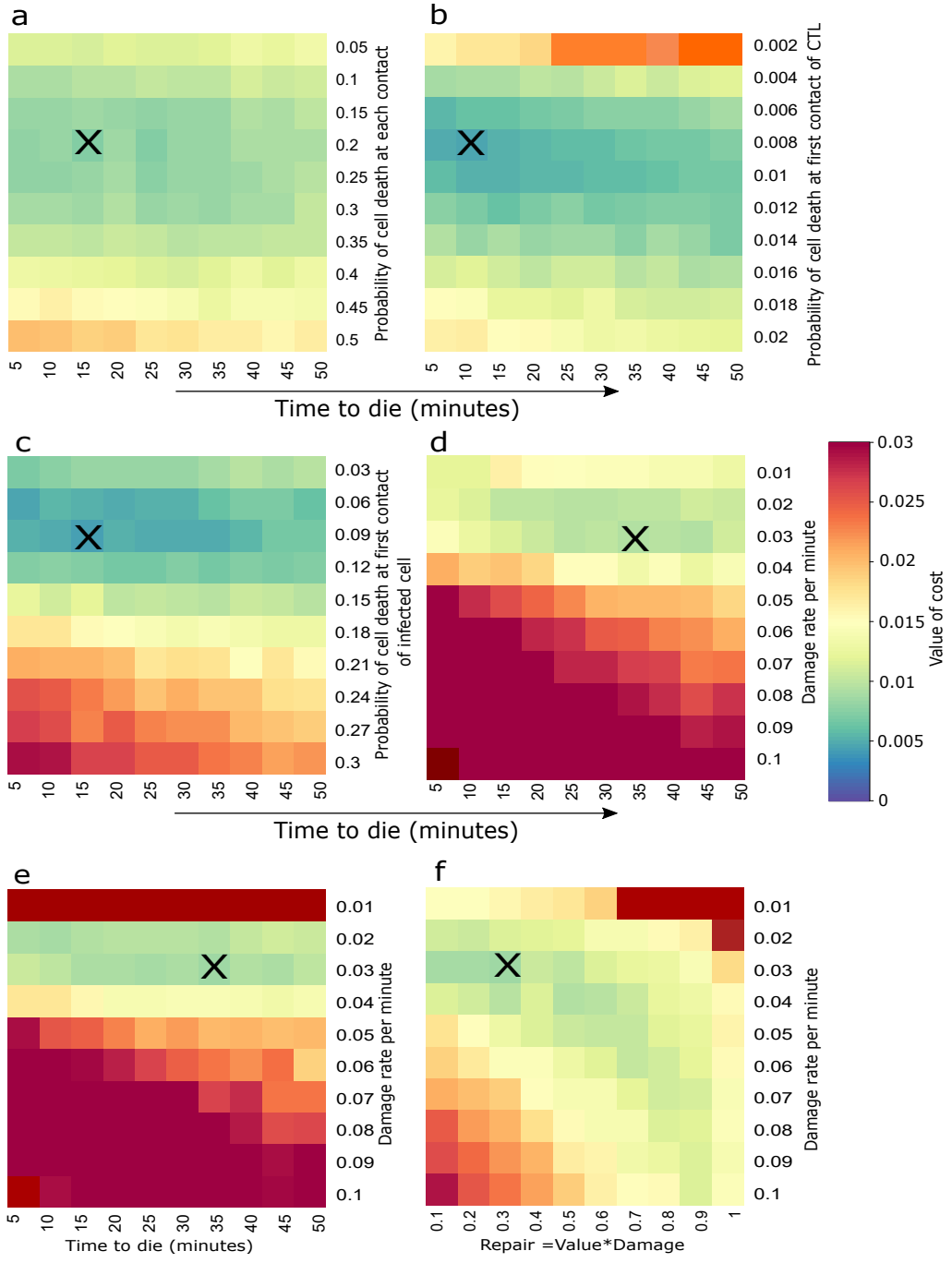

Figure 4.1: Heatmaps for all hypotheses in absence of zombie contacts. (a) Null hypothesis; (b) CTL contact integration hypothesis; (c) Infected cell contact integration hypothesis; (d) Constant damage hypothesis; (e) Saturated damage hypothesis; (f) Concomitant damage and repair hypothesis. Each point on the heatmap is obtained by calculating the average cost over 30 simulations for the respective parameter combination. 'X' represents the parameter combination with the lowest cost. For saturated damage hypothesis and damage and repair hypothesis, there are three variable parameters and the lowest costs were found scanning the 3D parameter space (data not shown).

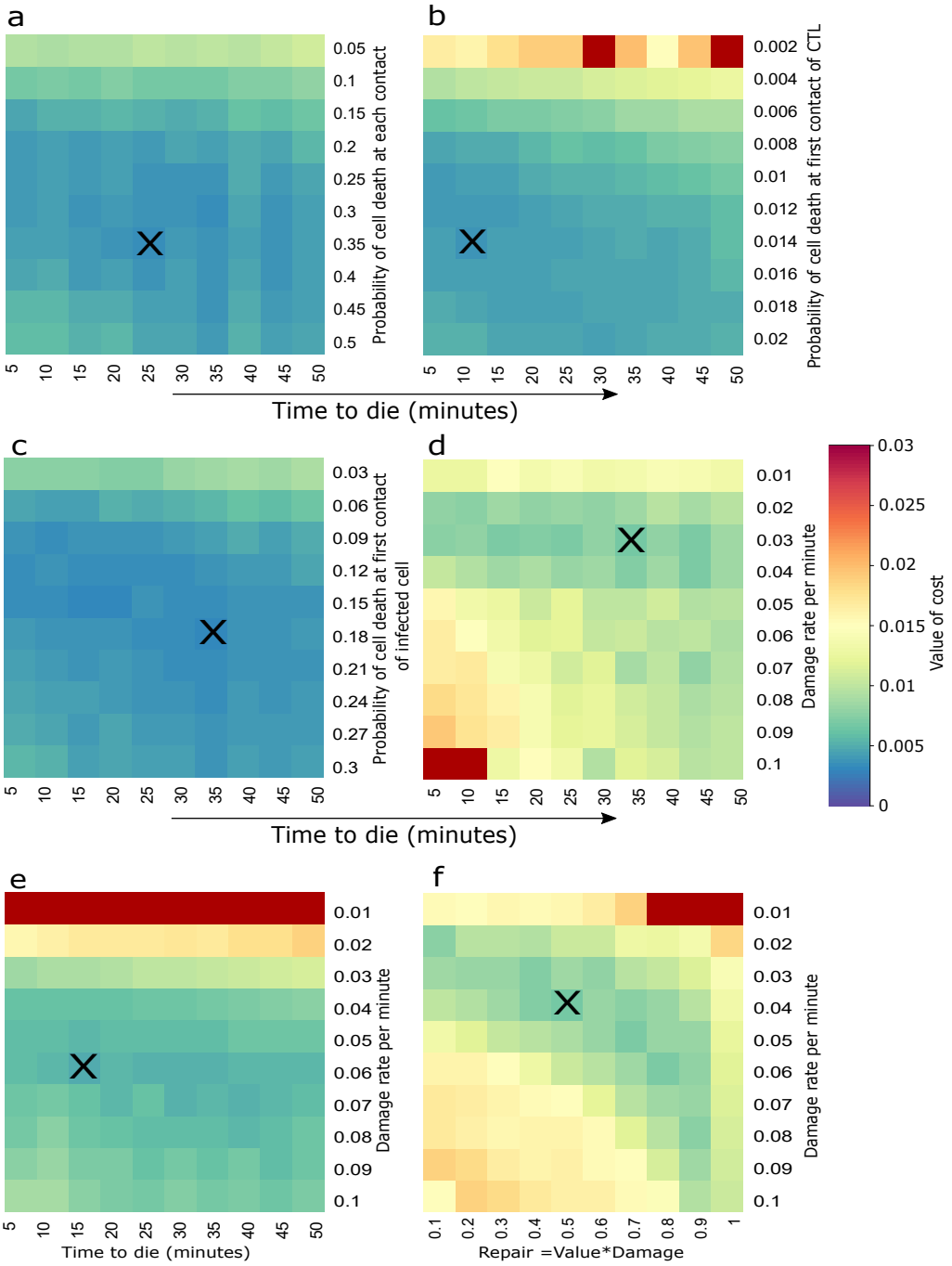

Figure 4.2: Heatmaps for all hypotheses in presence of zombie contacts. (a) Null hypothesis; (b) CTL contact integration hypothesis; (c) Infected cell contact integration hypothesis; (d) Constant damage hypothesis; (e) Saturated damage hypothesis; (f) Concomitant damage and repair hypothesis. The heatmaps are obtained using the same conditions described in Figure 4.1

CTLs killing infected cells. I obtained the best parameter from the heatmap (Figure 4.1a) and subsequently ran simulations for these parameter values (Figure 4.3, green lines).

In this model, the observed probability of killing infected cells with increasing interactions remains constant with increasing interaction numbers, as logically expected. The observed constant probability of killing at each contact is in disagreement with the experimental results. The testing of the Null hypothesis thus serves to verify the correctness of the model and confirms that the observed killing probability of infected cells with increasing interactions reflects the CTL-mediated mechanism of cell killing mediated in this context. Moreover, the result obtained shows that a killing probability independent of the contact history can not be a potential mechanism for explaining the *in vivo* datasets of Halle et al [111].

4.3 Contact Integration Hypotheses

4.3.1 CTL Contact Integration

In order to explain the increase in observed probability of killing infected cells with increasing interactions with CTLs (Figure 3.4a), I hypothesized that this could be a consequence of modulation of CTL killing capacity after each interaction with an infected cell. In this hypothesis, CTLs kill with a linearly increasing probability proportional to the number of target cell contacts the CTL had before. The cost of various parameters was plotted using heatmaps and an optimal set of parameters has been determined (Figure 4.1b).

For the obtained optimal parameter set, the observed probability of killing infected cells with increasing interactions with CTLs (Figure 4.3a, blue line) along with the corresponding plots for the other datasets (Figure 4.3b-h, blue lines) showed a good agreement of the model results with the experimental results. This indicates that a modulation of CTL killing capacity could be a potential mechanism that can reproduce the experimental observations.

4.3.2 Infected Cell Contact Integration

Next, I explored whether virus-infected cells might get more susceptible to death with increasing numbers of CTL contacts (infected cell contact integration hypothesis). As opposed to the previous hypothesis, here the infected cells retain memory of prior interactions with CTLs. In this scenario, the death susceptibility of infected target cells was modelled as a linearly increasing probability of death that is proportional to prior number of CTL visits (see Chapter 3). The simulation with the best parameter set (Figure 4.3, red lines) is in agreement with experimental data suggesting that infected cells may get more susceptible to cell death with increasing number of CTL contacts.

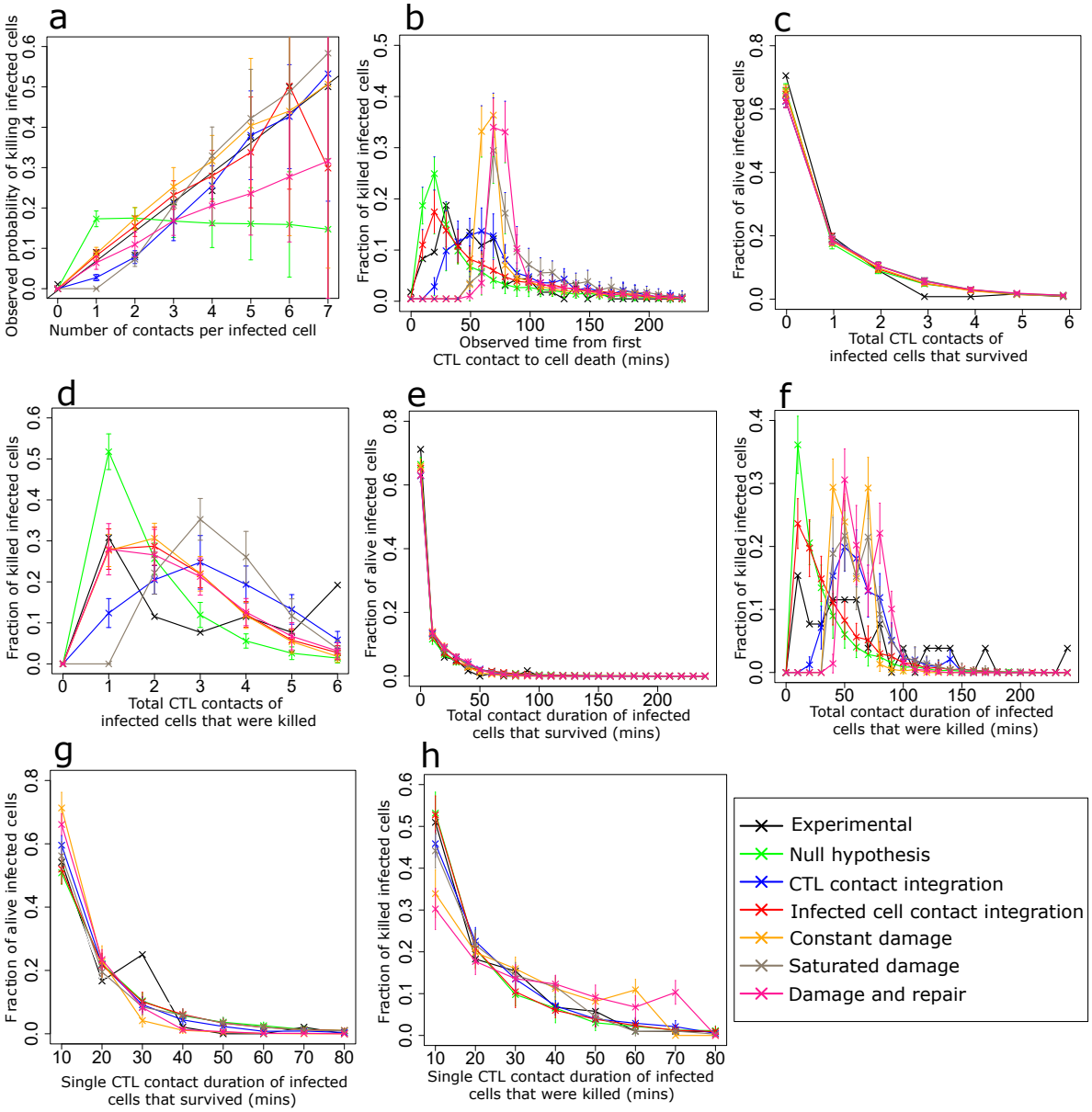

Figure 4.3: Plots for optimal parameters for all hypothesis in absence of zombie contacts. (a) Observed probability of killing infected cells in dependence on the number of interactions with CTLs, (b) distribution of observed times between first contact to a CTL and actual cell death for all killed infected cells, (c) distribution of the number of contacts with CTLs for all infected cells that survived during the observation period and, (d) were killed during the observation period, (e-h) distribution of total (e, f) and single (g, h) contact durations with CTLs for infected cells that survived during the observation period (e, g) and were killed during the observation period (f, h). Error bars represent SD from 30 simulations.

4.4 Damage-Based Hypotheses

In the previous hypothesis, I established that infected cells retaining memory of contacts with CTLs could be a potential mechanism. Next, I explored the mechanisms through which infected cells could retain memory of previous CTL contacts. I hypothesized that infected cells get damaged by interacting CTLs and once the damage of an infected cell reaches a threshold value of 1, the cell dies. The three damage-based hypotheses that were considered were constant damage, saturated damage, and damage and repair hypothesis (Figure 3.2d).

The constant damage hypothesis involves a constant rate of damage during interactions. In the saturated damage hypothesis, the damage process by the CTL halts after the duration of the ongoing interaction exceeds a threshold time ($T_{\max}$). This hypothesis was proposed because CTLs have a storage of cytolytic granules and are potentially unable to sustain a damage process for very long interactions, reaching up to 40 minutes in the *in vivo* dataset. Therefore, a possible biological factor that affects the killing observations could be T cell exhaustion during a single contact if the contact exceeds a certain threshold duration. I proposed that the interlude between two consecutive contacts is long enough for the CTLs to recuperate and be able to damage the infected cells again. In the damage and repair hypothesis, there is no T cell exhaustion. The CTLs damage the infected cells throughout the duration of the interaction and the infected cells also repair themselves. The repair mechanism continues irrespective of an ongoing interaction or even if the infected cell is not interacting at a given time.

I was able to reproduce the increasing probability of killing infected cells with increasing interactions with CTLs (Figure 4.3a, orange and grey lines respectively) for constant damage (Figure 4.1d) and saturated damage hypothesis (Figure 4.1e). Further calculations for both hypotheses show that the plot for observed time between the first contact to a CTL and the actual cell death obtained from the model does not coincide with the experimental distribution (Figure 4.3b, orange and grey lines respectively).

The best parameter set identified from the heatmap shows a damage rate of around 0.03 per minute for constant and saturated damage hypotheses (Figure 4.1d, e). For a cell to get a damage of 1, a total contact time of $1/d$ minutes is required (see Chapter 3). For a value of $d = 0.03$ per minute, the total contact time required for a damage of 1 is ~ 33.3 minutes which is also the minimum time a cell will take to die after the first observed CTL contact provided that the time between the fate decision for death and the actual dissolution of the cell is negligible. For the saturated damage hypothesis, the value would exceed ~ 33.3 minutes (see Chapter 3). For the damage and repair hypothesis, the optimal value for damage is 0.03 per minute and the value for repair is 0.009 (Figure 4.1f). The duration of one contact that is enough to induce a total damage of 1 is ~ 39.6 minutes (see Chapter 3). For an infected cell that dies, the observed time between the first contact with a CTL and the actual cell death will also consists of the time that passes

between consecutive contacts. As shown by the calculations above, for all of the damage-based hypothesis, no infected cell can die before an observed time of 30 minutes or less between the first CTL contact and cell death which is in disagreement with the experimental data (Figure 4.3b, pink line). All of the damage-based hypotheses that we described above have a constant rate of damage. Thus, I concluded that none of the damage-based hypotheses with a constant damage rate are compatible with all the experimental datasets.

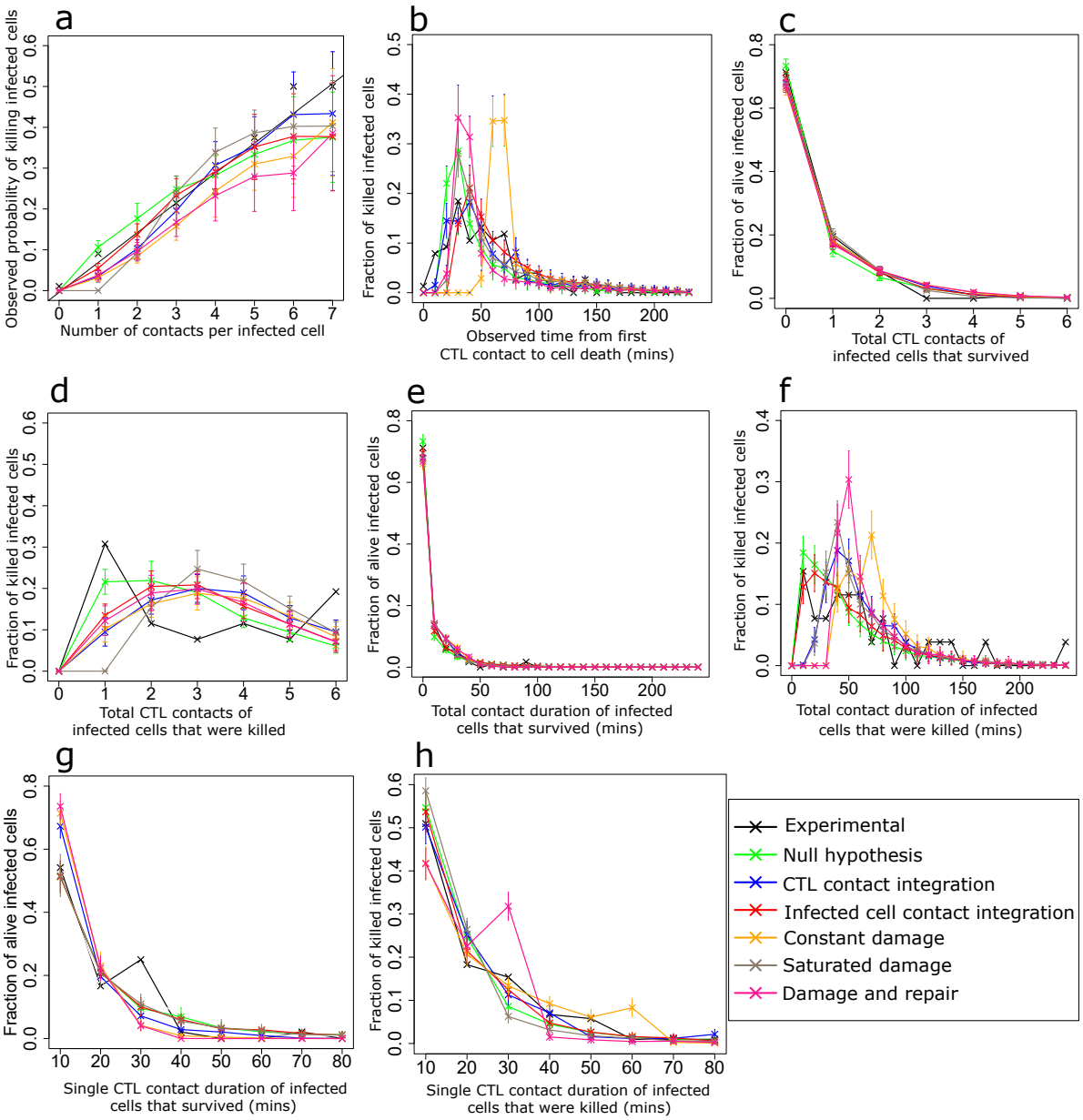

Figure 4.4: Impact of zombie contacts on model selection. Same as Figure 4.3 using the best fitted parameters (Figure 4.2) for each hypothesis in presence of zombie contacts. Error bars represent SD from 30 simulations

4.5 Zombie Contacts

4.5.1 Null Hypothesis

It is interesting to note that for all of the hypotheses above, the value of T_{death} is non-zero. The theory that an infected cell persists in the system in a state of activated apoptosis led me to explore the impact of contacts between CTLs and apoptotic infected cells. Thus, a target might receive multiple CTL contact events, even though the fate decision to die has already been made. It has been observed that once a target cells is disrupted, the remaining small so-called remnants of the target cells are only sometimes contacted by CTLs. A possible explanation could be that most of these remnants are taken up by local dendritic cells and macrophages, thus preventing direct access of the CTLs to the membrane or the remnants.

It is unknown how CTL interactions with target cells in the process of cytolysis might affect CTL killing mechanisms and estimates of CTL killing efficiency. To address this question, I next tested whether the allowance of "zombie contacts" impacts the observed probability of killing infected cells with increasing interactions with CTLs. I used the term "zombie contacts" to illustrate the interaction of a CTL with a target cell for which the intracellular pro-cell death signalling mechanisms have already passed a non-reversible cell death pathway checkpoint. Importantly, even the use of caspase reporter activity does not yet allow such data to be generated *in vivo*, therefore I used my agent-based model to better understand the possible impact of such zombie contacts.

Simulations with the Null hypothesis with zombie contacts were performed with different killing probabilities and T_{death} distributions (Figure 4.2a). An optimal parameter set could be identified, and the simulations for each separate dataset are shown (Figure 4.4a-h, green lines). Strikingly, although CTLs mechanistically kill with equal probability at each contact in the model under the Null hypothesis, the probability of killing infected cells shows an increase with increasing interactions with CTLs, in the presence of zombie contacts (Figure 4.4a, green line).

Due to zombie contacts, when following CTL killing activity *in vivo*, the time during which cells are already dying is counted in the analysis of the number of contacts. A consequence of counting these zombie contacts is that it leads to an over-estimation of number of contacts compared to the real number of contacts that lead to cell death. Thus, I showed that the zombie contacts have a significant impact on the probability of killing infected cells with increasing interactions with CTLs in case of a Null hypothesis. Consequently, the hypothetical possibility of zombie contacts introduces another uncertainty into the analysis of live-imaging data. An increase in probability of killing infected cells with increasing interactions with CTLs does not necessarily reflect a modulation of the CTL killing efficiency at the cellular level but could be an artefact that arises due to the presence of zombie contacts.

Interestingly, the Null hypothesis in the presence of zombie contacts is compatible with all other

datasets (Figure 4.4b-h, green lines). Even though, constant probability of killing at each contact can explain all datasets, there is an underlying assumption that zombie contacts do take place, and that the time to die would actually last 25 minutes (Figure 4.2a). In addition, after the 6th contact, the simulations show a saturation in the probability of killing infected cells with increasing interactions with CTLs while the experimental dataset continues increasing. Eventually, a longer observation time would increase the total number of observed contacts per target cells and allow discarding the Null hypothesis as possible mechanism.

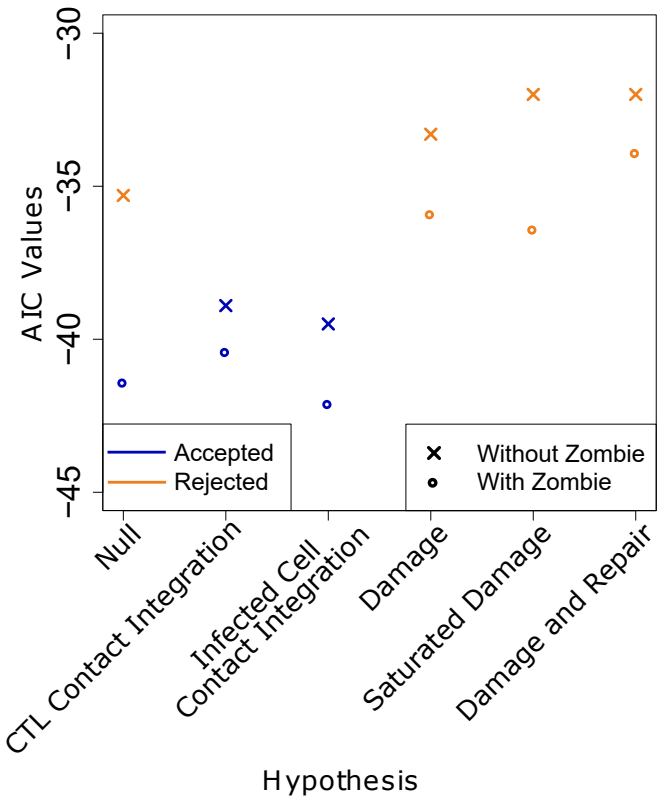

Figure 4.5: Comparison of AIC values for all hypotheses corresponding to their respective least cost. The data points in blue show the hypotheses that gave a good agreement with experimental results. The data points in orange show the hypotheses that were rejected.

4.5.2 Effect of Zombie Contacts

Considering the observed impact of zombie contacts in the Null hypothesis, I revisited all other hypotheses to test whether addition of zombie contacts to the ABM changes model performance in other scenarios as well (Figure 4.4b-f). In presence of zombie contacts, CTL contact integration and infected cell contact integration gave results in agreement with the experimental results but none of the damage-based hypotheses gave rise to plots that were in agreement with the experi-

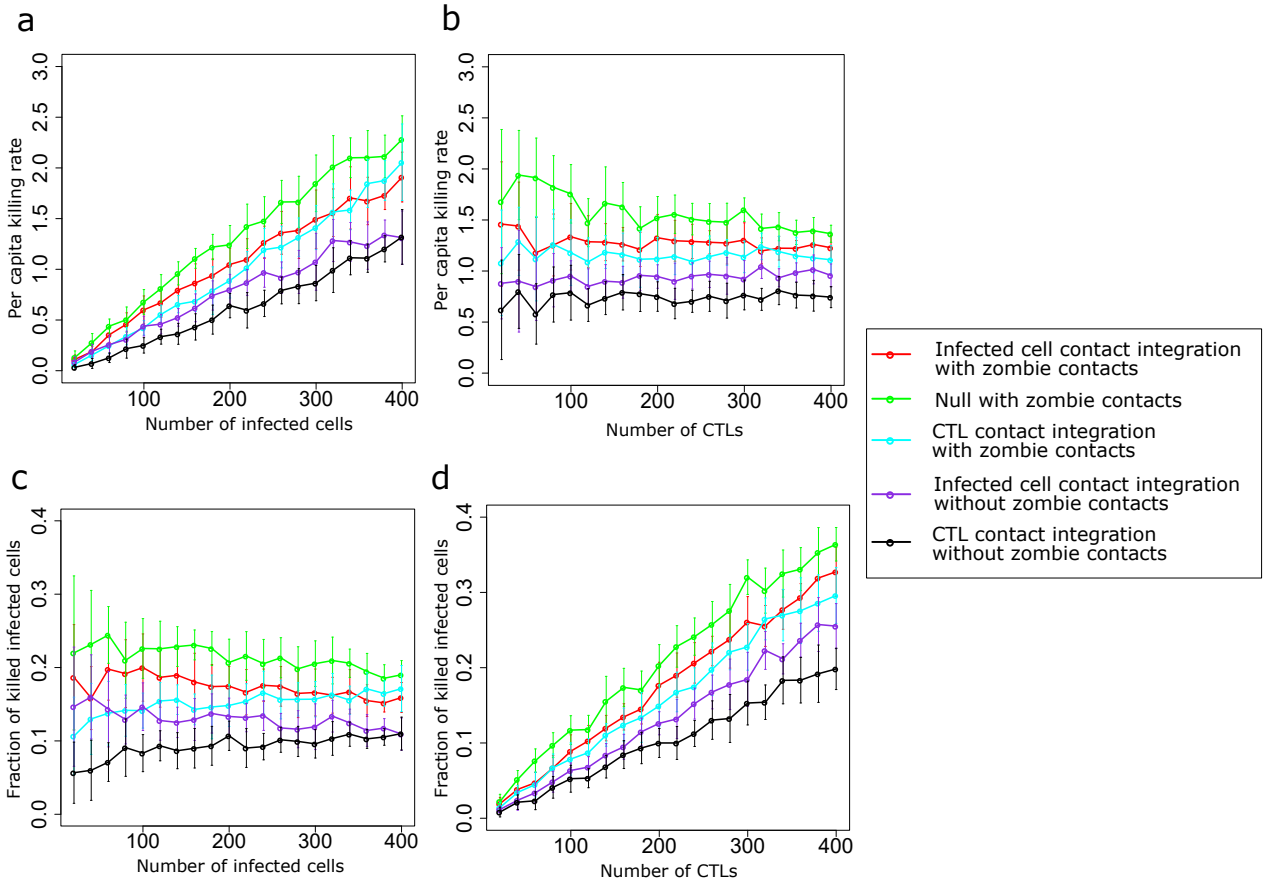

Figure 4.6: (a, b) PCKR values for variable number of infected cells (a) and of CTLs (b), (c, d) Fraction of killed cells for variable number of infected cells (c) and of CTLs (d). Error bars represent SD from 30 simulations.

Hypothesis	Killing parameter	T_{death}	Least cost	AIC
Infected cell contact integration	0.09	15	$4.35 * 10^{-3}$	-39.5
CTL contact integration	0.008	10	$4.70 * 10^{-3}$	-38.9
Null hypothesis	0.2	15	$7.35 * 10^{-3}$	-35.3
Damage	0.03	35	$9.37 * 10^{-3}$	-33.3
Damage and repair	d=0.03, r=0.009	40	$8.60 * 10^{-3}$	-32.0
Saturated damage	d=0.03, T_{max}=20	35	$8.64 * 10^{-3}$	-32.0

Table 4.1: Least cost for all Hypotheses in absence of zombie contacts in ascending order of AIC

Hypothesis	Killing parameter	T_{death}	Least cost	AIC
Infected cell contact integration	0.18	35	$3.12 * 10^{-3}$	-42.1
Null hypothesis	0.35	25	$3.41 * 10^{-3}$	-41.4
CTL contact integration	0.014	10	$3.90 * 10^{-3}$	-40.4
Saturated damage	d=0.06, T_{max}=10	15	$5.01 * 10^{-3}$	-36.4
Damage	0.03	35	$6.82 * 10^{-3}$	-35.9
Damage and repair	d=0.04, r=0.02	5	$6.83 * 10^{-3}$	-33.9

Table 4.2: Least cost for all Hypotheses in presence of zombie contacts in ascending order of AIC

mental results. This implies that apart from the Null hypothesis, the observed behaviour of the system remains the same irrespective of the presence or absence of zombie contacts. Note that all hypotheses showed a lower cost and a lower Akaike information criterion (AIC) value in presence of zombie contacts than in absence of zombie contacts as shown in Table 4.1 and Table 4.2 (Figure 4.5). This shows that the inclusion of zombie contacts gives rise to a better fit with experimental data.

4.6 Discriminating Between Best Hypotheses

4.6.1 Per Capita Killing Rate

By selecting the optimal parameter and plotting the readouts obtained from the experiments, various hypotheses were discarded. The five hypotheses that give a good agreement with all datasets in ascending order of cost are: (i) Infected cell contact integration in presence of zombie contacts, (ii) Null hypothesis in presence of zombie contacts, (iii) CTL contact integration hypothesis in presence of zombie contacts, (iv) infected cell contact integration in absence of zombie contacts, and (v) CTL contact integration hypothesis in absence of zombie contacts.

Since the datasets were not enough to discern between these five hypotheses, I sought to predict properties of the different hypotheses that could further help to discriminate them or to design

new predictive experiments. One property is the observed PCKR of CTLs, as a measure of 3D population killing efficiency. The PCKR is defined as the number of infected cells killed per CTL in 24 hours. Another important measure is the fractions of killed infected cells defined as the ratio of killed infected cells to the total number of infected cells in the system.

To understand how the number of infected cells affects the PCKR values, the number of CTLs was kept constant at 200 while the infected cell number was varied from 20 to 400 (Figure 4.6a). The other parameter values were kept fixed at the optimal parameter set obtained from the respective cost heatmaps of each hypothesis. For all five hypotheses, the values of PCKR increased with increasing number of infected cells however the increase was highest for the Null hypothesis.

Next, to elucidate the effect of the number of CTLs on the PCKR, the number of infected cells was kept constant at 250 while the CTL numbers were varied from 20 to 400 (Figure 4.6b). Surprisingly, even when the ratio of infected cells to CTLs is high, the values of PKCR remained constant for all hypotheses except the Null hypothesis where I saw a small drop in values of PCKR with increasing number of CTLs.

4.6.2 Fraction of Killed Infected Cells

Using the simulations describes above, I looked at the fraction of infected cells that are killed by CTLs for cases with different number of initial infected cells. A surprising result that is observed is that even for a low number of infected cells, CTLs fail in killing all infected cells within the 4-hour time window that is being analyzed (Figure 4.6c). In addition, while the fraction of cells killed showed a drop in values for Null hypothesis and infected cell contact integration hypothesis in presence and absence of zombie contacts, an increase in values is seen for CTL contact integration hypothesis in presence and absence of zombie contacts.

In contrast to the results obtained for variable number of infected cells, it is observed that for all four hypotheses, the fraction of infected cells killed increases with number of CTLs and at a higher number of CTLs, a much larger fraction of infected cells is killed (Figure 4.6d). Taken together, these results suggest that by keeping all other factors of a system constant and varying either the number of infected cells or the number of CTLs, we can differentiate between different killing hypotheses using PCKR and fraction of killed cells analysis.

4.7 Summary

The results obtained from the ABM show that retention of information about prior contacts by CTLs or infected cells, could be a phenomenon that explains all the observed datasets. A surprising result is that in the presence of contacts between dying infected cells and CTLs (zombie contacts) a contact history independent killing can give rise to an increase in the observed probability of killing infected cells with increasing interactions with CTLs. Interestingly, none of the linear

damage based hypotheses were consistent.

In general, I showed that only one dataset is not enough to discriminate hypotheses, but rather their combination. In the rejected hypotheses, the parameter sets that are consistent with one dataset are not consistent with the other one. Thus, in order to discriminate between the proposed hypotheses, all the datasets are important and need to be analyzed. I also proved that the hypotheses that work do so only for a short range of values, implying that for each successful hypothesis, the killing rates could be identified. Using a heatmap to find the best parameter range, even the values of the time to die T_{death} could be identified which is an important hidden biological parameter.

Chapter 5

Impact of Temporal Factors on Observed Results

In Chapter 2, I proposed a way to analyse the experimental data in [111] such that it accurately represents the killing properties of CTLs and is time independent. The PTA as I established can be employed to understand the dynamics of various systems that adhere to a certain set of rules that I have described in detail. The agent based model that I described in Chapter 3 can serve as a low cost and time efficient way to apply the PTA and to confirm if it gives expected results. Additionally, the ABM and PTA together can be used to understand the significance of observed properties for systems.

5.1 Constant System: Ratio of Killed Target Cells at Each Contact to Total Cells at Each Contact vs PTA

As discussed in equation (2.1), the equation for the ratio of killed target cells at each contact to total cells at each contact as calculated in [111] is:

$$R_{\mathrm{dead,i}} = \frac{D_{\mathrm{i}}}{A_{\mathrm{i}} + D_{\mathrm{i}}} \tag{5.1}$$

The equation for PTA that I have proposed in equation (2.5):

$$p_{\mathrm{obs,i}} = \frac{D_{\mathrm{i}}}{\sum_{k=i}^{m}(A_{\mathrm{k}} + D_{\mathrm{k}})} \tag{5.2}$$

To compare the differences between the results obtained by the methods of analysis outlined in equations (5.1) and (5.2) respectively, I analyzed observed data using these equations. As described in Chapter 2, I wanted to confirm whether the application of PTA to the Null hypothesis gives the same result for varying observation time windows.

To do so, I used the agent-based model described in Chapter 3 with the Null hypothesis. As discussed in Section (3.4), the probability of CTL mediated infected cell killing (p_0) remains constant as the number of CTL contacts increases in Null hypothesis. Thus, an observed change in calculated values will be a consequence of factors other than system dynamics. I ran simulations for the Null hypothesis with the probability of killing infected cells, p_0 as 0.2. I ran two simulations, one for a time of 120 minutes and another for 360 minutes respectively and analyzed the data using both methods of analyses (Figure 5.1a, b).

The plots obtained using the analysis method defined in equation (5.1) show a difference between observed killing frequencies when observed for different time windows. The plot for a longer time window shows a higher ratio of killed target cells at each contact to total target cells at each contact in comparison to the shorter time window. Another drawback of the method is that for either of the time windows, I am unable to obtain values for the probability of dead cells that accurately reflect the values that were input into the system. In this case, the value for cell death probability is p_0 at each contact. The value of p_0 was set to 0.2 but the values obtained from the observations are 0.3 and 0.4 for different time windows. On the other hand, the plots obtained by analysing the data using the new proposed method of analysis in equation (5.2) show no difference in values for different time windows. In addition to that, the values obtained from the analysis show a good agreement between the input and the observed value of $p_0 = 0.2$.

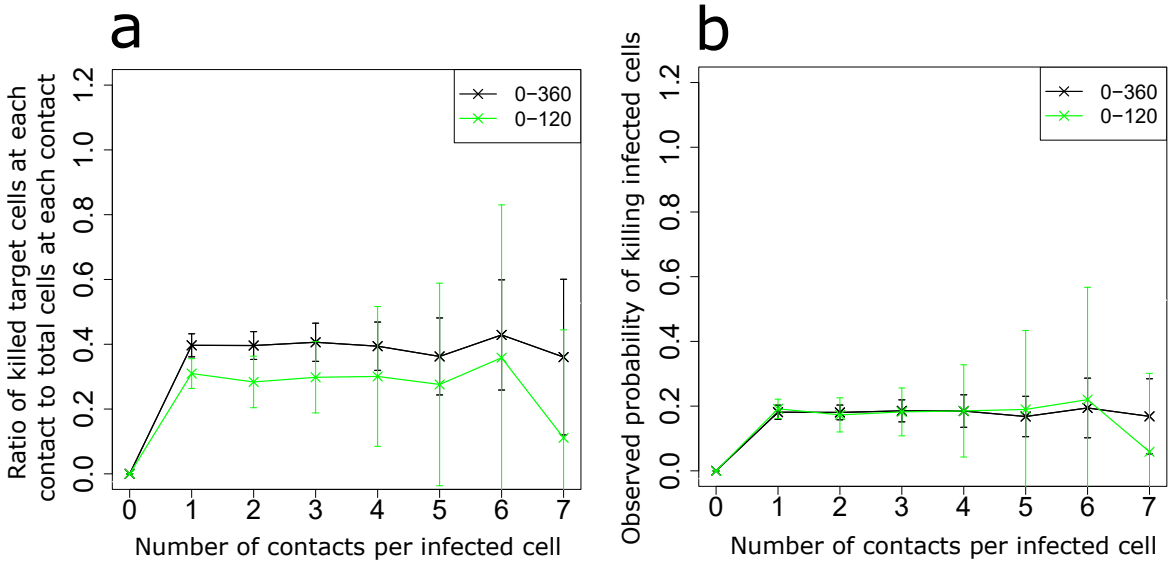

Figure 5.1: Comparison of data analysis methods for null hypothesis: (a) The ratio of killed target cells at each contact to total target cells at each contact for varying observation times gives a variation in results, (b) Observed probability of killing infected cells gives same values for both observation windows. Error bars represent SD from 50 simulations.

5.2 Application of PTA on Different Killing Hypotheses

Having established that the PTA gives a result that is not dependent on the duration of the observation window for the Null hypothesis, I investigated if the analysis gives a result that accurately describes the observed dynamics of the system.

I ran simulations for varying values of the p_0, k_T and k_I respectively for the three killing hypotheses described by Null hypothesis, CTL contact integration and infected cell contact integration. p_0 is the killing probability at each contact for the *Null hypothesis*, k_T is the probability of a CTL killing an infected cell at the first contact in *CTL contact integration hypothesis* and k_I is the probability of an infected cell getting killed at the first contact in *infected cell contact integration hypothesis*. I plotted the ratio of killed target cells at each contact to total cells at each contact (Figure 5.2 a-c) and the PTA values for all three hypotheses (Figure 5.2 d-f). The plots for the ratio of killed target cells at each contact to total cells at each contact for all three hypotheses show a difference for different parameter values but as discussed above, it is not possible to recover the values of probability of cell death after getting the i^{th} contact with a CTL (p_i) from these plots.

For all three killing hypotheses, the plots show dynamics that are easily distinguishable for varying parameter values (Figure 5.2 d-f). It is interesting to note that the plots for CTL contact integration killing hypothesis and infected cell contact integration killing hypothesis give rise to similar plots that show an increase in observed probability of killing infected cells with increasing number of contacts with CTLs (Figure 5.2e, f). An increase in CTL efficiency with increasing interactions (Figure 5.2e) and an increase of infected cell susceptibility (Figure 5.2f) to cell death, both show similar dynamics of an increase in the observed probability of killing infected cells with increasing CTL interactions. This implies that while the PTA can help differentiate the dynamics of the system, it cannot be used to know what causes the change in dynamics.

5.3 Varying Observation Times

A limitation of experimental systems is that the duration of observation window could vary. The same system under observation for varying time periods could show different results that could arise due to the difference in dynamics at a given time. Using PTA, I explored how various temporal variations in experimental systems affect the observations of various killing hypotheses.

Using the agent based model, I ran simulations for the (i) Null hypothesis; (ii) CTL contact integration; and (iii) infected cell contact integration. For each of these, I ran simulations for varying observation duration windows of 240 minutes, 360 minutes and 480 minutes and plotted the ratio of killed target cells at each contact to total cells at each contact (Figure 5.3 a-c) and the PTA values for all three hypotheses (Figure 5.3 d-f). For each of the hypothesis, I ran simulations

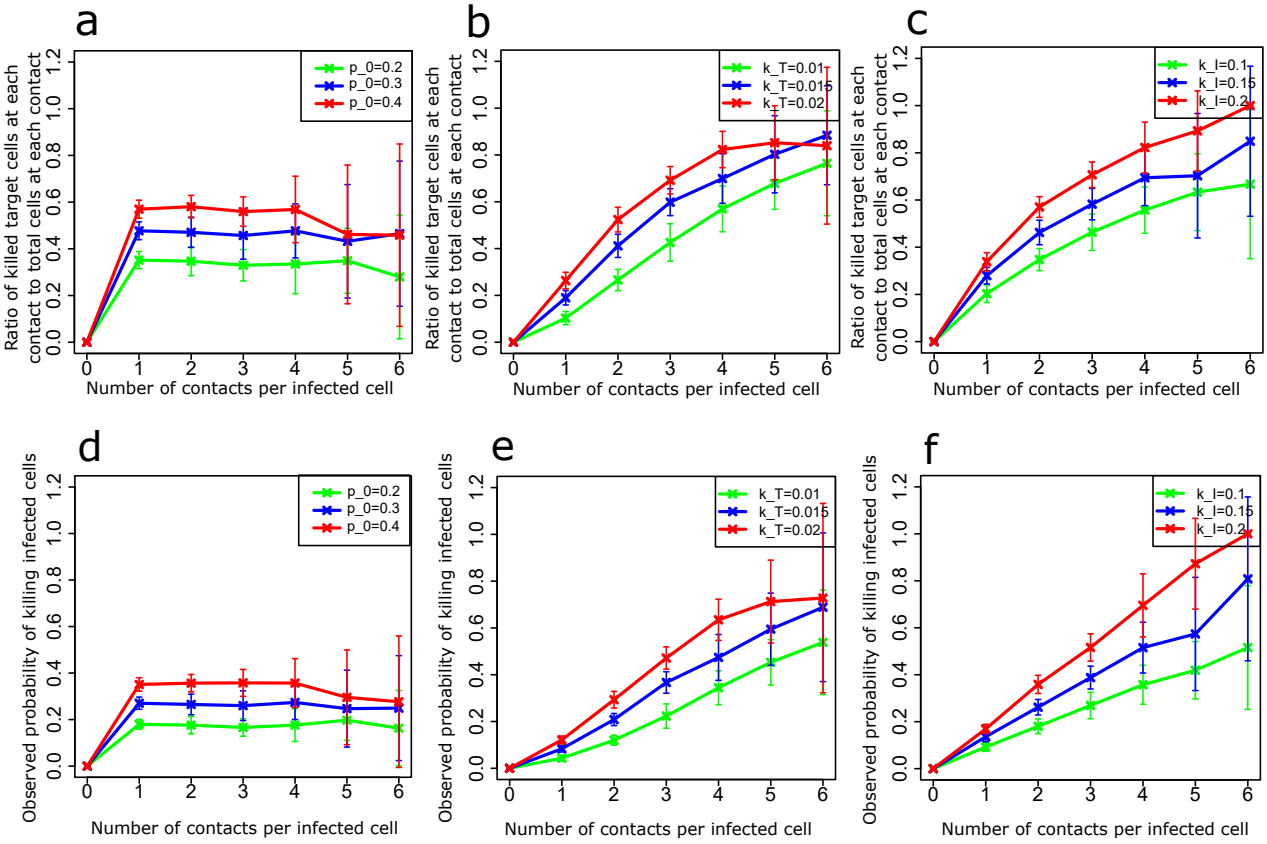

Figure 5.2: Computing the ratio of killed target cells at each contact to total cells at each contact and PTA to different killing hypotheses for varying parameter values for Null hypothesis for varying values of killing probability at each contact (p_0), CTL contact integration killing hypothesis for different probability of killing at first contact (k_{T}) and infected cell contact integration killing hypothesis for different probability of getting killed at first contact (k_{I}). The ratio of killed target cells at each contact to total cells at each contact for (a) Null hypothesis, (b) CTL contact integration killing hypothesis, (c) Infected cell contact integration killing hypothesis. PTA plots for (d) Null hypothesis, (e) CTL contact integration killing hypothesis, (f) Infected cell contact integration killing hypothesis. Error bars represent SD from 50 simulations.

from the optimal parameter values obtained in Chapter 4.

It is interesting to note that while the plots for the Null hypothesis do not show a difference for varying time windows, the same cannot be said for CTL contact integration or infected cell contact integration killing hypotheses. In the case of both the contact integration hypotheses, the system evolves as a consequence of increasing interactions. The number of interactions that the cells get changes with time. Hence, the system evolves with time. At two separate times, the population of infected cells will show different behavior in case of infected cell contact integration and the population of CTLs will show different behavior in case of CTL contact integration killing hypotheses. Thus, the PTA analysis gives different values at different times for systems whose properties evolve with time.

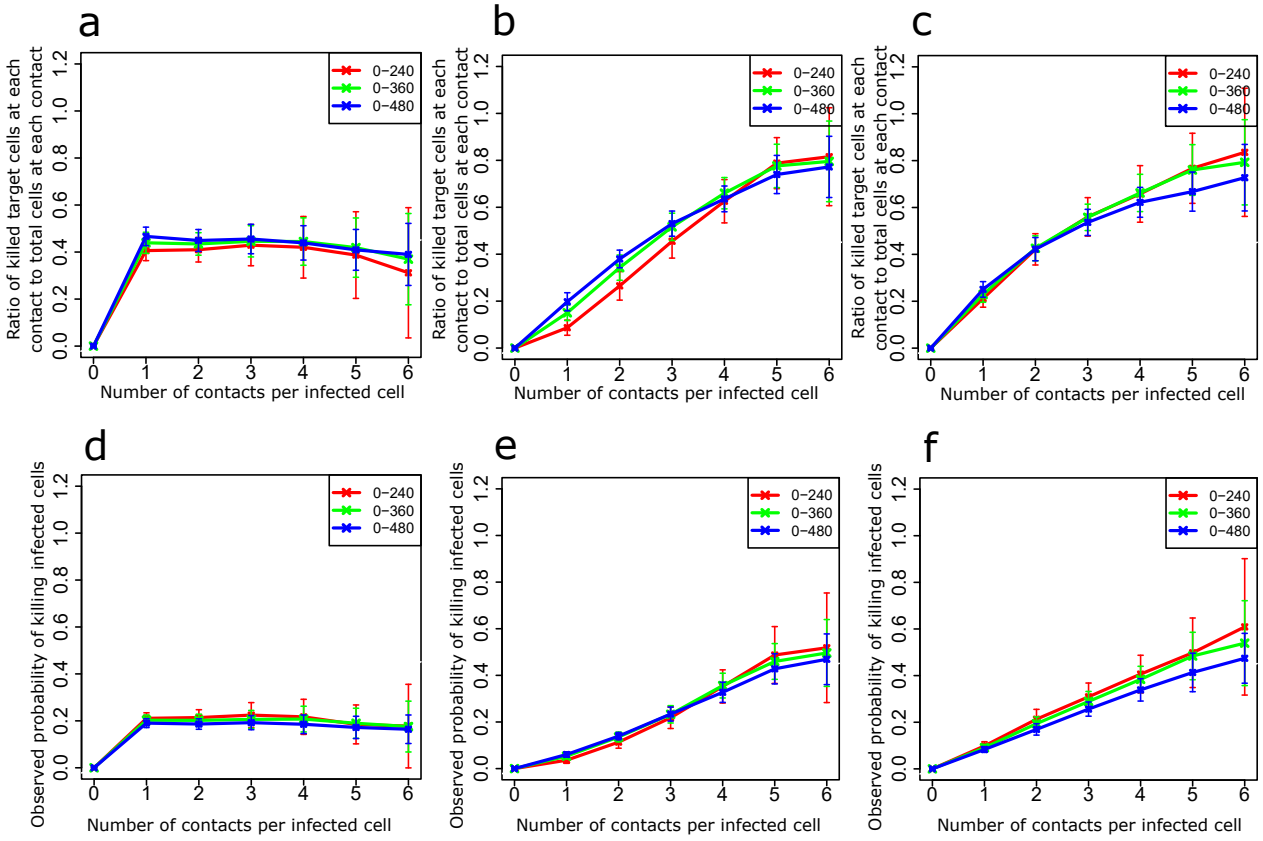

Figure 5.3: Varying observation windows to calculate the ratio of killed target cells at each contact to total cells at each contact and PTA to different killing hypotheses for Null hypothesis, CTL contact integration and infected cell contact integration. The ratio of killed target cells at each contact to total cells at each contact for (a) Null hypothesis, (b) CTL contact integration killing hypothesis, (c) Infected cell contact integration killing hypothesis. PTA plots for (d) Null hypothesis- The plots for varying observation windows are the same, (e) CTL contact integration killing hypothesis, (f) Infected cell contact integration killing hypothesis- The observed dynamics for the window of 0-240 minutes versus 0-480 minutes shows a significant difference (p-value=0.036). Error bars represent SD from 50 simulations.

5.4 Impact of Unknown History on Observed Results

Another temporal factor that affects the observed results is that experimental systems could have a history associated with them. Thus, in the system described in [111], the infected cells could already have had contacts with CTLs before the experimental observations were recorded.

Next, I investigated the effect of an unknown history on the observed plots. I ran the complete simulation for 480 minutes and observed the system for system for 240 minutes. This observation of 240 minutes was initiated at different time points (0 minutes, 120 minutes and 240 minutes). Thus, I compared how an unknown history of a system affects the plots obtained for the ratio of killed target cells at each contact to total cells at each contact (Figure 5.4a-c) and PTA (Figure 5.4d-f). Here I study how knowing the complete history (0 to 240 minutes) compares to having unknown history (120 minutes to 360 minutes and 240 minutes to 480 minutes).

It is interesting to note that for the Null hypothesis where the CTLs kill with an equal probability at each CTL-target cell contact, an unknown history does not affect the observed killing dynamics of the system (Figure 5.4d). That is due to the fact that the system does not evolve with time and the properties remain constant. On the other hand, for CTL contact integration and infected cell contact integration, the systems evolve with time and at a later time point, the system consists of more efficient CTLs and more susceptible infected cells respectively (Figure 5.4e, f). The value obtained from the PTA equals p_{i} (refer to Chapter 2, Table 2.1). For the case of Null hypothesis, the value of p_{i} remains unchanged with contacts but for CTL contact integration and infected cell contact integration, the value of p_{i} changes with contacts. Thus, as time progresses and CTLs and infected cells more contacts, the value of p_{i} for the cell population changes. Additionally, while the plots are different for the cases with unknown history and the complete known history, the plots do not show a significant difference for varying duration of unknown history for infected cell contact integration hypothesis (p-value=0.059). The system exhibits similar dynamics for an unknown history of 120 minutes and 240 minutes. This shows that in order to be able to compare two systems, it is important to start the observations at the same time to avoid any bias in results due to unknown history.

5.5 Summary

The PTA analysis for CTL mediated killing gives the probability of infected cell death at each contact. By comparing the plots for the ratio of killed target cells at each contact to total cells at each contact and PTA for Null hypothesis, I show that the PTA returns the value of p_{i} input into the system.

With the knowledge that PTA precisely represents the probability of killing infected cells at each contact, I could explore the impact of varying observation duration and unknown history on

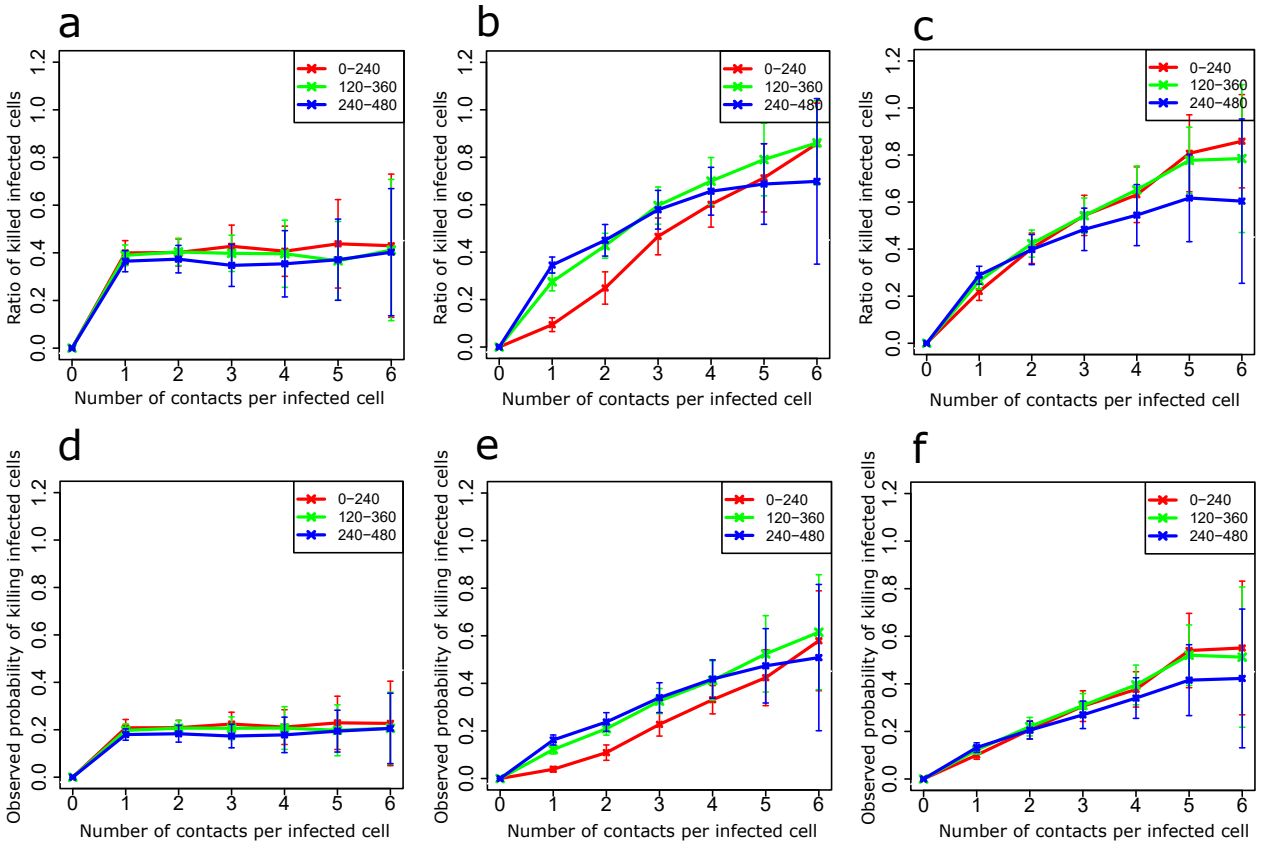

Figure 5.4: Varying unknown history duration to calculate the ratio of killed target cells at each contact to total cells at each contact and PTA to different killing hypotheses for Null hypothesis, CTL contact integration and infected cell contact integration. The ratio of killed target cells at each contact to total cells at each contact for (a) Null hypothesis, (b) CTL contact integration killing hypothesis, (c) Infected cell contact integration killing hypothesis. PTA plots for (d) Null hypothesis, (e) CTL contact integration killing hypothesis, (f) Infected cell contact integration killing hypothesis. Error bars represent SD from 50 simulations.

observed killing dynamics. In systems where the value of probability of infected cells to get killed at each contact varies with the number of contacts, the PTA gives rise to different results at different times. This result confirms that the PTA accurately gives the killing dynamics at different time points.

The varying PTA values obtained for varying time windows and unknown history also establish the futility of comparing two different experimental setups for the same system at different times. It also indicates that experiments involving CTL mediated killing should be planned to ensure that observations are taken at the same time.

Chapter 6

T Cell Activation

6.1 Introduction

T cell activation, as discussed in Chapter 1, takes place in the lymph node by forming transient and stable interactions between APCs and T cells. In 2015, Dong et al [114] showed that T cell motion changes as a consequence of antigen affinity. At steady state, T cells had high velocities and relatively persistent trajectories similar to amoeboid migration. In presence of low affinity antigen, T cells exhibit a switching migration mode that gives rise to T-cell exploratory behavior by means of partial deceleration and frequent direction changes. On the other hand, in the presence of high affinity antigen, T cells show pronounced deceleration. Whether the motion behaviour of T cells shows a gradual change with increasing signal integration still remains to be explored. To this end, Mayya et al studied the motion properties of T cells when they are getting activated. In this chapter, I have analyzed the motility properties of T cells with time and I have also studied the impact of increasing number of kinapses on the speed and turning angle.

Additionally, using PTA (refer to Chapter 2), I have computed the probability of T cell permanent arrest with increasing number of kinapses. I did this for different antigen concentrations, allowing me to explore the impact of antigen concentration on T cell arrest.

6.2 Methods

The lymph node is a dynamic, 3D environment and the study of kinapses and synapses proved to be difficult *in vivo* due to internal tissue movement and limitations of 3D rendering. To this end, in 2018, Mayya et al. used a system to observe the properties of T cell interactions with T cell receptor stimuli such that it was free of other influences that arise in an *in vivo* setup [207]. The system involved studying the behavior of freshly isolated human and mouse T cells. These T cells were introduced on a glass surfaces consisting of 2D stimulatory surfaces (Figure 6.1). The 2D

stimulatory spots, which were equally distributed along length and breadth of the glass surface were circular in shape. The radius of each antigen spot was 5 μm and the distance between the centres of each antigen spot was 30 μm. They were uniformly coated with ICAM1 and Okt3 antibody. The ICAM1 is an adhesion molecule whereas the anti-CD3 molecule interacts with antigen receptors associated with CD3 molecular complex on T cell surface to induce T cell activation [208]. This system is a general representation of the spatially uniform presentation of antigen to T cells by the dendritic cell network as seen *in vivo*. Using this setup, the motion properties of T cells were tracked for 2 hours. The experiment was done for three antigen concentrations on the spot: 1 μg/ml, 2 μg/ml and 4 μg/ml. As a control, one experimental setup also included the isotype (iso) antibody which does not trigger the TCR. This is a good control for confirming the temporal evolution of the system due to intermittent signaling.

At any given point in the experiment, prior to permanent arrest on the antigen spot, a T cell in motion could exist either in kinapse mode while interacting with an antigen spot or a T cell could be moving in the 2D space in a searching mode. Each of these kinapses are temporary interactions between T cells and antigen that eventually lead up to synapse formation which is the permanent arrest. The data recorded from the experiments consists of the x- and y-coordinate of T cells along with the associated time stamp. Thus, we can use this information to calculate the speed and turning angle of T cells. Since the two states that a T cell can exist in have different motility properties, I used the data obtained from the experimental data to study the impact of increasing number of kinapses with antigen spots on the motility properties of T cells during both phases.

The types of experimental data recorded at each time point in the experiments are:

1. x- and y-coordinate: The coordinates can be used to calculate the speed and to know if a T cell is arrested.

2. IRM attachment area: By making using of interference reflection microscopy (IRM), the area of attachment to the underlying substrate is recorded.

Using the above data, the speed over four steps is calculated and compared to the threshold speed ($v_{\text{threshold}}$). In the same way, the IRM attachment area of the T cell is compared to the IRM attachment area threshold ($a_{\text{threshold}}$). The values for $v_{\text{threshold}}$ and $a_{\text{threshold}}$ are based on observations of T cell arrest from experimental data. In this system, $v_{\text{threshold}} = 1.5\mu$m/s and $a_{\text{threshold}} = 5\mu\text{m}^2$.

The T cells can be in one of three possible states based on their motility properties and the three states can be separated using the coordinates and IRM attachment area values (Table 6.1).

T cell states	Speed	IRM attachment area
Searching mode	No condition	$< a_{\text{threshold}}$
Kinapse	$> v_{\text{threshold}}$	$> a_{\text{threshold}}$
Arrested	$< v_{\text{threshold}}$	$> a_{\text{threshold}}$

Table 6.1: Format of data output of infected cells killed by CTLs

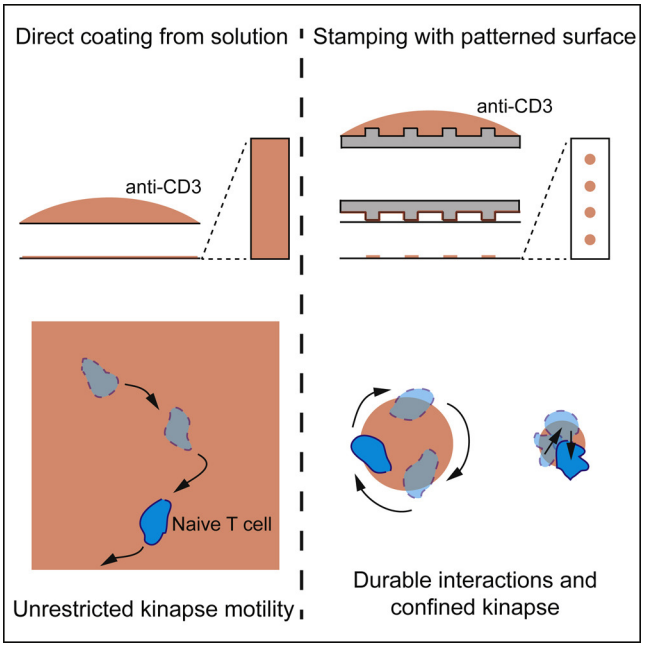

Figure 6.1: The experimental setup to study T cell motion properties consists of 2D stimulatory surfaces coated with antigen. Figure reproduced from [207].

6.3 Change in T cell Motility Properties Over Time

To quantify the change in T cell speed and turning angle over time, I divided the recorded data into time blocks of 20 minutes each. I started this analysis at 50 minutes to rid the analysis of any bias or perturbation caused by the introduction of T cells to the system. For each block of 20 minutes, I calculated the speed and turning angle using the recorded coordinates and time. These values were then pooled to give the average speed and turning angle (Figure 6.2).

There is a drop in the average speed of T cells in all cases except for where there is no antigen (Figure 6.2a). Another salient feature of the plot is that the average speed is lower at higher antigen concentrations (Figure 6.2a). On the other hand, the turning angle does not show a change with time but it is interesting to note that the turning angle is lower for the experiment with no antigen (Figure 6.2b).

Based on the patterns that the speed and turning angle follow, I hypothesized that T cells get arrested on the antigen spots as time progresses, leading to a decrease in speed values. To test this, I removed the arrested portions from the recorded data. The portions that remained after removing arrested portions were T cell tracks that were in kinapse or searching mode. Using

these T cell tracks, I repeated the analysis for 20 minutes time blocks (Figure 6.3). In contrast to what was observed previously, on removing the arrested T cell tracks, the average speed of T cells does not show any change with time till nearly 170 minutes. After 170 minutes, the average speed value for T cells shows a decrease for lower antigen concentration but remains the same for higher antigen concentration. Interestingly, the average speed value shows an increase in the absence of antigen. The turning angle, on the other hand, remained constant with time.

The average speed values of T cells (Figure 6.2a) for different antigen concentrations show smaller values for higher antigen concentration as time progresses but on excluding the arrested portions, the speed remains the same for all antigen concentrations till 170 minutes (Figure 6.3a) suggesting that the drop in speed observed in Figure 6.2a is a consequence of arrested T cell tracks. Together, Figure 6.2 and Figure 6.3, show that T cells get arrested on antigen spots leading to a decrease in the average speed of the T cell population. A sharper drop in T cells' speed indicates that a larger number of T cells are arrested on antigen spots. Thus, the results also show that a higher sub-population of T cells get arrested in the presence of higher antigen concentration.

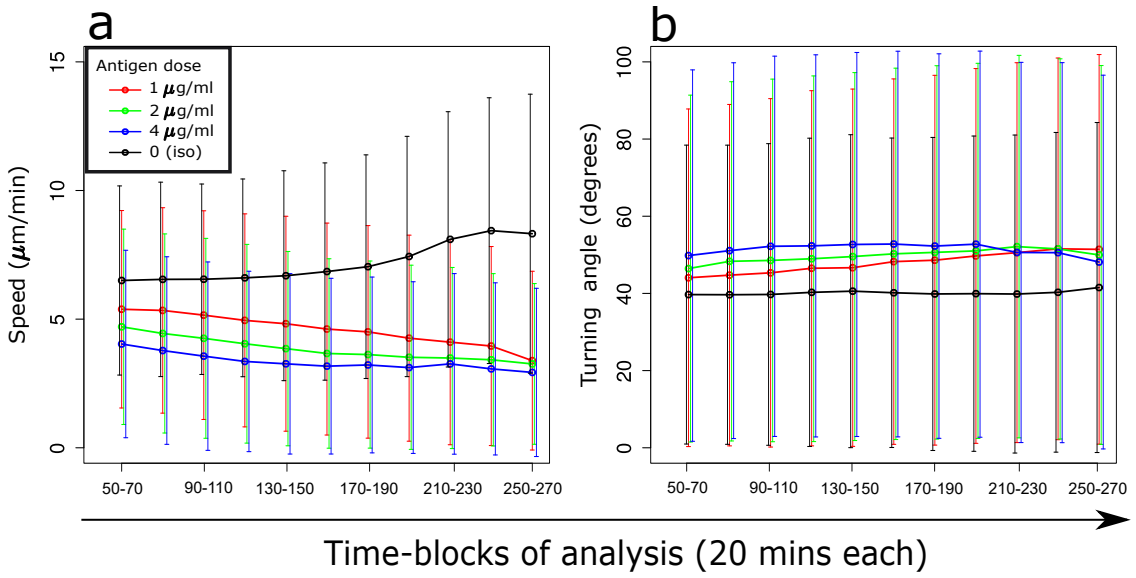

Figure 6.2: Motility properties of T cells over 20 minutes time blocks: (a) The speed of T cells decreases with increasing time, (b) The turning angle does not show significant change over time but the turning angle is lower for the setup with isotype antibody. Error bars represent SD. Mean and SD are computed by analysing 7592 cell tracks for 1 μg/ml antigen concentration, 15,288 cell tracks for 2 μg/ml antigen concentration, 12,313 cell tracks for 4 μg/ml antigen concentration and 14,183 cell tracks for isotype antibody.

6.4 Effect of Increasing Kinapses on T cell Motion Properties

The change in speed of T cells in the presence of antigen raised an interesting question about the effect of increasing number of kinapses on motility properties. In the system, as time progresses,

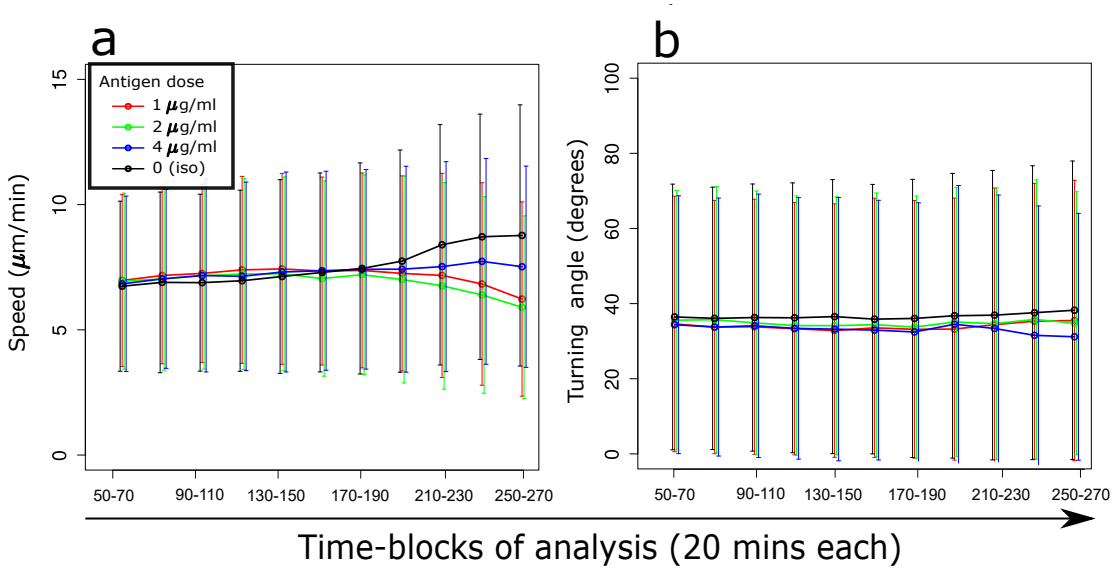

Figure 6.3: Motility properties of T cells over 20 minutes time blocks excluding arrested T cell tracks: (a) The value of speed for T cells remains constant with time, (b) The value of turning angle for T cells remains constant with time. Error bars represent SD. Mean and SD are computed by analysing 7592 cell tracks for 1 μg/ml antigen concentration, 15,288 cell tracks for 2 μg/ml antigen concentration, 12,313 cell tracks for 4 μg/ml antigen concentration and 14,183 cell tracks for isotype antibody.

T cells have multiple kinapses with antigen spots. We hypothesized that the motion properties of T cells change as a consequence of signal integration. To test if an increasing number of kinapses have an effect on the motion properties, I used the criteria defined above for kinapses and searching mode to separate the T cell tracks into the two phases. I plotted the T cell speed and turning angle in both phases as a function of the number of kinapses a T cell had had (Figure 6.4).

From the plots, it can be seen that neither the speed, nor the turning angles are impacted by the increasing number of kinapses that a T cell has had. These plots deny the presence of signal integration in T cells on the level of motion properties.

6.5 Duration of Kinapses

The separation of T cell tracks into kinapse and searching mode also gave an insight into the duration of kinapses of T cells with antigen spots. I questioned whether the duration of kinapses changes as a consequence of increasing number of kinapses. I used the T cell tracks to explore the effect of prior kinapses on the duration and plotted the duration of all kinapses as a function of the prior kinapses that the T cell had had (Figure 6.5). The obtained plot shows that the average duration of most kinapses in this setup is in the range of 70 to 90 seconds but the average remains unchanged with time and antigen concentration. Due to the large error bars seen in the plot, I am unable to draw any further conclusion on the effect of increasing number of kinapses on kinapse duration.

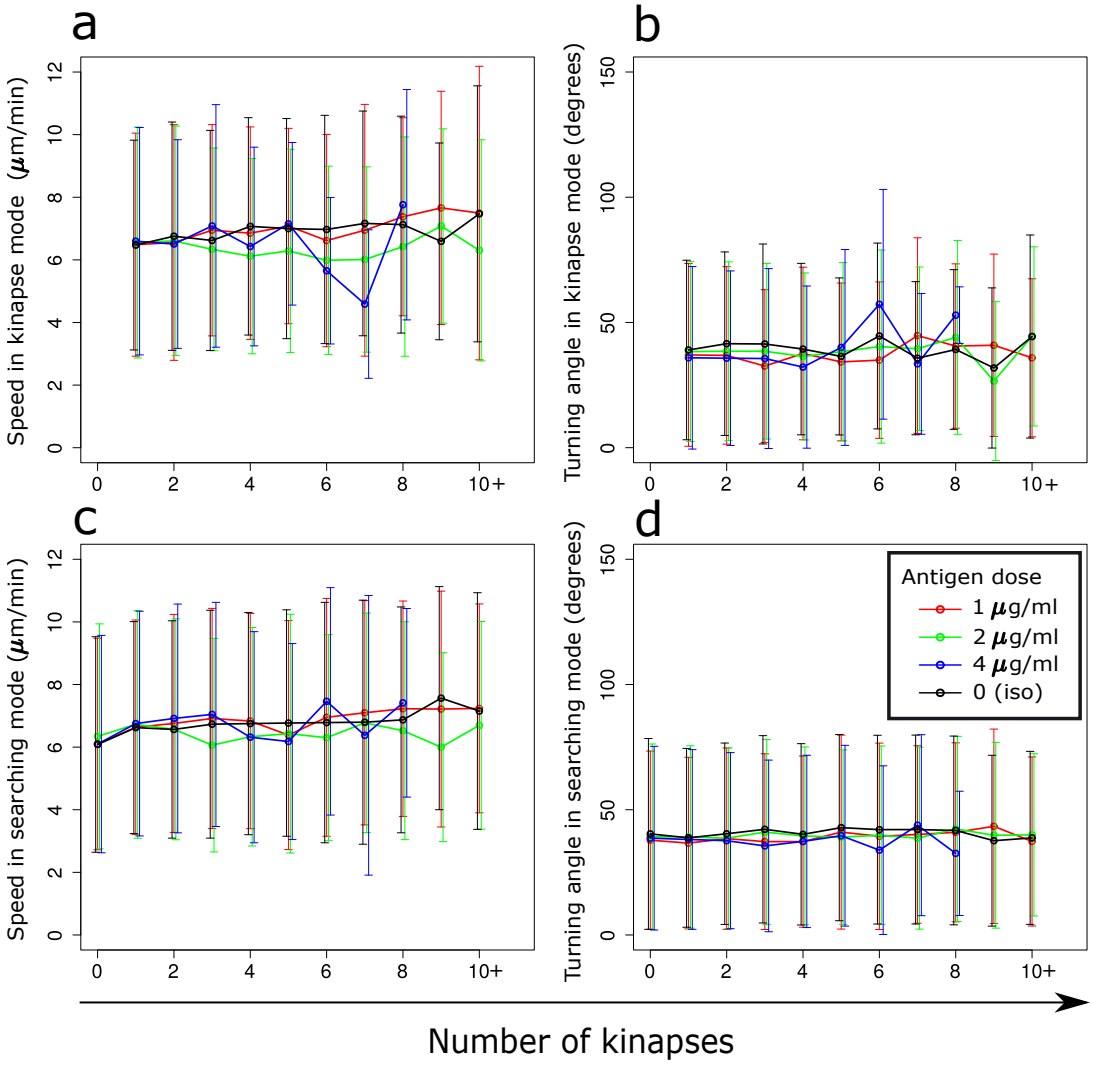

Figure 6.4: T cell motion properties as a function of the number of kinapses that the T cell has had: (a) Speed of T cells in kinapse mode, (b) Turning angle of T cells in kinapse mode, (c) Speed of T cells in searching mode, (d) Turning angle of T cells in searching mode. Error bars represent SD. Motion properties during kinapse and searching mode are computed by analysing 7592 cell tracks for 1 μg/ml antigen concentration, 15,288 cell tracks for 2 μg/ml antigen concentration, 12,313 cell tracks for 4 μg/ml antigen concentration and 14,183 cell tracks for isotype antibody.

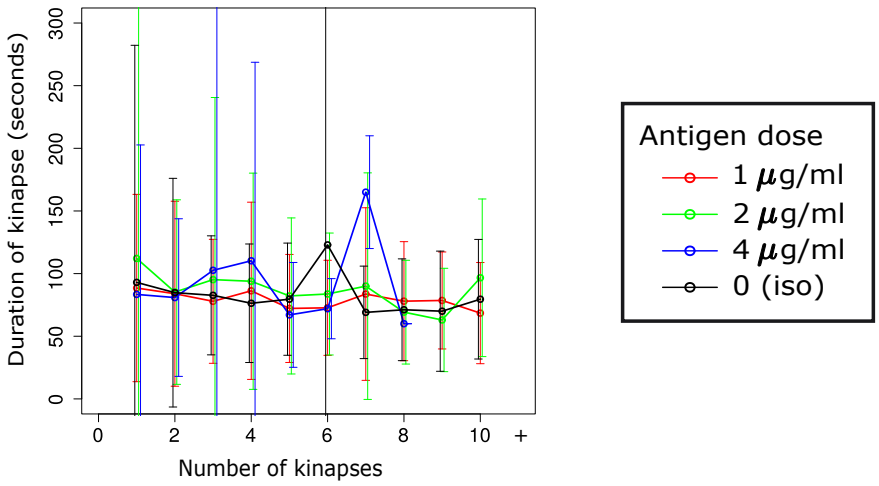

Figure 6.5: Duration of kinapses of T cells as a function of the number of prior kinapses that the T cell has had. The number of kinapses and SD for each antigen concentration were calculated by analysing 7592 cell tracks for 1 μg/ml antigen concentration, 15,288 cell tracks for 2 μg/ml antigen concentration, 12,313 cell tracks for 4 μg/ml antigen concentration and 14,183 cell tracks for isotype antibody.

6.6 Kinapses Needed for T cell Arrest

An interesting feature seen in Figure 6.5 is that while with lower antigen concentrations T cells go on to have more than 10 kinapses, T cells in the presence of 4 μg/ml do not get more than 8 kinapses prior to synapse formation. This led to a question about the number of kinapses needed before a T cell gets arrested at different concentrations.

With information about when T cells are in arrest and the number of kinapses that a T cell has before arrest, I plotted the number of T cells that are arrested as a function of the total kinapses that the T cell had had (Figure 6.6a). I also normalized the number of T cells arrested after each kinapse with all T cells that got permanently arrested by the end of the experiment (Figure 6.6b).

An interesting observation from these plots is that a large fraction of T cells needs just one kinapse to get permanently arrested on antigen spots. Another striking observation is that the fraction of cells that get permanently arrested to antigen spots is higher at higher antigen concentration values. This suggests that at higher antigen concentrations, T cells accumulate signal more quickly.

6.7 Probability of Permanent Arrest

On careful consideration of the system described above, it can be seen that it fits into the general framework of a system where the PTA can be applied. As described in Chapter 2, a system needs to consist of a species undergoing an irreversible change as a result of a recurring event. Here the species undergoing a change are the T cells, the recurring events are the kinapses with antigen spots and the irreversible change is T cell arrest on an antigen spot. This reinforces the versatility

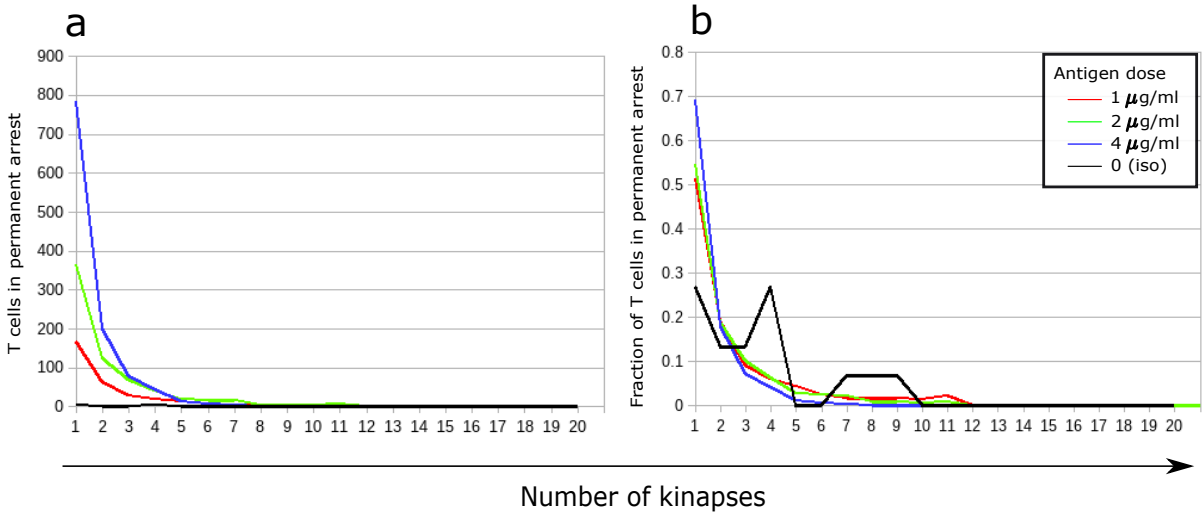

Figure 6.6: (a) Number of T cells forming synapses as a function of increasing number of kinapses, (b) Fraction of T cells forming synapse as a function of increasing number of kinapses. Number of T cells under permanent arrest as a function of number of kinapses calculated by analysing 7592 cell tracks for 1 μg/ml antigen concentration, 15,288 cell tracks for 2 μg/ml antigen concentration, 12,313 cell tracks for 4 μg/ml antigen concentration and 14,183 cell tracks for isotype antibody.

of PTA and opens up the possibility of exploring the impact of increasing number of kinapses on the probability of T cell arrest on antigen spot.

The equation for PTA as discussed in Chapter 2 is:

$$p_{\mathrm{calc,\,i}} = \frac{C_{\mathrm{i}}}{\sum_{k=i}^{m}(S_{\mathrm{k}} + C_{\mathrm{k}})} \tag{6.1}$$

where C_{i} is the number of elements that transitioned at exactly i recurring events and S_{i} is the number of elements that did not transition at exactly i recurring events. In the current system, C_{i} are the number of T cells in permanent arrest at exactly i kinapses and S_{i} are the T cells not in permanent arrest after i kinapses.

I analysed the experimental data for all three different antigen concentrations (1 μg/ml, 2 μg/ml and 4 μg/ml) to understand how different antigen concentrations affect the probability of arrest (Figure 6.7).

The analysis shows that while an increasing number of transient contacts do not lead to an increase in observed fraction of arrested T cells per contact, the antigen concentration plays a significant role in it. The fraction of arrested T cells is highest for 4 μg/ml and lowest for 1 μg/ml implying that the cells have a higher tendency to get arrested at higher antigen concentrations.

The conclusion that T cells have a higher probability of arrest at higher antigen concentrations also supports the trend seen in (Figure 6.2a). As discussed in Section 6.3, the decrease in speed values is greatest for an antigen concentration of 4 μg/ml and lowest for 1 μg/ml showing that a larger number of T cells get arrested at higher concentrations. This results suggests that a larger

number of arrested T cells would lead to higher number of activated T cells at higher antigen concentration and thus, a higher antigen concentration would lead to a stronger T cell response.

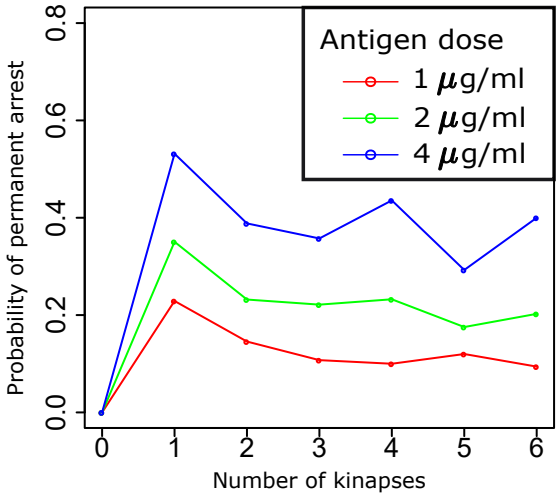

Figure 6.7: Probability of synapse formation with increasing number of kinapses

6.8 Summary

In this chapter, I have explored the change in T cell motion properties with time. The analysis of speed and turning angle with increasing kinapses did not give enough evidence for the effect of T cell signal integration on motion properties. Additionally, the probability of T cell arrest with increasing number of kinapses does not vary significantly showing that there is no signal integration on the level of synapses either.

On the other hand, I showed that T cells in the presence of higher antigen concentration have a higher probability of synapse formation as compared to T cells in the presence of lower antigen concentration. Interestingly, for all antigen concentrations, a majority of T cells form synapses after just one kinapse.

Chapter 7

Discussion

7.1 Probability of Transition Analysis

In vivo 2-photon microscopy-based imaging of CTL-mediated immunity [111] showed that infected cells need more than one contact with CTLs to get killed. But the exact impact of increasing number of interactions with CTLs on probability of killing infected cells remained unknown. As this finding was new and challenged the 'one kiss-one kill' dogma, the field critically lacked a method to analyze experimental data and give a quantification of killing at the cell level. To this end, I proposed the probability of transition analysis (PTA). The PTA involved extracting the probability that an infected cell would get killed as a function of contact number with CTLs.

7.1.1 Properties of PTA

The PTA gives the observed probability of death at exactly the i^{th} interaction ($p_{\text{obs, i}}$). The value of $p_{\text{obs, i}}$ is given by normalizing the number of dead infected cells with exactly i interactions by the number of infected cells that have survived the i^{th} interaction. For a system where the input probability of death equals p_{i} for the i^{th} interaction, the use of PTA gives:

$$p_{\text{obs, i}} = p_{\text{i}} \tag{7.1}$$

By mathematically deriving a general expression for the probability of killed infected cells at each contact, I showed that the results obtained from applying PTA are independent of other properties of the experimental setup such as time and density of cells. If the value of p_{i} was a function of time, the value obtained from PTA also changed with time but this change reflects how the killing dynamics of the system are changing with time. The results obtained from PTA accurately reflect the killing properties of the system.

To further test the PTA, I used the agent-based model (ABM) together with PTA. Each

hypothesis in the ABM had a hypothesis dependent killing parameter. For all hypothesis when I entered different values of the killing probability, I was able to recover the value of p_{i}, thus showing the benefit of PTA.

I used the PTA to analyze the experimental data obtained from [111] and showed that the observed probability of killing ($p_{\mathrm{obs,\,i}}$) infected cells linearly increased with increasing interactions with CTLs. This gave us a clear insight into the dynamics of CTL mediated killing of infected cells *in vivo* making it possible to propose different mechanisms for cell killing at the cellular level.

7.1.2 Versatility of PTA

The versatility of the PTA imply that it can be applied to a broader class of biological and non-biological problems. In particular, PTA is suited for the analysis of agents undergoing an irreversible change as a result of recurring events. Using PTA, we can understand the impact of the recurring event (T cell meeting cells loaded with antigen) on the irreversible change (activation or killing).

Further PTA can be used to differentiate between the signal integration hypothesis and probabilistic priming hypothesis of T cell priming in lymph nodes [209]. The signal integration regime would give rise to an increase in the value of $p_{\mathrm{calc,\,i}}$ with increasing i whereas the probabilistic priming regime would give a constant value of $p_{\mathrm{calc,\,i}}$ for increasing values of i.

Thus, I showed that the PTA is an elegant methodology and the successful application of PTA to two systems, reinforces its usefulness and versatility.

7.1.3 Positives and Negatives of PTA

The power of the PTA method is to reveal killing properties that change the observed behaviour of the system with time. For a system such as infected cell contact integration, at the initial time point all infected cells have had very few contacts and will therefore take more contacts to die. But for the same system, analyzed from at a later time point, infected cells have had contacts with CTLs and will get killed with a smaller observed number of contacts. The results obtained from the PTA will reflect that and the PTA will give rise to different results at different time points. But this is not an artefact of the PTA and instead shows us how the system behaviour evolves.

As a limitation of the PTA, it is only an analysis method that does not give a direct insight into the cause behind the observed dynamics. For instance, using PTA alone, an observed increase in probability of killing infected cells at increasing number of CTL contacts cannot be used to conclude if the increase is caused due to change in infected cell or CTL behavior. But by designing and studying an experimental setup with the number of CTLs as the limiting factor versus a system with the number of infected cells as the limiting factor and making using of the PTA, it would be possible to differentiate between the two possibilities. Additionally, observations taken at fixed

intervals in contrast to taking observations only at the end would also be a way to distinguish between hypotheses.

7.2 Modeling of T Lymphocyte Mediated Killing

The PTA showed that the probability of killing infected cell increased with increasing number of interactions with CTLs. Using the understanding of the system killing dynamics from PTA, I could propose various potential mechanisms that could give rise to the increase in observed probability. To differentiate between the proposed mechanisms, I developed a 3-dimensional agent-based model. This model was used to observe the killing patterns that emerge from various hypotheses, giving us possible ways to differentiate between hypotheses. The model consisted of CTLs which moved and initiated interactions with stationary infected cells in a three-dimensional space. The properties of the agent-based model such as the speed and turning angle of CTLs, the positioning of infected cells, the size of CTLs and infected cells were all taken from experimental data making the ABM an accurate representation of the experimental system.

Based on the different hypothesis, CTLs made a decision to kill infected cells during the interactions. I used the ABM to focus on the question of how to best model the CTL-mediated killing and or other mechanisms that could help to better explain the observed CTL killing dynamics.

The results from the ABM show that by assuming an immediate removal of infected cells from the system after the decision for cell death is taken, I was unable replicate the dataset for observed time between the first contact to a CTL and the actual cell death for all killing hypotheses. The failure to replicate the dataset led to a major result that infected cells are not removed immediately from the system. Instead, they persist in the system for a certain duration in a state of activated apoptosis (T_{death}) which is in agreement with previous studies [210]. T_{death} is an unknown parameter that affects the results significantly. A non-zero value of T_{death} raises questions about the behaviour of apoptotic infected cells. One such question is about the presence of interactions between CTLs and infected cells that are in a state of activated apoptosis (zombie contacts).

Using the agent-based model, I showed that the Null hypothesis in the absence of zombie contacts did not give rise to an increase in probability of killing infected cells at higher interactions. This is an observation that was to be expected as the Null hypothesis is a contact history independent killing mechanism. Instead, the absence of zombie contacts, retention of information about prior contacts, by either CTLs or infected cells, might be a phenomenon that explains all the observed datasets. Thus, I proposed damage-based hypotheses as potential mechanisms by which the retention of contacts by infected cells is implemented. Interestingly, the hypotheses of damage, saturated damage and concomitant damage and repair are not consistent, because a too low damage rate was imposed by the data (Figure 3.4a) leading to a contradiction of experimental

and simulated observed time between first CTL contact and cell death (Figure 3.4b). While the infected cell contact integration hypothesis describes a system where the number of CTL contacts determines cell death, the damage-based hypotheses also resolve the duration of the interactions, i.e. a longer interaction leads to a greater damage [211–213]. The simulation results suggest that the number of contacts with CTLs rather than the time integration of signals is critical for the target cell fate decision.

Surprisingly, in the presence of zombie contacts a contact history independent killing could give rise to an increase in the probability of killing infected cells with increasing interactions with CTLs. This observed increase in the presence of zombie contacts raises the question if in the experimental system, the killing is getting more efficient or it is an artefact of zombie contacts.

In addition, for all the hypotheses, a better fit with experimental data was found in the presence of zombie contacts, suggesting that there is a substantial time between the decision of death and actual disappearance of the cell, and that it is critical to study the behavior of cells during this period. The development and use of accurate reporters to identify the apoptotic state would be a useful next step. Notably, caspase activity reporter systems might be useful [214], but it is typically not clear at what stage of caspase activity does the pro-cell death pathway pass an "irreversibility threshold" in the context of ongoing CTL attack. Cell damage results in the initiation of Ca2+ signals, which trigger necrotic or apoptotic cellular death [215]. Thus, another way to know when an infected cell is dying is by the use of calcium sensors. Better *in vivo* sensors of target cell viability will be helpful to better define the "point of no return" of CTL-mediated target cell killing and can subsequently help in confirmation of zombie contacts.

The modulation of CTL properties with increasing number of contacts with infected cells could make CTLs less or more efficient. In the literature about CTL-mediated immunity against chronic infections or cancer, CTL exhaustion has been described [162,163]. Exhaustion in context to CTLs is usually defined as a reduced protective response in response to an ongoing antigenic activation. As an example, during virus infection, it is believed that exhausted CTL lose activities like direct killing and cytokine production [216, 217]. These mechanisms are in general viewed as negative modulation of the killing capacity of CTLs [169]. On the level of a single cell, a CTL that has interacted with multiple infected cells could become less cytotoxic. This would lead to a decrease in ability to kill target cells. As expected, none of the parameter values tested indicated the decreased killing of infected cells per contact (data not shown). This suggested that at the time point studied and within the duration of analysis and in this experimental setting, exhaustion at the time-scale of multiple contacts is not a viable hypothesis. All these results when taken together show that our data is compatible with a model where CTLs could increase their killing efficiency with each contact to target cells (CTL contact integration hypothesis). The CTL contact integration hypothesis eventually gives rise to a diverse population of CTLs that show heterogeneity during killing. This is in agreement with studies showing that CTLs have different killing properties

that contribute to a robust T cell response [218, 219].

It is important to note that the duration of contacts between alive infected cells and CTLs, and zombie contacts was taken from the same distribution. At present, the data from experiments gives one distribution for duration of contacts. The possibility of two distinct distribution of duration of contacts can be tested through sensors to detect apoptotic phase of infected cells.

In general, I showed that only one dataset is not enough to discriminate hypotheses, but rather their combination. For all the hypotheses, I was able to replicate the plot for observed probability of killing infected cells for a certain set of parameters. If the best hypothesis had to be selected on the basis of just the plot for observed probability of killing infected cells, it would not be possible. These sets of parameters that were optimum for a certain plot did not necessarily give a good agreement with other plots. In the rejected hypotheses, the parameter sets that are consistent with one dataset are not consistent with the other one. Thus, in order to discriminate between the proposed hypotheses, multiple datasets need to be analyzed.

I also proved that the hypotheses that work do so only for a short range of values, meaning that for each successful hypothesis, the killing rates could be identified. Using a heatmap to find the best parameter range, even the values of the time to die T_{death} could be identified which is an important hidden biological parameter. A fascinating aspect of the estimated value of T_{death} is the variation in calculated values between different hypotheses. The different values of T_{death} for different hypotheses could be used to distinguish between killing mechanisms. Also, the variation emphasizes the complexity of the ABM and the detail into which we can go with it.

The 2-photon imaging datasets shown in Figure 3.4 cannot directly identify whether the CTL-mediated killing rate is constant or integrated on the CTL or infected level. However, I showed here that more indicators can discriminate these remaining hypotheses. A first indicator is the killing efficiency of CTLs, as defined by per capita killing rate of CTLs (PCKR) which is defined as the number of infected cells killed per CTL in 24 hours [220]. The PCKR values obtained for the final hypotheses are different for varying number of initial CTLs and infected cells. The varying values of PKCR as a function of cell density suggest that a careful measurement of PKCR values for different cell numbers is suitable to discriminate the hypotheses. It is also surprising to note that even at very low number of infected cells, the CTLs still fail to kill all infected cells which contradicts the rapid CTL mediated killing seen in other studies [192]. This could be a consequence of random cell movement and raises the question whether directed cell movement where CTLs actively migrate towards infected cells is important to ensure successful elimination of more infected cells.

In [111], the PCKR values were found to range from 2 to 16. It is interesting that with our model, the hypothesis that gives the values most consistent with this range is the Null hypothesis in the presence of zombie contacts but this information isn't enough to reject the other hypotheses. The significance of cytotoxicity mediated by CTLs and the impact of the number of cells on

PCKR and fraction of killed infected cells are especially important due to the role of T cells in viral infections such as HIV, pneumonia and other diseases such as cancer [175, 221].

The fraction of total killed infected cells shows a linear increase with increasing number of CTLs, implying that CTL mediated killing follows mass action killing kinetics. Previous studies have shown that T cells show mass action killing kinetics in the spleen [197] and our results suggest a similar dynamic in the lymph node.

A recent study [222] reported a higher PCKR value at low CTL to infected cell ratio. In the simulations, we observe a similar behaviour when we vary the number of infected cells while keeping the number of CTLs constant (Figure 4.6b). But it was not in agreement with the results obtained when keeping the number of infected cells constant and varying the number of CTLs. Thus, our results suggest that instead of the ratio of CTLs to infected cells, the number of infected cells impact the PCKR values.

7.3 Limitation of Experimental Values

The experimental values used to discriminate between hypothesis gave us a detailed insight into the dynamics of the lymph node. But due to the complexity and length of the experiments, the sample size for all datasets was relatively small. The dataset for observed probability of killing infected cells had values for up to 14 CTL contacts. The number of cells which had 7 or more contacts with CTLs were just 3. Thus, I discarded these data points as they are not statistically significant. The limitation of rejecting these data points is that I could not discriminate between two hypothesis that were behaving similarly for smaller number of contacts and had different behavior for higher number of contacts.

In the experimental setup, CTLs exit and enter the area under observation. This implies that the history of all CTLs under observation is not known. This property of the experimental system makes it difficult to draw conclusions about the CTL behavior based on prior contacts. In the ABM, I have assumed that CTLs that leave from one side enter from the other making it possible to keep track of CTL history.

7.4 Comments on Model

7.4.1 Agent Based Modeling in Retrospect

The ABM developed in this study achieves a good level of accuracy without compromising on its simplicity. Including the speed, turning angle and duration of contact from experimental data makes the model similar in behaviour to an actual lymph node. Further, the inclusion of these values from experimental data accounts for the impact of other cells in the lymph node.

The reason for choosing the agent-based modeling technique was to zoom into the properties of the system that cannot otherwise be observed due to its bottom up approach [205]. These include things such as the killing mechanism, the value of T_{death} and the presence of zombie contacts. While other approaches to study CTL mediated killing such as differential equations and chemical kinetics have been employed extensively, the complexities that can be incorporated using the ABM gives cannot be done easily from other modeling approaches. An example of this would be to model the spatial heterogeneity of the system. With ABM, it is much easier to implement a heterogeneous space while EBMs work well for a homogeneous population. In the ABM developed in this study too, the infected cells are not distributed uniformly throughout the space and the implementation of this property was simple.

For the system described above, the other option would be to have an equation-based model (EBM). EBM employs a set of equations to describe the properties of the system. Ordinary and partial differential equations are two examples of this approach. The shortcoming of EBM in comparison to ABM is that it can only be used to model output with real system behavior on a systems level but the behavior of individual units cannot be validated [223, 224]. On the other hand, ABMs focus on the individual behavior of the components, thereby offering an additional layer of validation. This is also seen in the ABM of the lymph node, where all agents behave independently allowing for a greater variation between cell behavior, thus, making it more like an *in vivo* system.

The change in emergent phenomena by changing a single detail regarding zombie contacts highlights how agent-based modeling approach allows us to implement features in this model with an ease that would not be possible in other modeling pathways. While a similar model could be implemented by employing ordinary differential equations (ODEs) and partial differential equations (PDEs), it would be involve the addition of assumptions to reach a level of complexity that ABM does naturally.

For each of the hypotheses, I estimated the best parameter sets. These parameter set could be used to make predictions about previously unexplored system readouts such as PCKR and fraction of killed cells. An experimental setup to explore these values would span over months, if not years. In contrast, the ease and speed of the ABM makes it an ideal setup to explore system details in a short duration of time.

7.4.2 Limitations of Model

The ABM that I have developed is a representation of a lymph node. Yet, it includes just two types of cells- CTLs and infected cells. It is important to note that I have not yet included cells other than infected cells that might be able to interact with CTLs by processing and presenting extracellular antigens with MHC class I molecules to them. The speed, turning angle and duration

of contacts have been taken from experimental data. These values come from a system that has many other cell types. Thus, they already include the impact of other cells on this value. By including the experimental values in the system, I have also accounted for other cells but any other impact of the cells which have not been included remains unaccounted for.

While the model I have developed is an extremely versatile tool but a limitation of the estimated parameters obtained from the agent-based model is that they fit best for a specific system that describes an *in vivo* setup. As established with the PCKR and fraction of killed infected cell analyses, the results differ based on initial number of infected cells and CTLs. Thus, the parameters identified in the paper hold true for a certain experimental set-up and cannot be taken for different initial conditions. But the benefit of the model is the ease with which it can be adapted to various other initial conditions. Consequently, while the agent-based system described in the paper is for an *in vivo* system, it can be applied to different setting by varying the parameters. It can be used to study the killing mechanisms under different conditions.

7.5 Temporal Bias in Experimental Observations

The application of PTA on the results obtained from the ABM showed that a variable observation window gives rise to a variation in results for systems that evolve with time. On the other hand, the analysis results remain the same for systems with no change in dynamics over time, such as the contact history independent killing mechanism. This indicates the importance for observing experimental systems for the same duration as a comparison between the dynamics of two different systems could give the same observed results if observed at different duration giving rise to erroneous conclusions.

Similarly, observing the experimental setup after a certain time has elapsed gave rise to a history of cells that remains unobserved and unaccounted for. This too, gave a variation in results for systems that were changing with time. This suggests that while planning experiments where it is unknown if the system is evolving with time, it is imperative to ensure that the observations are being taken at a fixed time after initiation.

All these results together make a strong case for uniformity in experimental observations with respect to time. The observation duration for all experiments that are to be compared should be kept constant and the observation should be initiated after a fixed time.

7.6 Thoughts on T cell Activation

T cell activation has been shown to require an arrest on an APC [114]. Prior to this arrest, T cells move around the network of APC, alternating between a kinapse mode that occurs when the T cell has transient interactions with APCs and a searching mode that occurs when T cells move

around looking for APCs [99]. Further, it has been hypothesized that T cells integrate signals from APCs in order to get activated [101,225]. A study has also shown that the T cell and APC synapse can be broken and formed multiple times and this has the same effect on T cell proliferation as a long-lasting contact [118].

In the study by Mayya et al. [207], they used a 2D stimulatory surfaces with uniformly coated antigen at equidistant, uniform spots to study T cell motion and interaction with antigen spots. In a set of analysis, I explored the hypothesis of signal integration on T cell motility. The proposed hypothesis that I was exploring was that T cells change their motion properties as a consequence of signal integration. I analyzed the cell tracks to obtain the speed and turning angle values for time blocks of 20 minutes. The motion properties did not show any change with an increasing time. Since signal integration is a consequence of kinapses with antigen spots, I also computed the speed and turning angle in the kinapse mode and the searching mode as functions of the total number of kinapses that the T cell has had. For this analysis too, the motion properties remained largely unchanged. The results from the analysis did not provide enough evidence for a signal integration at the motility level in contrast to prior studies [226].

T cell get arrested on APCs after forming kinapses with antigen spots. Here, I also considered the effect of signal integration on T cell arrest. I studied the impact of increasing number of kinapses on T cell arrest using the PTA. Surprisingly, the probability of T cell arrest remained largely unchanged with increasing number of kinapses. But it is interesting to note that the probability of cell arrest was higher at higher antigen concentrations in accordance with previous studies [102, 227]. The fewer number of kinapses needed for permanent arrest at a higher antigen concentration suggests that T cells activation is dependent on antigen concentration. However, the probability of arrest with increasing number of kinapses computed using PTA suggests that there is no signal integration. Thus, while the effect of signal integration on the motion properties cannot be confirmed, the effect of signal integration on synapse formation is absent.

7.7 Future Perspectives

By making use of simple and universal properties of cells, the ABM described in this study encapsulates a system that is observed very commonly. Despite being defined by such basic properties, this system has the ability to estimate the behavior at a cellular level while on the other hand, it can also be used to predict emergent phenomena. With an increase in knowledge in the field, the properties of the agents could easily be updated thereby making the system more powerful and accurate. Due to the versatility and efficiency of the ABM, it can be used to expand our knowledge in various ways:

1. In ABM described above, it would be interesting to introduce calcium signaling and flux in the infected cells as a consequence of interaction with CTLs [111]. This could then be used

to study the heterogeneity in calcium signaling after single CTL contacts.

2. An interesting addition to the system would be introduction of varying affinities of T cells and infected cells with each other [228]. This would make the model more like an actual biological system and would help explore the mechanism of eliminating infected cells in a realistic setup.

3. The inclusion of other types of cells into the system would make the ABM more malleable. By making a general framework of a system with more cells, this model could then be used to study other *in vivo* and *in vitro* systems.

4. A more ambitious direction for the model involves the introduction of defense mechanisms by target cells. Melanoma cells have been shown to secrete enzymes that degrade perforin [229] whereas certain virus-infected cells have been shown to escape CTL detection by the expression of viral immune evasion proteins [230, 231]. The dynamic interplay that arises between CTLs and target cells would be a fascinating topic to study.

7.8 Final Statements

In 1984, G. J. V. Nossal [232] wrote "A readership consisting of primarily anatomists has every right to question the favorite sport of research workers in cell immunology. This is to take a lymphoid tissue and totally destroy its beautiful and elaborately designed architecture to obtain simple cell suspension of lymphocytes, which are then asked to do more or less all the jobs of the original anatomic masterpiece." With the wide use of *in silico* techniques today, computational biologists in the field of immunology have the same favorite sport as research workers in cell immunology. While the recreation of a lymphoid tissue using simple rules might seem like a step down, it is imperative to understand that even by employing simple rules, scientists have gained remarkable insight into the workings of a lymphoid tissue. Moreover, it is by using the insights gained from these systems as building blocks, that we can hope to have a complete understanding of the elegant workings of the immune system.

With this study, I have tried to further our knowledge of the lymph node by designing a simple ABM of CTL mediated killing of infected cells. By means of the ABM, I have proposed potential mechanisms that CTLs could employ to kill infected cells. Additionally, I have provided a way to quantify the impact of increasing number of contacts with CTLs on infected cell death. With the understanding that we obtain from PTA, we are one step closer to understanding how CTLs kill infected cells and how T cells are activated.

The importance of T cells as a part of the immune system cannot be stated enough. They play multiple roles in the adaptive immune system which include but are not limited to recognizing and killing antigens and infected cells, acting as helper cell to interact with B cells and acting as

regulatory cells to diminish the immune response. A deficiency in T cells can manifest as blood disorders, digestive problems and autoimmune disorders to name a few. Additionally, due to the function of killing infected cells, the use of T cells as a part of immunotherapy against cancer and chronic infectious diseases has confounded and intrigued scientists for over a century now [233].

In a field as dynamic as this, our knowledge is increasing in leaps and bounds and a clearer understanding of T cell killing and activation mechanisms will play an indispensable role in designing better immunotherapies. I hope that this study will help in pushing the envelope a little further in the field.

Bibliography

[1] F. P. Retief and L. Cilliers, "The epidemic of athens, 430-426 bc," *South African Medical Journal*, vol. 88, no. 1, pp. 50–53, 1998.

[2] W. T. Cefalu, "Inflammation, insulin resistance, and type 2 diabetes: back to the future?," *Diabetes*, vol. 58, no. 2, pp. 307–308, 2009.

[3] A. J. Filiano, Y. Xu, N. J. Tustison, R. L. Marsh, W. Baker, I. Smirnov, C. C. Overall, S. P. Gadani, S. D. Turner, Z. Weng, *et al.*, "Unexpected role of interferon-γ in regulating neuronal connectivity and social behaviour," *Nature*, vol. 535, no. 7612, p. 425, 2016.

[4] A. Takahashi, M. E. Flanigan, B. S. McEwen, and S. J. Russo, "Aggression, social stress, and the immune system in humans and animal models," *Frontiers in behavioral neuroscience*, vol. 12, p. 56, 2018.

[5] J. P. Konsman and R. Dantzer, "How the immune and nervous systems interact during disease-associated anorexia," *Nutrition*, vol. 17, no. 7-8, pp. 664–668, 2001.

[6] B. E. Leonard, "The concept of depression as a dysfunction of the immune system," in *Depression: From Psychopathology to Pharmacotherapy*, vol. 27, pp. 53–71, Karger Publishers, 2010.

[7] S.-K. Chen, P. Tvrdik, E. Peden, S. Cho, S. Wu, G. Spangrude, and M. R. Capecchi, "Hematopoietic origin of pathological grooming in hoxb8 mutant mice," *Cell*, vol. 141, no. 5, pp. 775–785, 2010.

[8] S. E. Turvey and D. H. Broide, "Innate immunity," *Journal of Allergy and Clinical Immunology*, vol. 125, no. 2, pp. S24–S32, 2010.

[9] A. Baroni, E. Buommino, V. De Gregorio, E. Ruocco, V. Ruocco, and R. Wolf, "Structure and function of the epidermis related to barrier properties," *Clinics in dermatology*, vol. 30, no. 3, pp. 257–262, 2012.

[10] R. L. Gallo and L. V. Hooper, "Epithelial antimicrobial defence of the skin and intestine," *Nature Reviews Immunology*, vol. 12, no. 7, p. 503, 2012.

[11] A. M. McDermott, "Antimicrobial compounds in tears," *Experimental eye research*, vol. 117, pp. 53–61, 2013.

[12] S. Akira, S. Uematsu, and O. Takeuchi, "Pathogen recognition and innate immunity," *Cell*, vol. 124, no. 4, pp. 783–801, 2006.

[13] H. Kumar, T. Kawai, and S. Akira, "Pathogen recognition by the innate immune system," *International reviews of immunology*, vol. 30, no. 1, pp. 16–34, 2011.

[14] C. A. Janeway Jr and R. Medzhitov, "Innate immune recognition," *Annual review of immunology*, vol. 20, no. 1, pp. 197–216, 2002.

[15] T. H. Mogensen, "Pathogen recognition and inflammatory signaling in innate immune defenses," *Clinical microbiology reviews*, vol. 22, no. 2, pp. 240–273, 2009.

[16] S. N. Shishido, S. Varahan, K. Yuan, X. Li, and S. D. Fleming, "Humoral innate immune response and disease," *Clinical immunology*, vol. 144, no. 2, pp. 142–158, 2012.

[17] B. Bottazzi, A. Doni, C. Garlanda, and A. Mantovani, "An integrated view of humoral innate immunity: pentraxins as a paradigm," *Annual review of immunology*, vol. 28, pp. 157–183, 2009.

[18] J. V. Sarma and P. A. Ward, "The complement system," *Cell and tissue research*, vol. 343, no. 1, pp. 227–235, 2011.

[19] J. A. Hoffmann, F. C. Kafatos, C. A. Janeway, and R. Ezekowitz, "Phylogenetic perspectives in innate immunity," *Science*, vol. 284, no. 5418, pp. 1313–1318, 1999.

[20] C. A. Janeway Jr, P. Travers, M. Walport, and M. J. Shlomchik, "Evolution of the innate immune system," in *Immunobiology: The Immune System in Health and Disease. 5th edition*, Garland Science, 2001.

[21] A. Aderem and D. M. Underhill, "Mechanisms of phagocytosis in macrophages," *Annual review of immunology*, vol. 17, no. 1, pp. 593–623, 1999.

[22] T. C. Theoharides, K.-D. Alysandratos, A. Angelidou, D.-A. Delivanis, N. Sismanopoulos, B. Zhang, S. Asadi, M. Vasiadi, Z. Weng, A. Miniati, *et al.*, "Mast cells and inflammation," *Biochimica et Biophysica Acta (BBA)-Molecular Basis of Disease*, vol. 1822, no. 1, pp. 21–33, 2012.

[23] W. M. Nauseef and N. Borregaard, "Neutrophils at work," *Nature immunology*, vol. 15, no. 7, p. 602, 2014.

[24] E. A. Jacobsen, A. G. Taranova, N. A. Lee, and J. J. Lee, "Eosinophils: singularly destructive effector cells or purveyors of immunoregulation?," *Journal of Allergy and Clinical Immunology*, vol. 119, no. 6, pp. 1313–1320, 2007.

[25] M. A. Caligiuri, "Human natural killer cells," *Blood*, vol. 112, no. 3, pp. 461–469, 2008.

[26] J. Banchereau, F. Briere, C. Caux, J. Davoust, S. Lebecque, Y.-J. Liu, B. Pulendran, and K. Palucka, "Immunobiology of dendritic cells," *Annual review of immunology*, vol. 18, no. 1, pp. 767–811, 2000.

[27] L. Wu and L. Van Kaer, "Natural killer t cells in health and disease," *Frontiers in bioscience (Scholar edition)*, vol. 3, p. 236, 2011.

[28] M. F. Flajnik and M. Kasahara, "Origin and evolution of the adaptive immune system: genetic events and selective pressures," *Nature Reviews Genetics*, vol. 11, no. 1, p. 47, 2010.

[29] K. M. Yatim and F. G. Lakkis, "A brief journey through the immune system," *Clinical Journal of the American Society of Nephrology*, vol. 10, no. 7, pp. 1274–1281, 2015.

[30] A. Fischer, F. Le Deist, S. Hacein-Bey-Abina, I. André-Schmutz, G. De Saint Basile, J.-P. De Villartay, and M. Cavazzana-Calvo, "Severe combined immunodeficiency. a model disease for molecular immunology and therapy," *Immunological reviews*, vol. 203, no. 1, pp. 98–109, 2005.

[31] A. Moise, F. Nedelcu, M. A. Toader, S. M. Sora, A. Tica, D. E. Ferastraoaru, and I. Constantinescu, "Primary immunodeficiencies of the b lymphocyte," *Journal of medicine and life*, vol. 3, no. 1, p. 60, 2010.

[32] F. A. Bonilla and H. C. Oettgen, "Adaptive immunity," *Journal of Allergy and Clinical Immunology*, vol. 125, no. 2, pp. S33–S40, 2010.

[33] Q. Qi, Y. Liu, Y. Cheng, J. Glanville, D. Zhang, J.-Y. Lee, R. A. Olshen, C. M. Weyand, S. D. Boyd, and J. J. Goronzy, "Diversity and clonal selection in the human t-cell repertoire," *Proceedings of the National Academy of Sciences*, vol. 111, no. 36, pp. 13139–13144, 2014.

[34] R. A. Manz, S. Arce, G. Cassese, A. E. Hauser, F. Hiepe, and A. Radbruch, "Humoral immunity and long-lived plasma cells," *Current opinion in immunology*, vol. 14, no. 4, pp. 517–521, 2002.

[35] M. K. Slifka, R. Antia, J. K. Whitmire, and R. Ahmed, "Humoral immunity due to long-lived plasma cells," *Immunity*, vol. 8, no. 3, pp. 363–372, 1998.

[36] E. J. Wing and J. S. Remington, "Cell-mediated immunity and its role in resistance to infection," *Western Journal of Medicine*, vol. 126, no. 1, p. 14, 1977.

[37] L. S. Walker and A. K. Abbas, "Regulation of cell-mediated immunity: The biology of checkpoints and regulatory t cells," *Cancer Immunotherapy Principles and Practice*, p. 95, 2017.

[38] E. Vivier, D. H. Raulet, A. Moretta, M. A. Caligiuri, L. Zitvogel, L. L. Lanier, W. M. Yokoyama, and S. Ugolini, "Innate or adaptive immunity? the example of natural killer cells," *science*, vol. 331, no. 6013, pp. 44–49, 2011.

[39] M. A. Cooper, M. Colonna, and W. M. Yokoyama, "Hidden talents of natural killers: Nk cells in innate and adaptive immunity," *EMBO reports*, vol. 10, no. 10, pp. 1103–1110, 2009.

[40] K. Rainwater-Lovett and W. J. Moss, "Immunologic basis for revaccination of hiv-infected children receiving haart," *Future virology*, vol. 6, no. 1, pp. 59–71, 2011.

[41] R. Rhoades and R. Pflanzer, "Human physiology 4th," *Thomson Learning*, 2002.

[42] Y.-H. Wang, Z. Zhang, P. D. Burrows, H. Kubagawa, S. L. Bridges, H. W. Findley, and M. D. Cooper, "V (d) j recombinatorial repertoire diversification during intraclonal pro-b to b-cell differentiation," *Blood*, vol. 101, no. 3, pp. 1030–1037, 2003.

[43] G. Asma, R. L. van den Bergh, and J. Vossen, "Development of pre-b and b lymphocytes in the human fetus.," *Clinical and experimental immunology*, vol. 56, no. 2, p. 407, 1984.

[44] K. Rajewsky, "Clonal selection and learning in the antibody system," *Nature*, vol. 381, no. 6585, p. 751, 1996.

[45] C. Brack, M. Hirama, R. Lenhard-Schuller, and S. Tonegawa, "A complete immunoglobulin gene is created by somatic recombination," *Cell*, vol. 15, no. 1, pp. 1–14, 1978.

[46] T. W. LeBien and T. F. Tedder, "B lymphocytes: how they develop and function," *Blood*, vol. 112, no. 5, pp. 1570–1580, 2008.

[47] N. E. Harwood and F. D. Batista, "Early events in b cell activation," *Annual review of immunology*, vol. 28, pp. 185–210, 2009.

[48] T. Okada, M. J. Miller, I. Parker, M. F. Krummel, M. Neighbors, S. B. Hartley, A. O'Garra, M. D. Cahalan, and J. G. Cyster, "Antigen-engaged b cells undergo chemotaxis toward the t zone and form motile conjugates with helper t cells," *PLoS biology*, vol. 3, no. 6, p. e150, 2005.

[49] I. C. MacLennan, K.-M. Toellner, A. F. Cunningham, K. Serre, D. M.-Y. Sze, E. Zúñiga, M. C. Cook, and C. G. Vinuesa, "Extrafollicular antibody responses," *Immunological reviews*, vol. 194, no. 1, pp. 8–18, 2003.

[50] D. Nemazee, "Mechanisms of central tolerance for b cells," *Nature Reviews Immunology*, vol. 17, no. 5, p. 281, 2017.

[51] C. C. Goodnow, S. Adelstein, and A. Basten, "The need for central and peripheral tolerance in the b cell repertoire," *Science*, vol. 248, no. 4961, pp. 1373–1379, 1990.

[52] E. Notidis, L. Heltemes, and T. Manser, "Dominant, hierarchical induction of peripheral tolerance during foreign antigen-driven b cell development," *Immunity*, vol. 17, no. 3, pp. 317–327, 2002.

[53] R. Pelanda and R. M. Torres, "Central b-cell tolerance: where selection begins," *Cold Spring Harbor perspectives in biology*, vol. 4, no. 4, p. a007146, 2012.

[54] F. Melchers, "Checkpoints that control b cell development," *The Journal of clinical investigation*, vol. 125, no. 6, pp. 2203–2210, 2015.

[55] A. Norvell and J. G. Monroe, "Acquisition of surface igd fails to protect from tolerance-induction. both surface igm-and surface igd-mediated signals induce apoptosis of immature murine b lymphocytes.," *The Journal of Immunology*, vol. 156, no. 4, pp. 1328–1332, 1996.

[56] D. M. Russell, Z. Dembić, G. Morahan, J. Miller, K. Bürki, and D. Nemazee, "Peripheral deletion of self-reactive b cells," *Nature*, vol. 354, no. 6351, p. 308, 1991.

[57] C. C. Goodnow, J. Crosbie, S. Adelstein, T. B. Lavoie, S. J. Smith-Gill, R. A. Brink, H. Pritchard-Briscoe, J. S. Wotherspoon, R. H. Loblay, K. Raphael, *et al.*, "Altered immunoglobulin expression and functional silencing of self-reactive b lymphocytes in transgenic mice," *Nature*, vol. 334, no. 6184, p. 676, 1988.

[58] D. A. Fulcher and A. Basten, "Reduced life span of anergic self-reactive b cells in a double-transgenic model.," *Journal of Experimental Medicine*, vol. 179, no. 1, pp. 125–134, 1994.

[59] D. Gay, T. Saunders, S. Camper, and M. Weigert, "Receptor editing: an approach by autoreactive b cells to escape tolerance.," *Journal of Experimental Medicine*, vol. 177, no. 4, pp. 999–1008, 1993.

[60] S. L. Tiegs, D. M. Russell, and D. Nemazee, "Receptor editing in self-reactive bone marrow b cells.," *Journal of Experimental Medicine*, vol. 177, no. 4, pp. 1009–1020, 1993.

[61] P. C. Sandel and J. G. Monroe, "Negative selection of immature b cells by receptor editing or deletion is determined by site of antigen encounter," *Immunity*, vol. 10, no. 3, pp. 289–299, 1999.

[62] R. Schwenk, L. V. Asher, I. Chalom, D. Lanar, P. Sun, K. White, D. Keil, K. E. Kester, J. Stoute, D. G. Heppner, *et al.*, "Opsonization by antigen-specific antibodies as a mechanism

of protective immunity induced by plasmodium falciparum circumsporozoite protein-based vaccine," *Parasite immunology*, vol. 25, no. 1, pp. 17–25, 2003.

[63] J. Pollara and M. Z. Tay, "Antibody-dependent cellular phagocytosis in antiviral immune responses," *Frontiers in immunology*, vol. 10, p. 332, 2019.

[64] D. P. Harris, L. Haynes, P. C. Sayles, D. K. Duso, S. M. Eaton, N. M. Lepak, L. L. Johnson, S. L. Swain, and F. E. Lund, "Reciprocal regulation of polarized cytokine production by effector b and t cells," *Nature immunology*, vol. 1, no. 6, p. 475, 2000.

[65] C. Mauri and A. Bosma, "Immune regulatory function of b cells," *Annual review of immunology*, vol. 30, pp. 221–241, 2012.

[66] J. Parkin and B. Cohen, "An overview of the immune system," *The Lancet*, vol. 357, no. 9270, pp. 1777–1789, 2001.

[67] J. S. Hale and P. J. Fink, "Back to the thymus: peripheral t cells come home," *Immunology and cell biology*, vol. 87, no. 1, pp. 58–64, 2009.

[68] J. C. Zúñiga-Pflücker, "T-cell development made simple," *Nature Reviews Immunology*, vol. 4, no. 1, p. 67, 2004.

[69] M. Nishino, S. K. Ashiku, O. N. Kocher, R. L. Thurer, P. M. Boiselle, and H. Hatabu, "The thymus: a comprehensive review," *Radiographics*, vol. 26, no. 2, pp. 335–348, 2006.

[70] L. Klein, B. Kyewski, P. M. Allen, and K. A. Hogquist, "Positive and negative selection of the t cell repertoire: what thymocytes see (and don't see)," *Nature Reviews Immunology*, vol. 14, no. 6, p. 377, 2014.

[71] G. L. Stritesky, Y. Xing, J. R. Erickson, L. A. Kalekar, X. Wang, D. L. Mueller, S. C. Jameson, and K. A. Hogquist, "Murine thymic selection quantified using a unique method to capture deleted t cells," *Proceedings of the National Academy of Sciences*, vol. 110, no. 12, pp. 4679–4684, 2013.

[72] A. C. Carpenter and R. Bosselut, "Decision checkpoints in the thymus," *Nature immunology*, vol. 11, no. 8, p. 666, 2010.

[73] N. D. Pennock, J. T. White, E. W. Cross, E. E. Cheney, B. A. Tamburini, and R. M. Kedl, "T cell responses: naive to memory and everything in between," *Advances in physiology education*, vol. 37, no. 4, pp. 273–283, 2013.

[74] R. C. Budd and K. A. Fortner, "T lymphocytes," in *Kelley and Firestein's Textbook of Rheumatology*, pp. 189–206, Elsevier, 2017.

[75] C. A. Chambers, "The expanding world of co-stimulation: the two-signal model revisited," *Trends in immunology*, vol. 22, no. 4, pp. 217–223, 2001.

[76] Z. Tatari-Calderone, R. T. Semnani, T. B. Nutman, J. Schlom, and H. Sabzevari, "Acquisition of cd80 by human t cells at early stages of activation: functional involvement of cd80 acquisition in t cell to t cell interaction," *The Journal of Immunology*, vol. 169, no. 11, pp. 6162–6169, 2002.

[77] D. J. Lenschow, T. L. Walunas, and J. A. Bluestone, "Cd28/b7 system of t cell costimulation," *Annual review of immunology*, vol. 14, no. 1, pp. 233–258, 1996.

[78] T. S. Lim, J. K. H. Goh, A. Mortellaro, C. T. Lim, G. J. Hämmerling, and P. Ricciardi-Castagnoli, "Cd80 and cd86 differentially regulate mechanical interactions of t-cells with antigen-presenting dendritic cells and b-cells," *PloS one*, vol. 7, no. 9, p. e45185, 2012.

[79] R. H. Schwartz, "T cell anergy," *Annual review of immunology*, vol. 21, no. 1, pp. 305–334, 2003.

[80] L. A. Kalekar, S. E. Schmiel, S. L. Nandiwada, W. Y. Lam, L. O. Barsness, N. Zhang, G. L. Stritesky, D. Malhotra, K. E. Pauken, J. L. Linehan, *et al.*, "Cd4+ t cell anergy prevents autoimmunity and generates regulatory t cell precursors," *Nature immunology*, vol. 17, no. 3, p. 304, 2016.

[81] F. Macián, S.-H. Im, F. J. Garcıa-Cózar, and A. Rao, "T-cell anergy," *Current opinion in immunology*, vol. 16, no. 2, pp. 209–216, 2004.

[82] Y. Xing and K. A. Hogquist, "T-cell tolerance: central and peripheral," *Cold Spring Harbor perspectives in biology*, vol. 4, no. 6, p. a006957, 2012.

[83] R. I. Nurieva, X. Liu, and C. Dong, "Molecular mechanisms of t-cell tolerance," *Immunological reviews*, vol. 241, no. 1, pp. 133–144, 2011.

[84] M. R. Von Essen, M. Kongsbak, P. Schjerling, K. Olgaard, N. Ødum, and C. Geisler, "Vitamin d controls t cell antigen receptor signaling and activation of human t cells," *Nature immunology*, vol. 11, no. 4, p. 344, 2010.

[85] A. Lanzavecchia, G. Iezzi, and A. Viola, "From tcr engagement to t cell activation: a kinetic view of t cell behavior," *Cell*, vol. 96, no. 1, pp. 1–4, 1999.

[86] S. K. Bromley, W. R. Burack, K. G. Johnson, K. Somersalo, T. N. Sims, C. Sumen, M. M. Davis, A. S. Shaw, P. M. Allen, and M. L. Dustin, "The immunological synapse," *Annual review of immunology*, vol. 19, no. 1, pp. 375–396, 2001.

[87] M. A. Williams and M. J. Bevan, "Effector and memory ctl differentiation," *Annu. Rev. Immunol.*, vol. 25, pp. 171–192, 2007.

[88] K. R. Garrod, H. D. Moreau, Z. Garcia, F. Lemaître, I. Bouvier, M. L. Albert, and P. Bousso, "Dissecting t cell contraction in vivo using a genetically encoded reporter of apoptosis," *Cell reports*, vol. 2, no. 5, pp. 1438–1447, 2012.

[89] K. K. McKinstry, T. M. Strutt, and S. L. Swain, "Regulation of cd4+ t-cell contraction during pathogen challenge," *Immunological reviews*, vol. 236, no. 1, pp. 110–124, 2010.

[90] A. Sharma, M. Campbell, C. Yee, S. Goswami, and P. Sharma, "Immunotherapy of cancer," in *Clinical Immunology*, pp. 1033–1048, Elsevier, 2019.

[91] V. Golubovskaya and L. Wu, "Different subsets of t cells, memory, effector functions, and car-t immunotherapy," *Cancers*, vol. 8, no. 3, p. 36, 2016.

[92] S. H. Kaufmann, "The contribution of immunology to the rational design of novel antibacterial vaccines," *Nature Reviews Microbiology*, vol. 5, no. 7, p. 491, 2007.

[93] H.-W. Mittrücker, A. Visekruna, and M. Huber, "Heterogeneity in the differentiation and function of cd8+ t cells," *Archivum immunologiae et therapiae experimentalis*, vol. 62, no. 6, pp. 449–458, 2014.

[94] H. Hamada, M. de la Luz Garcia-Hernandez, J. B. Reome, S. K. Misra, T. M. Strutt, K. K. McKinstry, A. M. Cooper, S. L. Swain, and R. W. Dutton, "Tc17, a unique subset of cd8 t cells that can protect against lethal influenza challenge," *The Journal of Immunology*, vol. 182, no. 6, pp. 3469–3481, 2009.

[95] A. Visekruna, J. Ritter, T. Scholz, L. Campos, A. Guralnik, L. Poncette, H. Raifer, S. Hagner, H. Garn, V. Staudt, *et al.*, "Tc9 cells, a new subset of cd8+ t cells, support th2-mediated airway inflammation," *European journal of immunology*, vol. 43, no. 3, pp. 606–618, 2013.

[96] G. Iezzi, K. Karjalainen, and A. Lanzavecchia, "The duration of antigenic stimulation determines the fate of naive and effector t cells," *Immunity*, vol. 8, no. 1, pp. 89–95, 1998.

[97] P. Bousso, "T-cell activation by dendritic cells in the lymph node: lessons from the movies," *Nature Reviews Immunology*, vol. 8, no. 9, p. 675, 2008.

[98] R. S. Friedman, P. Beemiller, C. M. Sorensen, J. Jacobelli, and M. F. Krummel, "Real-time analysis of t cell receptors in naive cells in vitro and in vivo reveals flexibility in synapse and signaling dynamics," *Journal of Experimental Medicine*, vol. 207, no. 12, pp. 2733–2749, 2010.

[99] M. L. Dustin, "Cell adhesion molecules and actin cytoskeleton at immune synapses and kinapses," *Current opinion in cell biology*, vol. 19, no. 5, pp. 529–533, 2007.

[100] J. B. Huppa, M. Gleimer, C. Sumen, and M. M. Davis, "Continuous t cell receptor signaling required for synapse maintenance and full effector potential," *Nature immunology*, vol. 4, no. 8, p. 749, 2003.

[101] S. Celli, F. Lemaître, and P. Bousso, "Real-time manipulation of t cell-dendritic cell interactions in vivo reveals the importance of prolonged contacts for cd4+ t cell activation," *Immunity*, vol. 27, no. 4, pp. 625–634, 2007.

[102] S. E. Henrickson, T. R. Mempel, I. B. Mazo, B. Liu, M. N. Artyomov, H. Zheng, A. Peixoto, M. P. Flynn, B. Senman, T. Junt, *et al.*, "T cell sensing of antigen dose governs interactive behavior with dendritic cells and sets a threshold for t cell activation," *Nature immunology*, vol. 9, no. 3, p. 282, 2008.

[103] H. D. Moreau, F. Lemaître, E. Terriac, G. Azar, M. Piel, A.-M. Lennon-Dumenil, and P. Bousso, "Dynamic in situ cytometry uncovers t cell receptor signaling during immunological synapses and kinapses in vivo," *Immunity*, vol. 37, no. 2, pp. 351–363, 2012.

[104] T. R. Mempel, S. E. Henrickson, and U. H. Von Andrian, "T-cell priming by dendritic cells in lymph nodes occurs in three distinct phases," *Nature*, vol. 427, no. 6970, p. 154, 2004.

[105] K. L. Rock, E. Reits, and J. Neefjes, "Present yourself! by mhc class i and mhc class ii molecules," *Trends in immunology*, vol. 37, no. 11, pp. 724–737, 2016.

[106] M. L. Dustin and E. O. Long, "Cytotoxic immunological synapses," *Immunological reviews*, vol. 235, no. 1, pp. 24–34, 2010.

[107] M. Norcross, "A synaptic basis for t-lymphocyte activation," in *Annales de l'Institut Pasteur/Immunologie*, vol. 135, pp. 113–134, Elsevier, 1984.

[108] N. Zhang and M. J. Bevan, "Cd8+ t cells: foot soldiers of the immune system," *Immunity*, vol. 35, no. 2, pp. 161–168, 2011.

[109] D. R. Fooksman, S. Vardhana, G. Vasiliver-Shamis, J. Liese, D. A. Blair, J. Waite, C. Sacristán, G. D. Victora, A. Zanin-Zhorov, and M. L. Dustin, "Functional anatomy of t cell activation and synapse formation," *Annual review of immunology*, vol. 28, pp. 79–105, 2009.

[110] A. Siokis, P. A. Robert, P. Demetriou, M. L. Dustin, and M. Meyer-Hermann, "F-actin-driven cd28-cd80 localization in the immune synapse," *Cell reports*, vol. 24, no. 5, pp. 1151–1162, 2018.

[111] S. Halle, K. A. Keyser, F. R. Stahl, A. Busche, A. Marquardt, X. Zheng, M. Galla, V. Heissmeyer, K. Heller, J. Boelter, *et al.*, "*In vivo* killing capacity of cytotoxic t cells is limited and involves dynamic interactions and t cell cooperativity," *Immunity*, vol. 44, no. 2, pp. 233–245, 2016.

[112] B. Malissen, "Dancing the immunological two-step," *Science*, vol. 285, no. 5425, pp. 207–208, 1999.

[113] M. Huse, B. F. Lillemeier, M. S. Kuhns, D. S. Chen, and M. M. Davis, "T cells use two directionally distinct pathways for cytokine secretion," *Nature immunology*, vol. 7, no. 3, p. 247, 2006.

[114] H. D. Moreau, F. Lemaître, K. R. Garrod, Z. Garcia, A.-M. Lennon-Duménil, and P. Bousso, "Signal strength regulates antigen-mediated t-cell deceleration by distinct mechanisms to promote local exploration or arrest," *Proceedings of the National Academy of Sciences*, vol. 112, no. 39, pp. 12151–12156, 2015.

[115] M. Gunzer, A. Schäfer, S. Borgmann, S. Grabbe, K. S. Zänker, E.-B. Bröcker, E. Kämpgen, and P. Friedl, "Antigen presentation in extracellular matrix: interactions of t cells with dendritic cells are dynamic, short lived, and sequential," *Immunity*, vol. 13, no. 3, pp. 323–332, 2000.

[116] A. Scholer, S. Hugues, A. Boissonnas, L. Fetler, and S. Amigorena, "Intercellular adhesion molecule-1-dependent stable interactions between t cells and dendritic cells determine cd8+ t cell memory," *Immunity*, vol. 28, no. 2, pp. 258–270, 2008.

[117] I. Munitic, P. E. Ryan, and J. D. Ashwell, "T cells in g1 provide a memory-like response to secondary stimulation," *The Journal of Immunology*, vol. 174, no. 7, pp. 4010–4018, 2005.

[118] M. Faroudi, R. Zaru, P. Paulet, S. Müller, and S. Valitutti, "Cutting edge: T lymphocyte activation by repeated immunological synapse formation and intermittent signaling," *The Journal of Immunology*, vol. 171, no. 3, pp. 1128–1132, 2003.

[119] A. Viola and A. Lanzavecchia, "T cell activation determined by t cell receptor number and tunable thresholds," *Science*, vol. 273, no. 5271, pp. 104–106, 1996.

[120] M. Huse, "Microtubule-organizing center polarity and the immunological synapse: protein kinase c and beyond," *Frontiers in immunology*, vol. 3, p. 235, 2012.

[121] A. T. Ritter, Y. Asano, J. C. Stinchcombe, N. Dieckmann, B.-C. Chen, C. Gawden-Bone, S. van Engelenburg, W. Legant, L. Gao, M. W. Davidson, *et al.*, "Actin depletion initiates events leading to granule secretion at the immunological synapse," *Immunity*, vol. 42, no. 5, pp. 864–876, 2015.

[122] J. C. Stinchcombe, E. Majorovits, G. Bossi, S. Fuller, and G. M. Griffiths, "Centrosome polarization delivers secretory granules to the immunological synapse," *Nature*, vol. 443, no. 7110, p. 462, 2006.

[123] M. Lettau, D. Kabelitz, and O. Janssen, "Lysosome-related effector vesicles in t lymphocytes and nk cells," *Scandinavian journal of immunology*, vol. 82, no. 3, pp. 235–243, 2015.

[124] R. Basu, B. M. Whitlock, J. Husson, A. Le Floc'h, W. Jin, A. Oyler-Yaniv, F. Dotiwala, G. Giannone, C. Hivroz, N. Biais, *et al.*, "Cytotoxic t cells use mechanical force to potentiate target cell killing," *Cell*, vol. 165, no. 1, pp. 100–110, 2016.

[125] F. Tamzalit, M. S. Wang, W. Jin, M. Tello-Lafoz, V. Boyko, J. M. Heddleston, C. T. Black, L. C. Kam, and M. Huse, "Interfacial actin protrusions mechanically enhance killing by cytotoxic t cells," *Science immunology*, vol. 4, no. 33, p. eaav5445, 2019.

[126] M. R. Jenkins and G. M. Griffiths, "The synapse and cytolytic machinery of cytotoxic t cells," *Current opinion in immunology*, vol. 22, no. 3, pp. 308–313, 2010.

[127] J. L. Harris, E. P. Peterson, D. Hudig, N. A. Thornberry, and C. S. Craik, "Definition and redesign of the extended substrate specificity of granzyme b," *Journal of Biological Chemistry*, vol. 273, no. 42, pp. 27364–27373, 1998.

[128] M. Bots and J. P. Medema, "Granzymes at a glance," *Journal of cell science*, vol. 119, no. 24, pp. 5011–5014, 2006.

[129] W. J. Grossman, P. A. Revell, Z. H. Lu, H. Johnson, A. J. Bredemeyer, and T. J. Ley, "The orphan granzymes of humans and mice," *Current opinion in immunology*, vol. 15, no. 5, pp. 544–552, 2003.

[130] J. A. Trapani and V. R. Sutton, "Granzyme b: pro-apoptotic, antiviral and antitumor functions," *Current opinion in immunology*, vol. 15, no. 5, pp. 533–543, 2003.

[131] I. Rousalova and E. Krepela, "Granzyme b-induced apoptosis in cancer cells and its regulation," *International journal of oncology*, vol. 37, no. 6, pp. 1361–1378, 2010.

[132] O. Krähenbühl and J. Tschopp, "Perforin-induced pore formation," *Immunology today*, vol. 12, no. 11, pp. 399–402, 1991.

[133] J. A. Trapani, "Granzymes: a family of lymphocyte granule serine proteases," *Genome biology*, vol. 2, no. 12, pp. reviews3014–1, 2001.

[134] G. Dennert and E. Podack, "Cytolysis by h-2-specific t killer cells. assembly of tubular complexes on target membranes.," *Journal of Experimental Medicine*, vol. 157, no. 5, pp. 1483–1495, 1983.

[135] J. A. Lopez, O. Susanto, M. R. Jenkins, N. Lukoyanova, V. R. Sutton, R. H. Law, A. Johnston, C. H. Bird, P. I. Bird, J. C. Whisstock, *et al.*, "Perforin forms transient pores on the target cell plasma membrane to facilitate rapid access of granzymes during killer cell attack," *Blood*, vol. 121, no. 14, pp. 2659–2668, 2013.

[136] S. S. Metkar, B. Wang, M. Aguilar-Santelises, S. M. Raja, L. Uhlin-Hansen, E. Podack, J. A. Trapani, and C. J. Froelich, "Cytotoxic cell granule-mediated apoptosis: perforin delivers granzyme b-serglycin complexes into target cells without plasma membrane pore formation," *Immunity*, vol. 16, no. 3, pp. 417–428, 2002.

[137] D. Kägi, B. Ledermann, K. Bürki, P. Seiler, B. Odermatt, K. J. Olsen, E. R. Podack, R. M. Zinkernagel, and H. Hengartner, "Cytotoxicity mediated by t cells and natural killer cells is greatly impaired in perforin-deficient mice," *Nature*, vol. 369, no. 6475, p. 31, 1994.

[138] C. M. Walsh, M. Matloubian, C.-C. Liu, R. Ueda, C. G. Kurahara, J. L. Christensen, M. Huang, J. Young, R. Ahmed, and W. Clark, "Immune function in mice lacking the perforin gene," *Proceedings of the National Academy of Sciences*, vol. 91, no. 23, pp. 10854–10858, 1994.

[139] M. Barry and R. C. Bleackley, "Cytotoxic t lymphocytes: all roads lead to death," *Nature Reviews Immunology*, vol. 2, no. 6, p. 401, 2002.

[140] A. Strasser, P. J. Jost, and S. Nagata, "The many roles of fas receptor signaling in the immune system," *Immunity*, vol. 30, no. 2, pp. 180–192, 2009.

[141] N. Itoh, S. Yonehara, A. Ishii, M. Yonehara, S.-I. Mizushima, M. Sameshima, A. Hase, Y. Seto, and S. Nagata, "The polypeptide encoded by the cdna for human cell surface antigen fas can mediate apoptosis," *Cell*, vol. 66, no. 2, pp. 233–243, 1991.

[142] P. Wong and E. G. Pamer, "Cd8 t cell responses to infectious pathogens," *Annual review of immunology*, vol. 21, no. 1, pp. 29–70, 2003.

[143] F. Kischkel, S. Hellbardt, I. Behrmann, M. Germer, M. Pawlita, P. Krammer, and M. Peter, "Cytotoxicity-dependent apo-1 (fas/cd95)-associated proteins form a death-inducing signaling complex (disc) with the receptor.," *The EMBO journal*, vol. 14, no. 22, pp. 5579–5588, 1995.

[144] M. Muzio, A. M. Chinnaiyan, F. C. Kischkel, K. O'Rourke, A. Shevchenko, J. Ni, C. Scaffidi, J. D. Bretz, M. Zhang, R. Gentz, *et al.*, "Flice, a novel fadd-homologous ice/ced-3–like protease, is recruited to the cd95 (fas/apo-1) death-inducing signaling complex," *Cell*, vol. 85, no. 6, pp. 817–827, 1996.

[145] H. Li, H. Zhu, C.-j. Xu, and J. Yuan, "Cleavage of bid by caspase 8 mediates the mitochondrial damage in the fas pathway of apoptosis," *Cell*, vol. 94, no. 4, pp. 491–501, 1998.

[146] G. M. Cohen, "Caspases: the executioners of apoptosis," *Biochemical Journal*, vol. 326, no. 1, pp. 1–16, 1997.

[147] D. R. McIlwain, T. Berger, and T. W. Mak, "Caspase functions in cell death and disease," *Cold Spring Harbor perspectives in biology*, vol. 5, no. 4, p. a008656, 2013.

[148] R. Bonecchi, C. Garlanda, A. Mantovani, and F. Riva, "Cytokine decoy and scavenger receptors as key regulators of immunity and inflammation," *Cytokine*, vol. 87, pp. 37–45, 2016.

[149] S.-L. Hsieh and W.-W. Lin, "Decoy receptor 3: an endogenous immunomodulator in cancer growth and inflammatory reactions," *Journal of biomedical science*, vol. 24, no. 1, p. 39, 2017.

[150] D. I. O'Brien, K. Nally, R. G. Kelly, T. M. O'Connor, F. Shanahan, and J. O'Connell, "Targeting the fas/fas ligand pathway in cancer," *Expert opinion on therapeutic targets*, vol. 9, no. 5, pp. 1031–1044, 2005.

[151] V. Poulaki, C. S. Mitsiades, and N. Mitsiades, "The role of fas and fasl as mediators of anticancer chemotherapy," *Drug Resistance Updates*, vol. 4, no. 4, pp. 233–242, 2001.

[152] E. E. Varfolomeev and A. Ashkenazi, "Tumor necrosis factor: an apoptosis junkie?," *cell*, vol. 116, no. 4, pp. 491–497, 2004.

[153] I. L. Ch'en, J. S. Tsau, J. D. Molkentin, M. Komatsu, and S. M. Hedrick, "Mechanisms of necroptosis in t cells," *Journal of Experimental Medicine*, vol. 208, no. 4, pp. 633–641, 2011.

[154] C. J. Kearney and S. J. Martin, "An inflammatory perspective on necroptosis," *Molecular cell*, vol. 65, no. 6, pp. 965–973, 2017.

[155] A. Linkermann and D. R. Green, "Necroptosis," *New England Journal of Medicine*, vol. 370, no. 5, pp. 455–465, 2014.

[156] B. L. Heckmann, B. Tummers, and D. R. Green, "Crashing the computer: apoptosis vs. necroptosis in neuroinflammation," *Cell Death & Differentiation*, p. 1, 2018.

[157] M. Sarhan, W. G. Land, W. Tonnus, C. P. Hugo, and A. Linkermann, "Origin and consequences of necroinflammation," *Physiological reviews*, vol. 98, no. 2, pp. 727–780, 2018.

[158] M. Elemans, A. Florins, L. Willems, and B. Asquith, "Rates of ctl killing in persistent viral infection in vivo," *PLoS computational biology*, vol. 10, no. 4, p. e1003534, 2014.

[159] V. Simon, D. D. Ho, and Q. A. Karim, "Hiv/aids epidemiology, pathogenesis, prevention, and treatment," *The Lancet*, vol. 368, no. 9534, pp. 489–504, 2006.

[160] Í. Caramalho, M. Faroudi, E. Padovan, S. Müller, and S. Valitutti, "Visualizing ctl/melanoma cell interactions: multiple hits must be delivered for tumour cell annihilation," *Journal of cellular and molecular medicine*, vol. 13, no. 9b, pp. 3834–3846, 2009.

[161] A. J. Zajac, J. N. Blattman, K. Murali-Krishna, D. J. Sourdive, M. Suresh, J. D. Altman, and R. Ahmed, "Viral immune evasion due to persistence of activated t cells without effector function," *Journal of Experimental Medicine*, vol. 188, no. 12, pp. 2205–2213, 1998.

[162] E. J. Wherry, "T cell exhaustion," *Nature immunology*, vol. 12, no. 6, p. 492, 2011.

[163] S. M. Kahan, E. J. Wherry, and A. J. Zajac, "T cell exhaustion during persistent viral infections," *Virology*, vol. 479, pp. 180–193, 2015.

[164] E. J. Wherry, J. N. Blattman, K. Murali-Krishna, R. Van Der Most, and R. Ahmed, "Viral persistence alters cd8 t-cell immunodominance and tissue distribution and results in distinct stages of functional impairment," *Journal of virology*, vol. 77, no. 8, pp. 4911–4927, 2003.

[165] M. J. Fuller and A. J. Zajac, "Ablation of cd8 and cd4 t cell responses by high viral loads," *The Journal of Immunology*, vol. 170, no. 1, pp. 477–486, 2003.

[166] H. W. Virgin, E. J. Wherry, and R. Ahmed, "Redefining chronic viral infection," *Cell*, vol. 138, no. 1, pp. 30–50, 2009.

[167] C. Wang, M. Singer, and A. C. Anderson, "Molecular dissection of cd8+ t-cell dysfunction," *Trends in immunology*, vol. 38, no. 8, pp. 567–576, 2017.

[168] E. J. Wherry and R. Ahmed, "Memory cd8 t-cell differentiation during viral infection," *Journal of virology*, vol. 78, no. 11, pp. 5535–5545, 2004.

[169] E. J. Wherry and M. Kurachi, "Molecular and cellular insights into t cell exhaustion," *Nature Reviews Immunology*, vol. 15, no. 8, p. 486, 2015.

[170] D. M. Pardoll, "The blockade of immune checkpoints in cancer immunotherapy," *Nature Reviews Cancer*, vol. 12, no. 4, p. 252, 2012.

[171] M. N. Wykes and S. R. Lewin, "Immune checkpoint blockade in infectious diseases," *Nature Reviews Immunology*, vol. 18, no. 2, p. 91, 2018.

[172] D. L. Barber, E. J. Wherry, D. Masopust, B. Zhu, J. P. Allison, A. H. Sharpe, G. J. Freeman, and R. Ahmed, "Restoring function in exhausted cd8 t cells during chronic viral infection," *Nature*, vol. 439, no. 7077, p. 682, 2006.

[173] B. Walker and A. McMichael, "The t-cell response to hiv," *Cold Spring Harbor perspectives in medicine*, vol. 2, no. 11, p. a007054, 2012.

[174] S. R. Stipp, A. Iniguez, F. Wan, and D. Wodarz, "Timing of cd8 t cell effector responses in viral infections," *Royal Society Open Science*, vol. 3, no. 2, p. 150661, 2016.

[175] A. K. Sewell, D. A. Price, A. Oxenius, A. D. Kelleher, and R. E. Phillips, "Cytotoxic t lymphocyte responses to human immunodeficiency virus: control and escape," *Stem Cells*, vol. 18, no. 4, pp. 230–244, 2000.

[176] L. Martínez-Lostao, A. Anel, and J. Pardo, "How do cytotoxic lymphocytes kill cancer cells?," 2015.

[177] C. H. June, R. S. O'Connor, O. U. Kawalekar, S. Ghassemi, and M. C. Milone, "Car t cell immunotherapy for human cancer," *Science*, vol. 359, no. 6382, pp. 1361–1365, 2018.

[178] A. N. Miliotou and L. C. Papadopoulou, "Car t-cell therapy: a new era in cancer immunotherapy," *Current pharmaceutical biotechnology*, vol. 19, no. 1, pp. 5–18, 2018.

[179] M. A. Alexander-Miller, G. R. Leggatt, and J. A. Berzofsky, "Selective expansion of high-or low-avidity cytotoxic t lymphocytes and efficacy for adoptive immunotherapy," *Proceedings of the National Academy of Sciences*, vol. 93, no. 9, pp. 4102–4107, 1996.

[180] P. G. Coulie, B. J. Van den Eynde, P. Van Der Bruggen, and T. Boon, "Tumour antigens recognized by t lymphocytes: at the core of cancer immunotherapy," *Nature Reviews Cancer*, vol. 14, no. 2, p. 135, 2014.

[181] J. Wang, O. W. Press, C. G. Lindgren, P. Greenberg, S. Riddell, X. Qian, C. Laugen, A. Raubitschek, S. J. Forman, and M. C. Jensen, "Cellular immunotherapy for follicular lymphoma using genetically modified cd20-specific cd8+ cytotoxic t lymphocytes," *Molecular Therapy*, vol. 9, no. 4, pp. 577–586, 2004.

[182] K. Brunner, J. Mauel, J.-C. Cerottini, and B. Chapuis, "Quantitative assay of the lytic action of immune lymphoid cells of 51cr-labelled allogeneic target cells in vitro; inhibition by isoantibody and by drugs," *Immunology*, vol. 14, no. 2, p. 181, 1968.

[183] R. Miller and M. Dunkley, "Quantitative analysis of the 51cr release cytotoxicity assay for cytotoxic lymphocytes," *Cellular immunology*, vol. 14, no. 2, pp. 284–302, 1974.

[184] R. R. Regoes, A. Yates, and R. Antia, "Mathematical models of cytotoxic t-lymphocyte killing," *Immunology and Cell Biology*, vol. 85, no. 4, pp. 274–279, 2007.

[185] S. Ariotti, J. B. Beltman, G. Chodaczek, M. E. Hoekstra, A. E. van Beek, R. Gomez-Eerland, L. Ritsma, J. van Rheenen, A. F. Marée, T. Zal, *et al.*, "Tissue-resident memory cd8+ t cells continuously patrol skin epithelia to quickly recognize local antigen," *Proceedings of the National Academy of Sciences*, vol. 109, no. 48, pp. 19739–19744, 2012.

[186] C. Kummerow, E. C. Schwarz, B. Bufe, F. Zufall, M. Hoth, and B. Qu, "A simple, economic, time-resolved killing assay," *European journal of immunology*, vol. 44, no. 6, pp. 1870–1872, 2014.

[187] J. Fassy, K. Tsalkitzi, M. Goncalves-Maia, and V. M. Braud, "A real-time cytotoxicity assay as an alternative to the standard chromium-51 release assay for measurement of human nk and t cell cytotoxic activity," *Current protocols in immunology*, vol. 118, no. 1, pp. 7–42, 2017.

[188] B. Bonavida, T. P. Bradley, and E. A. Grimm, "The single-cell assay in cell-mediated cytotoxicity," *Immunology Today*, vol. 4, no. 7, pp. 196–200, 1983.

[189] E. Grimm and B. Bonavida, "Mechanism of cell-mediated cytotoxicity at the single cell level: I. estimation of cytotoxic t lymphocyte frequency and relative lytic efficiency," *The Journal of Immunology*, vol. 123, no. 6, pp. 2861–2869, 1979.

[190] B. Weigelin and P. Friedl, "A three-dimensional organotypic assay to measure target cell killing by cytotoxic t lymphocytes," *Biochemical pharmacology*, vol. 80, no. 12, pp. 2087–2091, 2010.

[191] V. Garcia, K. Richter, F. Graw, A. Oxenius, and R. R. Regoes, "Estimating the in vivo killing efficacy of cytotoxic t lymphocytes across different peptide-mhc complex densities," *PLoS computational biology*, vol. 11, no. 5, p. e1004178, 2015.

[192] D. L. Barber, E. J. Wherry, and R. Ahmed, "Cutting edge: rapid in vivo killing by memory cd8 t cells," *The Journal of Immunology*, vol. 171, no. 1, pp. 27–31, 2003.

[193] R. K. Benninger and D. W. Piston, "Two-photon excitation microscopy for the study of living cells and tissues," *Current protocols in cell biology*, vol. 59, no. 1, pp. 4–11, 2013.

[194] P. T. So, "Two-photon fluorescence light microscopy," *eLS*, 2001.

[195] P. J. Goulder and D. I. Watkins, "Hiv and siv ctl escape: implications for vaccine design," *Nature Reviews Immunology*, vol. 4, no. 8, p. 630, 2004.

[196] C. L. Althaus and R. J. De Boer, "Dynamics of immune escape during hiv/siv infection," *PLoS computational biology*, vol. 4, no. 7, p. e1000103, 2008.

[197] V. V. Ganusov, D. L. Barber, and R. J. De Boer, "Killing of targets by cd8+ t cells in the mouse spleen follows the law of mass action," *PloS one*, vol. 6, no. 1, p. e15959, 2011.

[198] F. Graw and R. R. Regoes, "Investigating ctl mediated killing with a 3d cellular automaton," *PLoS computational biology*, vol. 5, no. 8, p. e1000466, 2009.

[199] S. J. Merrill, "Foundations of the use of an enzyme-kinetic analogy in cell-mediated cytotoxicity," *Mathematical Biosciences*, vol. 62, no. 2, pp. 219–235, 1982.

[200] A. Yates, F. Graw, D. L. Barber, R. Ahmed, R. R. Regoes, and R. Antia, "Revisiting estimates of ctl killing rates in vivo," *PloS one*, vol. 2, no. 12, p. e1301, 2007.

[201] R. R. Regoes, D. L. Barber, R. Ahmed, and R. Antia, "Estimation of the rate of killing by cytotoxic t lymphocytes in vivo," *Proceedings of the National Academy of Sciences*, vol. 104, no. 5, pp. 1599–1603, 2007.

[202] S. Gadhamsetty, A. F. Marée, J. B. Beltman, and R. J. de Boer, "A general functional response of cytotoxic t lymphocyte-mediated killing of target cells," *Biophysical journal*, vol. 106, no. 8, pp. 1780–1791, 2014.

[203] S. Gadhamsetty, A. F. Marée, J. B. Beltman, and R. J. de Boer, "A sigmoid functional response emerges when cytotoxic t lymphocytes start killing fresh target cells," *Biophysical journal*, vol. 112, no. 6, pp. 1221–1235, 2017.

[204] S. Gadhamsetty, A. F. Marée, R. J. de Boer, and J. B. Beltman, "Tissue dimensionality influences the functional response of cytotoxic t lymphocyte-mediated killing of targets," *Frontiers in immunology*, vol. 7, p. 668, 2017.

[205] C. M. Macal and M. J. North, "Tutorial on agent-based modeling and simulation," in *Proceedings of the Winter Simulation Conference, 2005.*, pp. 14–pp, IEEE, 2005.

[206] M. J. Miller, S. H. Wei, M. D. Cahalan, and I. Parker, "Autonomous t cell trafficking examined in vivo with intravital two-photon microscopy," *Proceedings of the National Academy of Sciences*, vol. 100, no. 5, pp. 2604–2609, 2003.

[207] V. Mayya, E. Judokusumo, E. A. Shah, C. G. Peel, W. Neiswanger, D. Depoil, D. A. Blair, C. H. Wiggins, L. C. Kam, and M. L. Dustin, "Durable interactions of t cells with t cell receptor stimuli in the absence of a stable immunological synapse," *Cell reports*, vol. 22, no. 2, pp. 340–349, 2018.

[208] C. D. Tsoukas, B. Landgraf, J. Bentin, M. Valentine, M. Lotz, J. Vaughan, and D. Carson, "Activation of resting t lymphocytes by anti-cd3 (t3) antibodies in the absence of monocytes.," *The Journal of immunology*, vol. 135, no. 3, pp. 1719–1723, 1985.

[209] J. Textor, S. E. Henrickson, J. N. Mandl, U. H. Von Andrian, J. Westermann, R. J. De Boer, and J. B. Beltman, "Random migration and signal integration promote rapid and robust t cell recruitment," *PLoS computational biology*, vol. 10, no. 8, 2014.

[210] S. Elmore, "Apoptosis: a review of programmed cell death," *Toxicologic pathology*, vol. 35, no. 4, pp. 495–516, 2007.

[211] S. Khailaie, P. A. Robert, A. Toker, J. Huehn, and M. Meyer-Hermann, "A signal integration model of thymic selection and natural regulatory t cell commitment," *The Journal of Immunology*, vol. 193, no. 12, pp. 5983–5996, 2014.

[212] J. Rachmilewitz and A. Lanzavecchia, "A temporal and spatial summation model for t-cell activation: signal integration and antigen decoding," *Trends in immunology*, vol. 23, no. 12, pp. 592–595, 2002.

[213] S. Valitutti, D. Coombs, and L. Dupré, "The space and time frames of t cell activation at the immunological synapse," *FEBS letters*, vol. 584, no. 24, pp. 4851–4857, 2010.

[214] G. P. McStay and D. R. Green, "Measuring apoptosis: caspase inhibitors and activity assays," *Cold Spring Harbor Protocols*, vol. 2014, no. 8, pp. pdb–top070359, 2014.

[215] G. Hajnóczky, E. Davies, and M. Madesh, "Calcium signaling and apoptosis," *Biochemical and biophysical research communications*, vol. 304, no. 3, pp. 445–454, 2003.

[216] M. J. Fuller, A. Khanolkar, A. E. Tebo, and A. J. Zajac, "Maintenance, loss, and resurgence of t cell responses during acute, protracted, and chronic viral infections," *The Journal of Immunology*, vol. 172, no. 7, pp. 4204–4214, 2004.

[217] J. S. Yi, M. A. Cox, and A. J. Zajac, "T-cell exhaustion: characteristics, causes and conversion," *Immunology*, vol. 129, no. 4, pp. 474–481, 2010.

[218] Z. Vasconcelos, S. Müller, D. Guipouy, W. Yu, C. Christophe, S. Gadat, S. Valitutti, and L. Dupré, "Individual human cytotoxic t lymphocytes exhibit intraclonal heterogeneity during sustained killing," *Cell reports*, vol. 11, no. 9, pp. 1474–1485, 2015.

[219] V. R. Buchholz, M. Flossdorf, I. Hensel, L. Kretschmer, B. Weissbrich, P. Gräf, A. Verschoor, M. Schiemann, T. Höfer, and D. H. Busch, "Disparate individual fates compose robust cd8+ t cell immunity," *Science*, vol. 340, no. 6132, pp. 630–635, 2013.

[220] M. Elemans, N.-K. S. Al Basatena, and B. Asquith, "The efficiency of the human cd8+ t cell response: how should we quantify it, what determines it, and does it matter?," *PLoS computational biology*, vol. 8, no. 2, p. e1002381, 2012.

[221] B. Farhood, M. Najafi, and K. Mortezaee, "Cd8+ cytotoxic t lymphocytes in cancer immunotherapy: A review," *Journal of cellular physiology*, vol. 234, no. 6, pp. 8509–8521, 2019.

[222] R. Khazen, S. Müller, F. Lafouresse, S. Valitutti, and S. Cussat-Blanc, "Sequential adjustment of cytotoxic t lymphocyte densities improves efficacy in controlling tumor growth," *Scientific Reports*, vol. 9, p. 12308, 2019.

[223] Y. Sun and L. Cheng, "A survey on agent-based modelling and equation-based modelling," *Department of Computer Science. Georgia State University. Atlanta. Disponível em: www. cs. gsu. edu/˜ csclicx/Csc8350/model. pdf*, 2005.

[224] H. V. D. Parunak, R. Savit, and R. L. Riolo, "Agent-based modeling vs. equation-based modeling: A case study and users' guide," in *International Workshop on Multi-Agent Systems and Agent-Based Simulation*, pp. 10–25, Springer, 1998.

[225] S. Celli, Z. Garcia, and P. Bousso, "Cd4 t cells integrate signals delivered during successive dc encounters in vivo," *The Journal of experimental medicine*, vol. 202, no. 9, pp. 1271–1278, 2005.

[226] T. H. Harris, E. J. Banigan, D. A. Christian, C. Konradt, E. D. T. Wojno, K. Norose, E. H. Wilson, B. John, W. Weninger, A. D. Luster, *et al.*, "Generalized lévy walks and the role of chemokines in migration of effector cd8+ t cells," *Nature*, vol. 486, no. 7404, p. 545, 2012.

[227] H. Zheng, B. Jin, S. E. Henrickson, A. S. Perelson, U. H. von Andrian, and A. K. Chakraborty, "How antigen quantity and quality determine t-cell decisions in lymphoid tissue," *Molecular and cellular biology*, vol. 28, no. 12, pp. 4040–4051, 2008.

[228] N. Anikeeva and Y. Sykulev, "Mechanisms controlling granule-mediated cytolytic activity of cytotoxic t lymphocytes," *Immunologic research*, vol. 51, no. 2-3, pp. 183–194, 2011.

[229] R. Khazen, S. Müller, N. Gaudenzio, E. Espinosa, M.-P. Puissegur, and S. Valitutti, "Melanoma cell lysosome secretory burst neutralizes the ctl-mediated cytotoxicity at the lytic synapse," *Nature communications*, vol. 7, p. 10823, 2016.

[230] X.-N. Xu, G. R. Screaton, F. M. Gotch, T. Dong, R. Tan, N. Almond, B. Walker, R. Stebbings, K. Kent, S. Nagata, *et al.*, "Evasion of cytotoxic t lymphocyte (ctl) responses by nef-dependent induction of fas ligand (cd95l) expression on simian immunodeficiency virus–infected cells," *Journal of Experimental Medicine*, vol. 186, no. 1, pp. 7–16, 1997.

[231] D. Horst, M. C. Verweij, A. J. Davison, M. E. Ressing, and E. J. Wiertz, "Viral evasion of t cell immunity: ancient mechanisms offering new applications," *Current opinion in immunology*, vol. 23, no. 1, pp. 96–103, 2011.

[232] G. Nossal, "The double cascade of lymphoid proliferation: current challenges and problem areas," *American journal of anatomy*, vol. 170, no. 3, pp. 253–259, 1984.

[233] C. O. Starnes, "Coley's toxins in perspective.," 1992.